UNIVERSITY OF CALIFORNIA
RIVERSIDE

The Behavior and Systematics of Extrafloral Nectary Associated *Orasema* (Hymenoptera: Eucharitidae)

A Thesis submitted in partial satisfaction
of the requirements for the degree of

Master of Science

in

Entomology

by

Judith Sierra Herreid

December 2015

Thesis Committee:
Dr. John Heraty, Chairperson
Dr. Dong-Hwan Choe
Dr. Richard Stouthamer

The Thesis of Judith Sierra Herreid is approved:

_____

_____

_____

Committee Chairperson

University of California, Riverside

Acknowledgements

I'd first like to thank my advisor, Dr. John Heraty. I'm exceedingly grateful for his help over the past few years. I appreciate the countless hours he's spent editing my work and the support he has given me in my research endeavors. Thanks to him I have been able learn so much and become a better entomologist. My guidance committee has also been very helpful during my time at UCR. I appreciate the insightful comments on my thesis from Dr. Dong-Hwan Choe, the many ideas Dr. Richard Stouthamer provided me and Dr. Edith Allen's encouragement. I also could not have completed my studies without the help and support I received from the members of the Heraty lab and I am exceeding grateful to my undergraduate researchers that dissected numerous ant heads. Finally, I would like to thank my family. Without the constant support and love from my parents and brother I would not have been able to make it this far, I will forever appreciate that. Last but not least I am grateful for the love and encouragement from Levi Zahn. He has made grad school an exceedingly happy experience even when times were incredibly stressful for the both of us.

This research was supported by NSF-DEB 1257733 to Dr. John Heraty and the Harry Scott Smith Scholarship. I also appreciate all of the collectors and institutions that have provided me with my collection materials.

Table of Contents

List of Figures

List of Tables

1. Introduction

The family Eucharitidae is from one of the most diverse and species rich orders of insects, Hymenoptera (Grissell, 1999; Sharkey, 2007). Hymenoptera includes roughly 75% of all insect parasitoids (Eggleton and Belshaw, 1992), but eucharitids are the only family known to be strictly parasitoids of ant immature stages (Lachaud and Pérez-Lachaud, 2012). This is unique because although a variety of insects parasitize and exploit the resource rich ant nest (Lachaud et al., 2012; Lachaud and Pérez-Lachaud, 2012), a relatively small proportion of insect parasitoids target ants. Very few parasitoids or predators have been able to negotiate the nest defense mechanisms to attack the ant brood (Hölldobler and Wilson, 1990; Schmid-Hempel, 1998; Murray et al., 2013).

Eucharitids, all of whom first parasitize the ant larva and then develop on the ant pupa, have been able to overcome these defenses with a uniquely modified lifecycle that involves ovipositing into or on plant tissue with a mobile first instar (planidia) gaining access to its host (Clausen, 1940b; Clausen, 1941). Eucharitidae, which comprises 54 genera and over 470 species, is divided into four subfamilies (Lachaud and Pérez-Lachaud, 2012). These subfamilies are Akapalinae, Oraseminae, Eucharitinae, Gollumiellinae (Heraty, 2002; Lachaud and Pérez-Lachaud, 2012; Heraty and Murray, 2013; Murray et al., 2013; Murray, 2014). These ant parasitoids use a plethora of different behaviors to access their immature host without entering the ant nest as an adult (Heraty, 1985; Heraty and Barber, 1990; Heraty, 2002).

These behaviors begin with the placement of eggs away from the host ant's nest into or on a variety of plant structures (Heraty and Murray, 2013). Eggs are randomly scattered onto leaves, placed on seeds later dispersed by the wind, oviposited into overwintering or expanding leaf or flower buds, or inserted into leaf or fruit tissues (Parker and Thompson, 1925; Clausen, 1940b; Clausen, 1941; Heraty and Barber, 1990). Once the planidia emerge they exhibit various behaviors that facilitate entrance into their host ant's nest. The planidia may use phoresy to enter the nest by attaching to foraging ants or the host ant's food source such as an immature thrips or auchenorrhynchous hemipteran (Parker, 1937; Ayre, 1962; Johnson et al., 1986; Heraty and Barber, 1990; Heraty, 2000; Heraty, 2002). Planidia are also possibly picked directly up in the mouthparts of foraging adult ants through feeding (Heraty and Barber, 1990).

The focus of the research herein will be on eucharitids whose unique behavior for host access involves a close association with extrafloral nectaries (EFNs). Extrafloral nectaries (EFNs) are nectar-secreting glands found on plants that are generally located independent of the flower (Heil et al., 2001; Marazzi et al., 2013b; Weber and Keeler, 2013). These glands attract a number of insects with their nectar, and often ants are among these visitors (González-Teuber and Heil, 2009; Heil, 2011). Eucharitids from several different species have been found to deposit eggs in close association to EFNs and their planidia are often found near to or in an EFN (Carey et al., 2012; Schwitzke et al., 2015). It seems likely that this close proximity to an EFN facilitates transfer to their ant host. My research examines the systematic relationships and behaviors of two EFN associated species groups from the genus *Orasema* (Eucharitidae: Oraseminae). I study how EFN associated

eucharitids gain host access by studying the *simulatrix*- and *wayqecha*-groups. Members of these species groups are revised, morphological descriptions are provided, and taxonomic placement is examined with a molecular phylogeny. Biology for members of both species groups is provided based on past and recent field observations. This biological information includes choice of ant and plant hosts, distributions and oviposition behaviors. Host access mechanisms are further studied in the field and with laboratory experiments.

The first chapter is a taxonomic revision of the *simulatrix*- and *wayqecha*-groups. Members of the *simulatrix*-group, *O. aureoviridis*, *O. beameri* and *O. simulatrix* are revised while *O. cancellata* **n.sp.**, *O. difrancoae* **n.sp.**, and *O. zahni* **n.sp.** are newly described. *Orasema wayqecha* **n.sp.** and *O. quadrimaculata* **n.sp.** from the *wayqecha*-group are described for the first time. A key is provided for these species, and their phylogenetic relationships are examined and discussed. This chapter uses an integrative taxonomic type approach to delimit species and looking at phylogenetic relationships. Morphology, molecular data, geographic distributions and behavior is considered in this chapter. The *simulatrix*- and *wayqecha*-groups are found to potentially have a sister group relationship based on a combined molecular analysis, a shared EFN association and morphological characteristics. The new species names from this thesis are not available for scientific record until published.

Chapter 2 examines planidia-ant relationships both in the field and in a laboratory setting. It is initially proposed that planidia of EFN associated *Orasema* are transferred to

the nest via the infrabuccal pocket of their host ant. Their host ant is foraging on plants whose EFNs have planidia near or in them and during this time the ant comes into contact with the immature *Orasema*. The planidia may access the ant's infrabuccal pocket either by attaching to the ant's body and being groomed into the mouthparts or by direct transfer into the mouthparts when the ant is feeding at the nectaries. To test this hypothesis three different studies were done. What ants carry planidia in their mouthparts must first be determined. For this, all ants foraging near to or on the host plant of *Orasema simulatrix* were collected, identified and the contents of their mouthparts examined. To further determine if the host ant carries planidia in its mouthparts, nests of *O. simulatrix* and *O. wayqecha* host ants were excavated and workers collected so their mouthpart contents could be determined. Finally laboratory trials using *Pheidole desertorum*, the host of *O. simulatrix*, were run to determine if planidia attached to the body are transferred to the infrabuccal pocket. The results from this study and recently discovered information allowed for a better understanding, and the adoption of a new hypothesis about how EFN associated planidia are being transferred to their host in the ant nest.

This research broadly examines EFN associated eucharitids. Two EFN associated species groups are revised using integrative taxonomy. Integrative taxonomy is an approach that uses multiple disciplines and methods for systematic research as opposed to traditional taxonomy which uses a single method such as morphology (Dayrat, 2005; Padial et al., 2010; Schlick-Steiner et al., 2010). Their means of host access are further examined with studies that look at behaviors in a field and laboratory environment.

Species in the genera *Kapala* Cameron (Eucharitinae) (Heraty pers. comm.) and *Chalcura* Kirby (Eucharitinae) potentially have EFN associations (Schwitzke et al., 2015). In the future this type of research could encompass more members of Eucharitidae, potentially allowing for EFN associations to be discussed in a phylogenetic context across all of the family.

2. Chapter 1

Species of *Orasema* (Hymenoptera: Eucharitidae) with a shared extrafloral nectary association

2.1 Abstract

Extrafloral nectaries (EFNs) are nectar secreting glands found on plants independent of their flowers. EFNs are diverse in form, present on a wide variety of plants, and their secretions are known to recruit ants. However, much less information has been published on insects with known EFN associations other than ants. Two distinct species groups of *Orasema* Cameron (Hymenoptera: Eucharitidae) are associated with EFNs of their plant hosts. The *Orasema simulatrix*- and *wayqecha*- species groups are proposed as sister groups based on morphological and molecular evidence. The *simulatrix*-group is comprised of six species found in deserts and xeric shrublands of the southwestern United States and Mexico. This species group is revised, retaining *O. aureoviridis*, *O. beameri* and *O. simulatrix* as valid species, and describing *O. cancellata* **n.sp.**, *O. difrancoae* **n.sp.**, and *O. zahni* **n.sp.**. The *wayqecha*-group is from Peru and Colombia and includes the newly described *O. wayqecha* **n.sp.** and *O. quadrimaculata* **n.sp.**. Members of the *simulatrix*-group oviposit near EFNs of *Chilopsis linearis* Cav. (Bigoniaceae), *Prosopis glandulosa* Torr. (Fabaceae), *Prosopis velutina* Wooton (Fabaceae) and *Populus angustifolia* James (Salicaceae), whereas *Orasema wayqecha* oviposits on leaves of two species of *Myrsine* (Myrsinaceae). Relationships are proposed based on a molecular analysis of ribosomal (28S and 18S) and mitochondrial (COI)

DNA, and their shared behavioral association with EFNs is discussed. Adults from both species groups have an expanded postgenal margin that encloses the mouthparts, but are otherwise morphologically distinct. The planidia of both groups also share several features, including long cerci that may facilitate their movements within EFNs. Oviposition near EFNs is proposed as a means of increasing encounter rates of the first-instar larvae with their myrmicine ant host.

Note: Nomenclatorial acts within this thesis chapter are not for the scientific record.

2.2 Introduction

Using an array of morphological, chemical and behavioral specializations, *Orasema* Cameron belongs to one of the few families of insect parasitoids that have infiltrated the complex social system of ants (Clausen, 1940a; Gross, 1993; Schmid-Hempel, 1998; Howard et al., 2001; Murray et al., 2013). A considerable amount of information is available on the within-nest biology of these ant parasitoids (Heraty et al., 1993; Heraty, 2000), yet there is still uncertainty over how their minute first-instar larvae gain access to brood within the ant nest. Different strategies of host access have been proposed across Eucharitidae. Eggs are laid away from the host and the active first-instars (planidia) must gain access to the host brood (Heraty, 1994a; Carey et al., 2012; Heraty and Murray, 2013). Within Oraseminae, proposed strategies for transport include either direct transfer by foraging ants or by phoretic transfer of planidia through their attachment to immature thrips or auchenorrynchous hemipterans, which then can be carried as prey to the ant brood (Clausen, 1940b; Das, 1963; Johnson et al., 1986; Heraty, 2000). The mechanism

of direct transfer is not well understood, but Ayre (1962) proposed that larvae attached to workers and then migrated to the ant mouthparts for later transfer to the brood.

An extrafloral nectary (EFN) association was first discovered in *Orasema simulatrix* Gahan, whereby females oviposit in close proximity to fluid-filled EFNs of desert willow, *Chilopsis linearis* Cav. (Bignoniaceae) (Carey et al., 2012). EFNs can be extremely diverse in form and have been found in a fifth of vascularized plant families (Marazzi et al., 2013a; Weber and Keeler, 2013). The function of EFNs has been proposed as either a plant defense mechanism attracting insect predators and parasitoids, or as a diversion to keep insects away from the floral nectary sources (Bentley, 1976; Stephenson, 1982; Wagner and Kay, 2002; González-Teuber and Heil, 2009). In either case, EFNs are highly attractive to ants and often facilitate a mutualistic ant-plant relationship (Heil et al., 2001; Díaz-Castelazo et al., 2013; Koptur et al., 2013). Some of these ant-plant relationships become obligate associations, with EFN nectar tailored to attract and provide nourishment for only their resident ant species (Heil et al., 2005). On *Chilopsis*, EFNs are foraging sites for a variety of ants, including *Pheidole desertorum* Wheeler (Myrmicinae), which is the known host of *O. simulatrix* (Carey et al., 2012). Oviposition occurs almost exclusively in association with the EFN, and the planidia are found both in and around the EFN. It is unclear if the ants collect the larvae while feeding at the EFN (a novel strategy), or if larvae attach to foraging ants while near EFNs, similar to the more general phoretic attachment described by Clausen (1940) and Ayre (1962). Herein I describe two species groups, the *simulatrix*- and the *wayqecha*-groups, that contain species known to oviposit near EFNs.

Orasema is present worldwide in subtropical regions, and in the Nearctic Region as far north as southern Canada (Heraty, 1994b; Heraty, 2002). Species are almost exclusively parasitoids of ant brood from the subfamily Myrmicinae (Heraty, 1985; Heraty et al., 1993; Heraty, 1994b; Heraty, 2000; Varone and Briano, 2009). Female *Orasema* deposit single stalked eggs into plant tissue using an expanded scimitar-shaped ovipositor. The planidia are transferred to ant larvae by workers, complete their development on ant pupae, and emerge as adults in the nest. Within the nest, wasps likely pick up host colony odors (cuticular hydrocarbons) through contact with their ant hosts (Vander Meer et al., 1989). This chemical camouflage not only allows them to survive within the nest, but also to exit the nest unharmed.

Originally described by Cameron (1884), *Orasema* includes 61 currently described species (Heraty, 1994b; Heraty, 2002; Heraty, 2014; Burks et al., 2015). Gahan (1940) provided the first key to a selection of New World species, with the Old World species revised by Heraty (1994). The species of *Orasema* have been partitioned into 13–17 species groups (Heraty, 1994b; Heraty, 2000). Seven to nine species groups have been recognized in the New World; however only the *festiva*- and *xanthopus*-groups from South America have been revised (Heraty et al., 1993; Burks et al., 2015).

Gahan's (1940) identification key grouped *Orasema aureoviridis* Gahan, *Orasema beameri* Gahan and *O. simulatrix*, based on having a strong axillular sulcus and a broad shallow medial depression on the scutellar disc. Heraty (1994, 2000) recognized these as the *simulatrix*-group. Herein I define the group and recognize six species within the

Nearctic region. The *wayqecha*-group is newly described, and based on two new species from western South America. A sister group relationship between the *wayqecha*- and *simulatrix*-groups was discovered that is based on adult and planidial morphological features, molecular characters, and a common behavior of depositing eggs on leaves near EFNs. While their monophyly is supported, this is in contrast to their morphological and geographic distinctness within *Orasema* which provides support for their recognition as distinct species groups.

2.3 Materials and Methods

The research includes: morphological studies of museum and collected specimens to create taxonomic descriptions; a molecular phylogenetic analysis that facilitates the understanding of relationship between and within the *wayquecha*- and *simulatrix*-groups; life history observations of their plant and ant host associations and behaviors.

2.3.1 Morphological Studies

Specimens examined are from the following collections: American Museum of Natural History, New York, USA (**AMNH**); Canadian National Collection of Insects, Ottawa, Canada (**CNC**); Florida State Collection of Arthropods, Gainesville, USA (**FSCA**), The Museum of Comparative Zoology, Cambridge, USA (**MCZ**); Fundación e Instituto Miguel Lillo, Tucuman,Argentina (**IMLA**); Lund University, Lund, Sweden (**MZLU**); San Diego Natural History Museum, San Diego, USA (**SDNH**); University of Arizona Insect Collection, Tucson, USA (**UAIC**); University of California, Davis, USA (**UCDC**); University of California Entomology Research Museum, Riverside, USA (**UCRC**);

University of Michigan Zoology Museum, Ann Arbor, USA (**UMMZ**); National Museum of Natural History, Washington, USA (**USNM**); and the W.F. Barr Entomological Collection, Moscow, USA (**WFBM**). All specimens are labeled with a UCRCENT barcode label indicating the museum of deposition and a unique specimen identification number. Georeference points estimated from Google Earth are italicized in the specimen lists. Specimen data were recorded in an internal FileMakerPro database. In the database all unique specimen identification numbers are prefaced with UCRENT. The UCRCENT is not included in the materials examined section.

Photographs of pinned specimens were taken using a Leica Imaging System with a Z16 APOA microscope with a 5 megapixel camera (model: DFC 450C), with images captured using the Leica Application Suite v4.4. Slide mounted specimens were imaged with a Zeiss Axioskop 2 mounted with a 1.4 megapixel CCD camera (model LW1165C; Lumenera Corp., Ottawa, Ontario, Canada), with images captured using ARCHIMED v5.4.1. Image stacks were montaged with Zerene Stacker (version 1.04, © Zerene Systems, LLC). Photographs from this manuscript, including additional images of holotype specimens and labels, are deposited in Morphbank in the following collection: 858553.

Morphological terminology follows Heraty (2002) and Heraty et al. (2013), and measurements (Fig. 10) follow Heraty (2002). Measurements were taken using an ocular micrometer with a Zeiss Stemi SV6 light microscope, with a 1.6x objective lens and a 16x eyepiece. All measurement ranges were acquired from at least 5 different specimens

unless otherwise stated. Abbreviations used in the descriptions are as follows: HDW- Head Width; HDH- head height; IOD- inner ocular distance; EYH- eye height; GNL- genal length; FLG- flagellar length; F2L- 2nd flagellomere length; F2W- 2nd flagellomere width; F3L- 3rd flagellomere length; FWL- forewing length; FWW- forewing width; ML- mesosoma length (pronotum to frenal groove).

Taxonomic descriptions initially were generated using DELTA (Description Language for Taxonomy) (Dallwitz, 1980; Dallwitz et al., 1993; Dallwitz et al., 1999). A set of 124 characters were used to code all characters, and then relevant information was pruned and edited into the descriptions herein. Taxonomic characters were vetted through the HAO ontology tool (Yoder et al., 2010).

2.3.2 Molecular Phylogenetic Analysis

The molecular dataset is based on 41 specimens of *Orasema*. Ten specimens are outgroups selected from five different new world species groups of *Orasema* (Table 1). The 31 *wayqecha*- and *simulatrix*-groups were sampled from Arizona, California, Colorado, New Mexico, Texas and Peru. Four individuals of *O. wayquecha* were sequenced (vouchers D3603 ♂, D3613 ♀, D3614 ♂, D4130 ♀), but only one was used in the analyses because they were identical in sequence. All specimens were collected into 95% ethanol, stored frozen, and after extraction pin-mounted and vouchered in the UCRC with a DNA voucher code and specimen identifier. Images of all vouchers are deposited in MorphBank (858457). Specimens and GenBank accession numbers are listed in Table 1.

The dataset includes three nuclear gene regions (18S, 28S D2, 28S D3–D5) and the mitochondrial gene region (COI). Primers for all gene regions are listed in Table 2. DNA was extracted from specimens using either a modified Chelex extraction protocol (Walsh et al., 1991) or the DNeasy Blood and Tissue kit (Qiagen). Gene regions were amplified via PCR following Murray et al. (2013). PCR products were purified using the GeneClean kit (MP Biomedicals) and submitted to either the Genomics Core at the University of California, Riverside, or Retrogen Inc., San Diego, for sequencing.

Sequences were edited with Sequencher v4.8 sequence analysis software (Gene Codes Corp.). Each gene region was aligned using the MAFFT v7 online server (Katoh and Standley, 2013), implementing the E–INS–i algorithmic model and default settings, except that the scoring matrix parameter for the nuclear gene regions was set to '1PAM/k = 2' for aligning closely related sequences (Mottern and Heraty, 2014). Mitochondrial genes were verified by translating to amino acid sequences using Mesquite v2.75 (Madison and Madison, 2011). Nuclear and mitochondrial gene regions were concatenated in SequenceMatrix v1.7.8 (Vaidya et al., 2011). Phylogenetic analyses were performed using Maximum likelihood, Bayesian and parsimony methods, with trees visualized with Fig tree v1.4.0 (Rambaut, 2012).

Maximum likelihood (ML) analyses were done using RAxML v8.2.4 (Stamatakis, 2014) through the CIPRES science gateway v3.3 (Miller et al., 2010). Data were analyzed using a GTR+Γ model (Stamatakis et al., 2008) with 1000 rapid bootstraps and five gene partitions: 18S, 28S D2, 28S D3–5, COI codon positions 1 and 2, and COI

codon position 3. RAxML analyses were repeated 10 times using different random starting seed values for parsimony inferences and rapid bootstrapping, and the tree chosen that had the highest final likelihood score.

Bayesian analyses were done using MRBAYES v3.2.3 (Ronquist et al., 2012) through the online CIPRES portal V.3.3 (http://www.phylo.org). The same gene partitions were used as in the likelihood analyses. A mixed model approach was implemented to determine the model of sequence evolution and search all possibilities within the GTR substitution model family (Huelsenbeck et al., 2004). The analysis included two runs, each with four chains running for 50 million generations, with trees sampled every 5000 generations and excluding a 20 percent (10 million generation) burnin rate. The average standard deviation of split frequencies was < 0.01 suggesting that both runs converged. Tracer v1.6.0 (Rambaut et al., 2014) was used to confirm that the effective sample size was greater than 200 in both runs. The maximum clade credibility tree was used with posterior probabilities exported from CIPRES.

Maximum Parsimony (MP) analyses were implemented using TNT v1.1 (Goloboff et al., 2008). Heuristic searches were performed with a new technology search. Default settings were retained except using 10 rounds of sectorial searches with RSS, CSS and XSS; 200 iterations of ratchet and a weighting probability of 5%; tree drifting of 50 cycles; 5 runs of tree fusing; a best score hit of 25 times; and finally an iteration of TBR performed. A traditional search yielded the same results. Support values were calculated by resampling for standard bootstraps with 1000 replicates.

2.3.3 Life History

Study Localities: Ant and plant associations were determined during collection events in the United States and Peru. Within the *simulatrix*-group, host associations were found across the American southwest (see materials examined). Particular sites for further investigation included: *Orasema aureoviridis* Lake Corpus Christi State Park (28°04'04"N 97°52'56"W) in San Patricio County, Texas; *O. beameri* along county road 126 (39°15'58"N 105°16'06"W) near Deckers, Colorado; *O. simulatrix* on Foothills Road (31°55'01"N 109°07'41"W) near Portal, Arizona and in Whitewater Canyon, California (33°57'51"N 116°39'03"W); and *O. zahni* in southeastern Arizona in several locations in Cochise, Pima and Santa Cruz County. *Orasema wayqecha* host information was collected at the Wayqecha Biological Station in the Cusco province of Peru, and specifically along the Perdiz Trail (13°10'38"S 71°35'04"W).

Plant Host Records: Sweep net collections were used to search for novel host plants. Vegetation with *Orasema* was collected and leaves inspected for oviposition punctures, EFNs and planidia of *Orasema*. Plant voucher specimens were pressed, mounted, given unique collector codes and deposited at UCR. Andrew Sanders from the UCR Herbarium assisted in plant identifications. Distribution data for host plants, *Chilopsis linearis* and *Prosopis glandulosa* are from USGS maps and Little (1976).

Ant Host Records: Parasitized ant brood was excavated from study sites in Arizona and Peru. Both brood and mature ants were collected and preserved in 95% EtOH. For large collections, soil, brood and ants from nest excavations were placed in fluon lined plastic

containers until they could be sorted and examined for evidence of parasitoids. Brood and ants were then preserved in at least 95% EtOH. Vouchers of preserved minors, majors and alates were pinned and used to identify ants collected. Vouchers of both *Orasema* and the ant hosts pin mounted, were given unique specimen identifier labels and deposited in UCRC.

2.4 Results

The following section reports phylogenetic relationships with a discussion of morphology and EFN associations, a key to species of the *wayqecha*- and *simulatrix*-groups and species descriptions.

2.4.1 Phylogenetic Relationships

Our analyses are based on four species from the *wayqecha*- and *simulatrix*-group, and 10 outgroup *Orasema*. These combined molecular analyses included three nuclear and one mitochondrial gene (partial 18S, 28S D2, 28S D3–5 and COI). COI had no stop codons or insertions. The alignment of 2951 bp was partitioned into 5 regions for likelihood (RAxML) and Bayesian analyses. The *simulatrix*-group were consistently monophyletic, but there were differences in support for the monophyly of the *O. simulatrix* and *O. wayqecha* clade.

The resulting trees from the Bayesian (BA), Maximum Likelihood (ML) and Parsimony (MP) analyses are similar but not identical. A sister-group relationship between the *wayqecha*- and *simulatrix*-groups had moderate support (PP 82%) in the BA

analysis (Fig. 1a). The 10 iterations of the ML (RAxML) analyses produced a single topology that differed from the BA results only by placing the *wayqecha*-, *bakeri*- and *simulatrix*-groups as monophyletic (BS 63) with the *bakeri*-group sister to the *simulatrix*-group (BS 53). The MP analyses produced 4,235 equally parsimonious trees (EPT) with a best score of 526 steps and a retention index of 0.83. The strict consensus tree (Fig. 1b) found the same relationships between the *wayqecha*-, *bakeri*- and *simulatrix*-groups as in the ML analyses but with bootstrap values of less than 50.

A monophyletic *simulatrix*-group was a consistent result in all three analyses with high levels of support (100), but species relationships within this group vary between analyses (Figs 1a & 1b). All three analyses placed *O. simulatrix* and *O. zahni* as monophyletic with support values ≥ 97. The parsimony analyses found a monophyletic *O. aureoviridis* and *O. beameri* (BS 58) to be sister to the *O. simulatrix* and *O. zahni* clade (BS 68), but placement of *O. aureoviridis* and *O. beameri* is unresolved in both the Bayesian and ML analyses.

When a larger sampling of taxa is included, a monophyletic *wayqecha*- and *simulatrix*-group is consistently supported in ML and BA (Mottern et al. unpublished). Further support morphological support for the monophyly of these two species groups includes convergent postgenae extending over the subforaminal bridge and labiomaxillary complex (Figs 2, 5), and planidia with elongate cerci and an emarginated tergite IX (Fig. 53). The habit of ovipositing near EFNs (Figs 60–62) appears to be a unique behavioral

apomorphy for this larger clade, although the manner of oviposition is unknown for many taxa.

Monophyly of the *simulatrix*-group is supported by a strongly impressed axillular sulcus (Figs 20, 23, 26, 29, 32, 35). Other features found in all members this group include an evenly reticulate sculpture on the face (Figs 8–13) and mesosoma (Figs 21, 24, 27, 30, 33, 36), a 4-digitate labrum (Fig. 3), and 7 funiculars (Figs 17–19). A monophyletic *wayqecha*-group is supported by a labrum with 7–10 segments (Fig. 6) and female wings with infuscate spots (Figs 49, 51), which occurs nowhere else in Oraseminae.

All species of the *simulatrix*-group oviposit into plant hosts with some form of nectar association. *Orasema simulatrix* oviposits into *Chilopsis* (Fig. 63), *O. aureoviridis* and *O. zhani* share *Prosopis* (Fabaceae) as a host plant, including the same species *P. glandulosa* Torr. (Figs 65–66), and the host plant of *O. beameri* is *Populus angustifolia* James (Salicaceae) (Fig. 64). In all analyses *O. simulatrix* is recovered as sister to *O. zahni*. *Orasema aureoviridis* and *O. zhani* were never recovered as monophyletic despite both ovipositing into *Prosopis*. Instead the parsimony results place *O. aureoviridis* in a clade with *O. beameri*, whose host plant is very different. However this relationship is unresolved in BA and ML (Fig. 1a).

2.4.2 Key to species in the *Orasema simulatrix*- and *O. wayqecha*- species groups

1) Postgenae not expanded over labiomaxillary complex (most species). If postgenae expanded, then face noticeably setose and mesosoma elongate (one undescribed species) .....other *Orasema*

- Postgenae expanded over labiomaxillary complex (Figs 2, 5). Face not noticeably setose and mesosoma roughly as long as tall (Figs 20, 23, 26, 29, 32, 35, 43) .... ***simulatrix*- and *wayqecha*-groups**, 2

2) Face evenly reticulate (Figs 8–13). Labrum with four digits (Fig. 3). Postmarginal vein short, similar in length to stigma (Figs 38, 39). Flagellum with 7 funiculars (Figs 17–19). Forewing hyaline (Figs 38, 39) ..... ***simulatrix*-group**, 3

- Face glabrate with at most scattered punctures or longitudinal striations near eye (Figs 47, 48). Labrum with 7–10 digits (Fig. 6). Postmarginal vein long, reaching 0.4–0.6X distance to apex (Figs 49–52). Flagellum with 8 funiculars. Forewing with dark spots at least along cubital vein (Figs 49–52) ..... ***wayqecha*-group**, 8

3) Forewing with posterior marginal fringe (Figs 38, 40) 4

- Forewing without marginal fringe (Figs 39, 41) ..... *Orasema simulatrix* Gahan

4) First funicular equal to or only slightly longer than pedicel (Figs 17, 18). Acropleural sulcus not evenly foveate (Figs 20, 23, 29, 35). Propodeal disc may be

laterally reticulate or completely reticulate-areolate, and with or without a median carina (Figs 22, 25, 31, 37) 5

- First funicular 1.5 times longer than pedicel (Fig 19). Acropleural sulcus evenly foveate (Fig. 32) Propodeal disc always laterally reticulate with reticulate-areolate median carina present (Fig. 34) ..... *Orasema difrancoae* **sp. n.**

5) Costal cell with up to 20 setae. Scutellar disc is longer than broad (Figs 20, 30, 36). Clypeus reticulate with lateral margin fairly straight (Figs 8, 11, 13) 6

- Costal cell with 20–35 setae (Fig. 38). Scutellar disc roughly equal in length and width (Fig. 24). Clypeus mostly smooth with rounded lateral margin (Fig. 9)..... ..... *Orasema cancellata* **sp.n.**

6) Female femur basally infuscate to dark with metallic luster. Bluish green or dark metallic body with gaster concolorus or brown (Fig. 16). Axillula reticulate, similar to mesosomal mid lobe (Figs 30, 36) 7

- Female femur yellow. Bright metallic green body color (Fig. 20). Axillula rugose and similar to scutellar disc (Fig. 21) ..... *Orasema aureoviridis* Gahan

7) Axillular groove with or without a small carina extending towards the median furrow of scutellar disc (Fig. 36). Female acrosternite rounded in ventral view (Fig. 14). Face without longitudinal groove (Fig. 13)..... *Orasema zahni* **sp.n.**

- Axillular groove with distinct carina extending towards the median furrow of scutellar disc (Fig. 30). Female acrosternite subtriangular in ventral view (Fig. 15). Face with slightly impressed longitudinal groove (Fig. 8) .... *Orasema beameri* **sp.n.**

8) Forewing of female with 3–4 dark spots, post-stigmal pigmentation not reaching wing apex and sometimes very light (Fig. 49); wing spot absent in male (Fig. 50). Labrum with 7–8 digits (Fig. 6). Frons with vertical and often distinct striae medial to eye (Fig. 47) ..... *Orasema wayqecha* **sp.n.**

- Forewing with four dark spots in both male and female, post-stigmal pigmentation reaching wing apex (Figs 51–52). Labrum with 9–10 digits. Frons weakly rugose medial to eye (Fig. 48) ..... *Orasema quadrimaculata* **sp.n.**

2.4.3 *Orasema simulatrix*-group

Diagnosis. Recognized from all other *Orasema* by the following combination of character states: postgena expanded and covering maxillary complex (Fig. 2); labrum with four digits (Fig. 3); and face mostly reticulate (Figs 8–13). Additional descriptive features include occiput strigate (Fig. 2), with dorsal margin abrupt and shallowly emarginate; eye bare with inner margin vertical and straight; anteclypeus present; flagellum with 7 funiculars (Figs 17–19); scape usually yellow, sometimes brown with a metallic luster in males; mesosoma bare and entirely rugose-reticulate (Figs 21, 24, 27, 30, 33, 36); axillular sulcus well-defined and distinctly crenulate (Figs 20, 23, 26, 29, 32,

35); prepectus triangular in dorsal half, strongly narrowed ventrally; hind femur and tibia slender and uniformly setose; wing hyaline with light brown venation; forewing rounded apically; basal cell and speculum bare; submarginal vein mostly bare with several setae in apical half; marginal vein covered with minute setae; postmarginal vein short, 1–2x as long as stigmal vein (Figs 38, 39); acrosternite crenulate (Figs 14, 15); hypopygium with a few minute setae apically. Ovipositor slightly curved cephalad; first valvula with subapical ridge and lateral line of 6–8 small narrowly separated teeth; second valvula with 7–10 lateral annuli that are broadly separated and smooth medially or weakly coalescing.

Planidium (Fig. 53). Length 0.12–0.18 mm. Antenna, labial plates and tergopleural line absent. Tergites I and II (TI, TII) separate. TI, TII, TIII with dorsal seta. TII, TVI with very short lateral seta. TI, TIII, TV, TVII with ventral seta. TIX emarginate. Caudal pad present; caudal cerci present and long, about as long as apical 6–7 tergites.

Biology. The plant and ant host are known for four members of the *simulatrix*-group. *Orasema aureoviridis*, *O. beameri*, *O. simulatrix* and *O. zahni* oviposit onto leaf surfaces either with or near EFNs. Planidia are often found within or around an EFN. In all species where planidia have been described, the caudal cerci are flexible and long, exceeding the apical five tergites in length (Fig. 53). Adults of these four species have been collected off other non-host plants but oviposition punctures have only been observed on their respective host plant. More detailed biology and host information for *O. aureoviridis*, *O. beameri*, *O. simulatrix* and *O. zahni* are characterized herein.

Distribution. Southwestern United States (Figs 68–70): Arizona, California, Colorado, New Mexico, Texas; Mexico (Fig. 70): Aguascalientes, Guerrero, Hidalgo, Jalisco, Michoacán, Morelos, Nuevo Leon, San Luis Potosi, Veracruz.

2.4.4 Species descriptions

2.4.4.1 *Orasema aureoviridis* (Gahan)

(Figs 11, 20–22, 66, 69)

Orasema aureoviridis Gahan 1940: 448-449. Holotype: 1 ♀; label information: "Uvalde Tex. 5-22-33" "A.W. Lindquist collector". Deposited in USNM, type number no. 53555.

Type image: http://usnmhymtypes.com/default.asp?Action=Show_Types&Single_Type=True&TypeID=7007

Diagnosis. This species most closely resembles *O. difrancoae*, but can be distinguished by its body color which often has a more metallic green lustre and by F2 being roughly the same length as the pedicel. *Orasema aureoviridis* is recognized from other species within the *simulatrix*-group by the following combination of characters: clypeus glabrate with 15–20 setose punctations (Fig. 11); axilla rugose-areolate (Fig. 21); propodeum reticulate-areolate with a distinct areolate median carina (Fig. 22); marginal wing fringe complete; hind femur light yellow (female) or light metallic brown apically (male).

Female. Length 2.7–3.4 mm. Body and coxae bright metallic green with coxae and petiole sometimes darker; pedicle and anellus yellow to brown; flagellum brown;

mandibles yellow to light brown with darker outline; maxilla and labrum yellowish brown; legs yellow.

Head (Fig. 11), HDW:HDH 1.2–1.5. Face reticulate with some portions weakly rugose; lacks longitudinal groove; scrobal impression with similar sculpture to face. IOD:EYH 1.7–1.8. Malar space only shallowly impressed between mouth and eye margin; GNL:EYH 0.72–0.88. Clypeus glabrate to weakly reticulate with 15–20 distinct setae over punctures; epistomal sulcus strongly impressed; ventral margin of clypeus straight; supraclypeal area sculptured similarly to clypeus, slightly broader than long and shorter than clypeus.

Antenna (Fig. 11) with scape reaching 0.8X distance to median ocellus; anellus stout, close to twice as broad as long; FLG:HDH 0.63–0.97; F2L:F2W 1–1.5; F2L:F3L 1.2–1.5; following flagellomeres subequal in length, gradually increasing in diameter.

Mesosoma (Figs 20–22) with mid and lateral lobes mostly reticulate with some rugose areas; axilla sculpture coarser than the rugose-areolate mesosoma; posterior margin of axilla broadly rounded, scutellar disc on roughly same plane as axilla (Fig. 20). Notauli moderately to deeply impressed and foveate. Scutellar disc reticulate with a rugose-areolate overlay, median channel; longer than broad; separated medially from TSA by a broadly impressed foveate channel; frenal line generally a weak crenulate groove, frenum and axillula with similar sculpture to scutellar disc, rugose-areolate. Propodeal disc reticulate with a rugose-areolate overlay, median carina visible and rugose-areolate (Fig. 22); callus rugulose; metapleuron rugose-areolate. Acropleural sulcus rugose but

indistinct. Upper mesepimeron reticulate. Lower mesepimeron reticulate to rugose. Transepimeral sulcus not very visible. Femoral groove rugose to finely reticulate and broadly impressed; mesepisternum rugose. Prepectus reticulate with some rugose overlay. Hind coxa reticulate dorsally and smooth ventrally.

Forewing. FWL:FWW 2.2–2.4; FWL:ML 2.1–2.3; costal cell with 5–15 minute setae, wing disc setose; marginal fringe present; stigmal vein 2.0–2.5X as long as broad; postmarginal vein as long as stigmal vein.

Metasoma with petiole 1.1–1.5X as long as hind coxa, 1.9–2.9X as long as broad and rugose; acrosternite subtriangular in ventral view.

Male. Length, 2.1–2.6 mm. Similar to female except for following: hind femur dark brown to infuscate basally; other femora yellow; FLG:HDH 0.78–0.84; scape yellow; F2L:F2W 0.6–0.8; metasoma with petiole 2.6–3.4X as long as hind coxa; petiole 6.3–7.4X as long as broad.

Oviposition Behavior and Immature Stages. *Orasema aureoviridis* has been observed to deposit eggs in somewhat straight lines on the ventral surface of leaves of *Prosopis glandulosa* (Fig. 66). Up to 67 egg punctures were found on a single leaf. Extrafloral nectaries are located on the stems at the base of both the leaflets and the pinnae (Fig. 66). EFNs are distributed at the base of leaflets along the rachis but not at the base of every leaflets. Punctures are concentrated at leaflets with an EFN at their base (Fig. 66). Planidia of *O. aureoviridis* were not collected and the ant host is unknown.

Distribution. USA: South Texas (Fig. 69: black triangle). Collecting locality habitats are arid regions with *Prosopis* present. All localities are found in or near the Chihuahuan desert.

Paratype: USA: Texas: Uvalde Co., Uvalde, 338m, *29°21'06"N, 99°45'39"W*, 2 May 1933, A.W. Lindquist [2♂ 1♀, USNM: 00416747–48]. **Additional material examined: USA: Texas:** Burnet Co., Inks Lake St.Park, South Trail, *30°43'58"N, 98°21'59"W*, 2 May 1987, J.S. Noyes, sweep [1♂ 1♀, BMNH: 00309467–68]; Cameron Co., Brownsville, 10m, *25°54'06.3"N, 97°29'50.9"W*, 1921, J.C. Bridwell [1♂, USNM: 00247871]; Crockett Co., 12 mi. W Jct. Hwy 29 & 137, 200m, *30°20'35"N, 97°41'49"W,* 10 Jun 1972, W.E. Clark [1♀, TAMU: 00426684]; 2 mi. W jct. 29 & 163, 200m, *30°20'35"N, 97°41'49"W*, 1 Jun 1973, Gaumer and Clark, beating mesquite [1♂, TAMU: 00426685]; San Patricio Co., Lake Corpus Christi St. Pk., 35m, 28°04'04"N, 97°52'56"W, 30 Jun 2014, A. Baker & S. Heacox, swp mesquite [2♂ 2♀, UCRC: 00436480, 00436484, 00436489, 00447151]; Starr Co., Falcon Lake St. Park, 100m, *26°34'54"N, 99°08'54"W*, 20 Apr 1985, J.B. Woolley [3♀, TAMU: 00426687–89]; near Falcon Dam, 80m, *26°33'32"N, 99°09'53"W*, 20 Apr 1985, J.B. Woolley [1♂, TAMU: 00426690]; Val Verde Co., 15 miles SE of Del Rio, 300m, *29°12'45"N, 100°43'44"W*, 20 Aug 1965, J.C. Schaffner [1♀, TAMU: 00426691]; Seminole Canyon St. Pk., 427m, *29°41'13"N, 101°19'03"W*, 20 Jul 1986, J.B. Woolley & G. Zolnerowich, Rio Grande Trail [1♀, TAMU: 00426692].

2.4.4.2 *Orasema beameri* Gahan

(Figs 8, 15, 17, 29–31, 64, 69)

Orasema beameri Gahan 1940: 447-448. Holotype: 1 ♀; label information: "Ridgeway Colo 7-1-37 R. H. Beamer". Deposited in USNM, type number no. 53554.

Type image:
http://usnmhymtypes.com/default.asp?Action=Show_Types&Single_Type=True&TypeID=7009

Diagnosis. This species most closely resembles *O. difrancoae*, but can be recognized by a rugose acropleural sulcus (Fig. 29) and multiple small but distinct carinae that extend from the axillular groove towards the median furrow of the scutellar disc (Fig. 30). It is recognized from other species by following combination of characters: shallowly impressed longitudinal groove (Fig. 8); marginal wing fringe present; notaulus strongly impressed; inner margin of coxae always strongly reticulate.

Female. Length 3.2–3.8 mm. Body and coxae dark to bluish green metallic luster; pedicle and anellus brown; flagellum brown to black; mandibles yellowish brown with darker outline; maxilla and labrum yellowish brown; femora with basal two thirds dark brown with metallic reflections; tibiae and tarsi yellow.

Head (Fig. 8), HDW:HDH 1.0–1.3. Face reticulate and broadly rounded with slightly impressed longitudinal groove; scrobal impression with similar sculpture to face. IOD:EYH 1.7–1.9. Malar space distinctly impressed between mouth and eye margin;

GNL:EYH 0.77–0.83. Clypeus weakly reticulate; epistomal sulcus strongly impressed; ventral margin of clypeus straight to slightly rounded; supraclypeal area with weak striations but sculptured similarly to clypeus, longer than broad and about 1.2X as long as clypeus.

Antenna (Fig. 17) with scape almost reaching median ocellus; anellus small but visible; FLG:HDH 0.65–0.98; F2L:F2W 0.9–1.5; F2L:F3L 0.9–1.4; following flagellomeres subequal in length, gradually increasing in diameter.

Mesosoma (Figs 29–31) with mid and lateral lobes reticulate with some fine rugose-areolate sections; axilla reticulate with an areolate overlay (Fig. 30); posterior margin of axilla abrupt or broadly rounded, scutellar disc below or on roughly same plane as dorsal margin of axilla. Notauli moderately to deeply impressed and foveate. Scutellar disc rugose-areolate and slightly longer than broad, separated medially from TSA by a broadly impressed or narrow foveate channel (Fig. 30); frenal line a shallow and often weak crenulate groove, frenum and axillula with similar sculpture to scutellar disc, rugose-areolate. Propodeal disc laterally reticulate-areolate, with median carina (Fig. 31); callus and metapleuron weakly rugose. Upper mesepimeron reticulate. Lower mesepimeron rugose to rugose-areolate. Transepimeral sulcus weakly impressed. Femoral groove rugose; mesepisternum rugose. Prepectus reticulate sometimes with a weak rugose overlay. Hind coxa finely reticulate sometimes smooth ventrally.

Forewing. FWL:FWW 2.4–2.5; FWL:ML 2.5–2.7; costal cell with 12–20 setae, wing disc setose; marginal fringe present; stigmal vein 2.0–2.5X as long as broad; postmarginal vein 1.5–2X as long as stigmal vein.

Metasoma with petiole 1.1–1.4X as long as hind coxa, 2.0–2.4X as long as broad and rugose; acrosternite subtriangular in ventral view (Fig. 15).

Male. Length, 2.2–2.5 mm. Similar to female except for following: femora mostly dark brown with metallic relections basally; FLG:HDH 0.8–0.9; scape metallic brown; F2L:F2W 0.7–0.9; metasoma with petiole 2.7–3.3X as long as hind coxa; petiole 6.6–9.7X as long as broad.

Oviposition Behavior and Immature Stages. *Orasema beameri* deposit eggs in grouped lines into the ventral leaf surface of *Populus angustifolia* James (Salicaceae) (Fig. 64). As many as 30 oviposition punctures have been found together and multiple oviposition groupings have been observed on a single leaf. Over 100 oviposition punctures have been found on a single leaf. Oviposition punctures are always found dorsal to the nectaries along the leaf margin and are more common at the base of the leaves (Fig. 64). *Populus angustifolia* possesses small nectar secreting glands found along the serrated edge of the leaf and at the base of the leaf near the petiole (Trelease, 1881). Planidia were observed near the nectaries at the base of the leaf near the petiole.

Planidia of *O. beameri* are 0.16–0.17 mm in length and are identical to the *simulatrix*-group description as illustrated in Fig. 53. The ant host is unknown.

Distribution. USA: Colorado (Fig. 70: black circle). Specimens have been collected at elevations of 2000–2184 m. Collecting locality habitats are a mix of deciduous and coniferous montane forest.

Paratypes: USA: Colorado: Ouray Co., Ridgway, 2100m, *38°09'09"N*, *107°45'32"W*, 1 Jul 1937 [3♂ 7♀, USNM: 00416750–56, 00416769, 00425349, 00425362]. **Additional material examined: USA: Colorado:** Douglas Co., ditch along CR 126, 2184m, 39°15'58.1"N, 105°16'06.6"W, 20 Jul 2015, J. Herreid, narrow leaf cottonwood, swp [4♂ 7♀, UCRC: 00446404–07, 00447164–70]; El Paso Co., Manitou, 1942m, *38°51'03"N*, *104°55'02"W*, 1877, Morrison [2♀, MCZ: 00316395–96]; Jefferson Co., Pine Groove, 2000m, *39°24'32"N*, *105°19'26"W*, 23 Mar 1907, C. Hill [1♀, UMMZ: 00243584]. **Planidia Slides: USA: Colorado:** Douglas Co., ditch along CR 126, 2180m, 39°15'58"N, 105°10'07"W, 5 Aug 2015, J. Herreid, narrow leaf cottonwood [4, UCRC: 00447234–37].

2.4.4.3 *Orasema cancellata* sp. nov.

(Figs 9, 18, 23–25, 38, 70)

Diagnosis. This species most closely resembles *O. aureoviridis* but can be distinguished by a scutellar disc that is roughly equal in length and width (Fig. 24) and a clypeus that is glabrate with rounded lateral margins (Fig. 9) instead of reticulate with a straight lateral margin. *Orasema cancellata* can be recognized from other members of the *simulatrix*-group by the following combination of characters: wing pilose, costal cell with over 20

setae and marginal wing fringe present (Fig. 38); propodeum evenly rugose-areolate with no median carina (Fig. 25); female petiole usually 3–4 times as long as broad.

Female. Length 2.7–4.0 mm. Body and coxae bluish to dark green; gaster brown; pedicle and anellus light brown; flagellum brown; mandibles brown with dark outline; maxilla and labrum yellow to yellowish brown; femora mostly all dark brown basally, sometimes only slightly infuscate; tibia and tarsi yellowish brown.

Head (Fig. 9), HDW:HDH 1.1–1.2. Face reticulate with some portions weakly rugose and longitudinal groove occasionally present; scrobal impression with similar sculpture to face. IOD:EYH 1.6–1.9. Malar space shallowly impressed adjacent to mouth; GNL:EYH 0.70–0.9. Clypeus glabrate; epistomal sulcus wide and weakly impressed; ventral margin of clypeus broadly rounded; supraclypeal area weakly sculptured, longer than broad and about equal length to clypeus.

Antenna (Fig. 18) with scape almost reaching median ocellus; anellus stout, close to twice as broad as long; FLG:HDH 0.79–0.90; F2L:F2W 1.0–1.2; F2L:F3L 1–1.3; following flagellomeres subequal in length, equal in width.

Mesosoma (Figs 23–25) with mid and lateral lobes reticulate with a rugose-areolate overlay; axilla similar but slightly coarser like scutellar disc (Fig. 23); posterior margin of axilla broadly rounded, scutellar disc on roughly same plane as axilla (Fig. 24). Notauli moderately to deeply impressed and foveate. Scutellar disc rugose-areolate and as long as broad, separated medially from TSA by narrow foveate channel; frenal line a distinct but small crenulate groove, frenum and axillula with similar sculpture to scutellar disc,

rugose-areolate. Propodeal disc rugose-areolate, median carina absent (Fig. 25); callus weakly rugose; metapleuron rugose-areolate. Upper and lower mesepimeron rugose-areolate. Transepimeral sulcus weakly impressed and not prominently visible. Femoral groove rugose; mesepisternum rugose-areolate. Prepectus rugose-areolate. Hind coxa finely reticulate and smooth ventally.

Forewing. FWL:FWW 2.2–2.3; FWL:ML 2.4–3.1; costal cell (20–35 setae) and wing disc setose; marginal fringe present (Fig. 38); stigmal vein 1.5–2.0X as long as broad; postmarginal vein as long as stigmal vein.

Metasoma with petiole 1.4–1.7X as long as hind coxa, 2.6–3.9X as long as broad and rugose-areolate; acrosternite semicircular or subtriangular in ventral view.

Male. Length, 2.1– 2.7 mm (n=4). Similar to female except for the following: hind femur dark brown to infuscate basally; other femora yellow; FLG:HDH 0.8–1.1 (n=3); scape metallic brown; F2L:F2W 0.9–1.3 (n=3); metasoma with petiole 2.8–3X as long as hind coxa (n=4); petiole 5.5–8.0X as long as broad (n=4).

Oviposition Behavior and Immature Stages. Unknown.

Distribution. Mexico: Jalisco, Veracruz (Fig. 73: black square).

Etymology. From Latin meaning to have a grid/lattice pattern, name refers to sculpture on the dorsal mesosoma.

Holotype: Mexico : Jalisco: 17 mi. N of Guadalajara, 1624m, *20°55'08"N, 103°26'05"W*, 6 Jul 1984, J.B. Woolley [1♀, TAMU: 00426693]; **Paratypes: Mexico :**

Jalisco: 17 mi. N of Guadalajara, 1624m, *20°55'08"N*, *103°26'05"W*, 6 Jul 1984, J.B. Woolley [2♀, TAMU: 00426694–95]; 8.3 mi. S Autlan, Hwy. 80, 1309m, *19°40'49"N*, *104°55'39"W*, 8 Jul 1984, J.B. Woolley [1♂ 1♀, TAMU: 00426696–97]; **Veracruz:** 33 mi. S. Nautla, 2111m, *19°43'25"N*, *96°46'16"W*, 31 Oct 1982, A. Gonzalez & J.T. Huber, screen swp [3♂ 4♀, UCRC: 00435183–89].

2.4.4.4 *Orasema difrancoae* sp. nov.

(Figs 10, 19, 32–34, 70)

Diagnosis. This species most closely resembles *O. beameri* but can be recognized by an evenly reticulate acropleural sulcus (Fig. 32) and the first funicular segment is 1.5 times longer than pedicel (Fig 19) instead of roughly equal in length to pedicel. It is recognized from other species by the following combination of characters: femoral groove finely reticulate to punctate and impressed (Fig. 32); margin between femoral groove and mesepisternum raised and often weakly rugose (Fig. 32); costal cell contains 14–20 setae; posterior marginal wing fringe present; propodeal disk laterally reticulate and rugose-areolate medially (Fig. 34); body has a dark blue green, purple or black metallic luster as well as the basal ½ to ¾ of the femur (Fig. 33).

Female. Length 3.1–3.8 mm. Body and coxae dark green blue to black with metallic green and purple luster; pedicel dark to light brown, anellus concolorus or lighter than pedicel; flagellum brown to black; mandibles brown with dark outline; maxilla and

labrum yellowish to dark brown; femora with basal ½ to ¾ dark brown with metallic reflections; tibiae and tarsi yellow.

Head (Fig. 10), HDW:HDH 1.1–1.2. Face finely reticulate and lacks longitudinal groove; scrobal impression sculpture similar to face. IOD:EYH 1.5–1.9. Malar space impressed, sometimes shallowly, between mouth and eye margin; GNL:EYH 0.70–0.96. Clypeus weakly to strongly reticulate; epistomal sulcus strongly to weakly impressed; ventral margin of clypeus straight; supraclypeal area reticulate, roughly the same length as clypeus (Fig. 10).

Antenna (Fig. 19) with scape reaching 0.8X distance to median ocellus; anellus small but visible; FGL:HDH 0.67–0.85; F2L:F2W 1.5–1.9; F2L:F3L 1.3–1.5; following flagellomeres subequal in length, equal in width.

Mesosoma (Figs 32–34) with mid and lateral lobes mostly reticulate with finely rugose-areolate sculpture (Fig. 33); axilla sculpture similar to mesosoma; posterior margin of axilla broadly rounded to abrupt, scutellar disc on roughly same plane as or slightly below dorsal margin of axilla (Fig. 32). Notauli deeply impressed and foveate. Scutellar disc weakly rugose and slightly longer than broad (Fig. 33), separated medially from TSA by a broadly or narrowly impressed foveate channel; frenal line a distinct crenulate groove, frenum finely rugose; axillula with similar sculpture to mesosomal mid lobe, mostly reticulate. Propodeal disc rugose-areolate median carina with shallow reticulations laterally (Fig. 34); callus reticulate sometimes with rugose overlay; metapleuron reticulate. Acropleural sulcus distinct and evenly reticulate. Upper

mesepimeron reticulate sometimes with weak rugose overlay. Lower mesepimeron similar but more reticulate (Fig. 32). Transepimeral sulcus irregularly foveate channel. Femoral groove finely reticulate and broadly impressed; mesepisternum rugose. Prepectus reticulate or weakly rugose. Hind coxa finely reticulate sometimes completely.

Forewing. FWL:FWW 2.3–2.6; FWL:ML 1.4–2.3; costal cell with 14–20 setae, wing disc setose; marginal fringe present; stigmal vein 2.0–2.5X as long as broad; postmarginal vein 1.5–2X as long as stigmal vein.

Metasoma with petiole 1.1–1.4X as long as hind coxa, 1.2–2.9X as long as broad and reticulate to weakly rugose; acrosternite generally subtriangular in ventral view.

Male. Length 2.8–3.6 mm. Similar to female except for the following: setae in costal cell and wing disc longer and more distinct; FLG :HDH 0.8–1.0; scape brown with metallic luster; F2L:F2W 1.0–1.3. Metasoma with petiole 2.6–3.1X as long as hind coxa; petiole 8.2–9.9X as long as broad.

Oviposition Behavior and Immature Stages. A single planidium was found on the gaster of an *O. difrancoae* adult female (USNM: 00248052). It is 0.13 mm in length with caudal cerci identical to the *simulatrix*-group description. Other planidial characters from the group description are unobservable. Oviposition behaviors and hosts are unknown.

Distribution. Mexico: Aguascalientes, Guerrero, Hidalgo, Jalisco, Michoacán, Morelos, Nuevo Leon, San Luis Potosi (Fig. 73: black triangle).

Etymology. Named after the musician Ani Difranco.

Holotype: Mexico: Morelos: Cuernavaca, *18°55'27"N*, *99°13'18"W*, May 1945, N.L.H. Krauss [1♀, USNM: 00247863]; **Paratypes: Mexico: Aguascalientes:** 10 mi. NE Calvillo, 2053m, *21°54'15"N*, *102°35'28"W*, 5 Jul 1984, J.B. Woolley [1♂, TAMU: 00426698]; **Mexico:** 13 miles W of Aguascalientes, 2000m, *21°53'27"N*, *102°26'55"W*, 5 Jul 1984, JB Woolley [1♂, UCRC: 00322698]; 8 mi. E Calvillo, 1991m, *21°53'30"N*, *102°36'19"W*, 11 Jul 1983, Kovarik, Schaffner, Harrison [1♀, TAMU: 00426699]; **Guerrero:** 17 miles E Tixtla, 1551m, *17°33'19"N*, *99°12'42"W*, 11 Jul 1985, J. Woolley, G. Zolnerowich [1♀, TAMU: 00426700]; **Hidalgo:** 16.0 km. E. Pachuca Jct. 115 & 130, 2587m, *20°03'08"N*, *98°36'56"W*, 20 May 1973, Erwin & Hevel [3♀, USNM: 00248050, 00248052–53]; **Jalisco:** 16 mi. S of Encarnacion, 2011m, *21°16'59"N*, *102°14'19"W*, 21 Mar 1953, Creighton [1♂, CNC: 00320659]; 3 km. NW Arenal, *20°47'16"N*, *103°42'36"W*, 16 Jul 1981, John D. Pinto [1♀, UCRC: 00435997]; Guadalajara, *20°39'35"N*, *103°20'59"W*, McConnell [1♀, USNM: 00248002]; **Michoacan:** Cotija, 1643m, *19°48'26"N*, *102°42'06"W*, 14 Sep 1975, B.Villegas [1♀, UCDC: 00280009]; **Morelos:** Cuernavaca, 1200m, *18°49'48"N*, *99°13'05"W*, Jun 1959, N.L.H. Krauss [1♀, USNM: 00247872]; Cuernavaca, *18°55'27"N*, *99°13'18"W*, May 1945, N.L.H. Krauss [7♂ 1♀, USNM: 00247862, 00247864–70, 00247873]; Cuernavaca, *18°56'02"N*, *99°13'53"W*, Jul 1965 [1♀, USNM: 00247741]; **Nuevo Leon:** 5.3 miles S La Escondida, 1895m, *24°02'15"N*, *99°58'16"W*, 8 Jul 1986, Kovarik, Schaffner [1♀, TAMU: 00426701]; **San Luis Potosi:** 65 mi. NW San Luis Potosi, 2255m, *22°48'40"N*, *101°43'34"W*, 30 Jun 1971, Ward & Brothers [1♀, USNM: 00247861].

2.4.4.5 *Orasema simulatrix* Gahan

(Figs 2–4, 12, 26–28, 39, 41, 53, 54, 60, 63, 68)

Orasema simulatrix Gahan 1940: 450. Holotype: 1 ♀; label information: “Oracle Ar 14.7” “Hubbard & Schwarz”. Deposited in USNM, type number no. 53556.

Type image: http://usnmhymtypes.com/default.asp?Action=Show_Types&Single_Type=True&TypeID=7179

Diagnosis. This species most closely resembles *O. zahni* but is recognized by the absence of a marginal wing fringe (Figs 39, 41). It can be differentiated from other species by following combination of characters: clypeus strongly reticulate with straight ventral margin (Fig. 12); female femora generally yellow to slightly infuscate with some exceptions; acropleural sulcus not prominently visible (Fig. 26); reticulate axillula (Fig. 27); propodeum with a reticulate-areolate median carina (Fig. 28)

Female. Length 2.8–3.3 mm. Body and coxae metallic green with purple and blue lustre or black with metallic green and purple lustre; gaster either concolorus with body or brown; pedicle and anellus light brown; flagellum brown; mandibles yellow to light brown with dark outline; maxilla and labrum yellow to yellowish brown; legs yellow hind femur sometimes slightly infuscate; tibiae and tarsi yellow.

Head (Fig. 12), HDW:HDH 1.2–1.3. Face reticulate sometimes with a slightly impressed longitudinal groove; scrobal impression with similar sculpture to face.

IOD:EYH 1.8–1.9. Malar space distinctly impressed between mouth and eye margin; GNL:EYH 0.7–0.9. Clypeus strongly reticulate; epistomal sulcus strongly impressed; ventral margin of clypeus straight; supraclypeal area sculptured similarly to clypeus with weak striations, longer than broad and about equal length to clypeus.

Antenna with scape almost reaching median ocellus; anellus small but visible; FLG:HDH 0.7–0.8; F2L:F2W 1.1–1.6; F2L:F3L 1.1–1.6; following flagellomeres subequal in length, gradually increasing in diameter.

Mesosoma (Figs 26–28) with mid and lateral lobes finely reticulate; axilla sculpture similar to the mesosoma; posterior margin of axilla relatively flat dorsally, scutellar disc on same plane as axilla. Notauli moderately to deeply impressed and foveate (Fig. 27). Scutellar disc reticulate with an areolate overlay and about 1.5X longer than broad (Fig. 27), separated medially from TSA by a broadly impressed foveate channel; frenal line a distinct but small crenulate groove, frenum and axillula with similar sculpture to scutellar disc, reticulate. Propodeal disc laterally reticulate, with rugose-areolate median carina overlaying reticulate sculpture (Fig. 28); callus weakly rugose to reticulate; metapleuron reticulate. Upper and lower mesepimeron reticulate. Transepimeral sulcus weakly impressed. Femoral groove finely reticulate and broadly impressed; mesepisternum rugose. Prepectus reticulate. Hind coxa finely reticulate and usually smoother ventrally.

Forewing (Fig. 39), FWL:FWW 2.4–2.6; FWL:ML 2.2–2.5; costal cell with 13–17 setae, wing disc setose; marginal fringe absent (Figs 39, 41); stigmal vein 2.0–2.5X as long as broad; postmarginal vein 1.5–2X as long as stigmal vein.

Metasoma with petiole 1.1–1.2X as long as hind coxa (n=5), 1.7–2.3X as long as broad and reticulate or weakly rugose; acrosternite subtriangular in ventral view.

Male. Length, 2.0–2.6 mm. Similar to female except for the following: femora usually mostly all dark brown with metallic reflections basally; FLG:HDH 0.6–0.9X; scape brown with metallic luster; F2L:F2W 0.7–1.0; metasoma with petiole 2.3–3.2X as long as hind coxa; petiole 4.1–6.5X as long as broad; adeagus broad; parameres long with three setae; 6 lateral spines on digitus; expanded genital capsule between intervolsellar process and volsella.

Oviposition Behavior and Immature Stages. *Orasema simulatrix* oviposit 1–27 eggs in straight lines on the surface of *Chilopsis linearis* leaves (Fig. 63) (Carey et al., 2012). EFNs are found on leaves of *Chilopsis linearis* and range from dry to wet to fluid filled. A fluid filled EFN is three times more likely to have fresh oviposition punctures than a dry EFN and once planidia emerge they are found most often near or in wet EFNs (Fig. 60) (Carey et al., 2012).

This association with EFNs seemingly facilitates their access to the ant host brood via the adult ants. EFNs are known to attract foraging ants to their valuable nectar (Heil, 2008; Marazzi et al., 2013b). The ant host for this wasp, *Pheidole desertorum* (Wheeler), can be found foraging and likely visiting EFNs on *C. linearis* at night (Carey et al., 2012). It is likely that the planidia comes in contact with or is picked up by the foraging host ant while ant is feeding at an EFN and is then vectored to the immature host brood to continue its lifecycle.

Planidium (Fig. 53): length 0.16–0.20 mm; identical to the *simulatrix*-group description. Pupa (Fig. 54): length 2.9 mm; recognized by: three pronounced tubercles over petiole; five prominent transverse ridges on abdomen; lateral swelling by mesothoracic spiracle.

Distribution. USA: Arizona, California, New Mexico, Texas (Fig. 68: black circle). Specimens have been collected broadly across the southwestern United States in arid regions with *C. linearis* present. Collecting localities are found in the Mojave, Sonoran and Chihuahuan Deserts.

Material Examined. USA: Arizona: Cochise Co., 1 mi. E Portal, 1432m, *31°54'49"N, 109°08'29"W*, 31 Jul 1982, G. Gibson [4♀, CNC: 00425775–77, UCRC: 00320394]; 2 mi. ESE Portal, 4500m, 31°54'00"N, 109°06'00"W, 5 Jun 1979, H.A. Hespenheide, *Chilopsis* [6♂ 2♀, UCRC: 00320433, 00447152–57, 00447160]; 2 mi. ESE Portal, 4500m, 31°54'00"N, 109°06'00"W, 8 Jun 1979, H.A. Hespenheide, *Chilopsis* [2♀, UCRC: 00447158–59]; 20 mi. N Warren, 1376m, *31°38'16"N, 111°02'39"W*, 21 Jun 1956 [1♀, USNM: 00247740]; 6.8 mi. SE Apache Tr. mouth Skeleton Cyn., 1371m, *31°35'39"N, 109°04'08"W*, 14 Aug 1982, G. Gibson [13♂ 8♀, CNC: 00321012–15, 00321017–24, 00321037, UCRC: 00320361–62, 00320372–74, 00320384, 00320386–87]; Canadian Lane, 1425m, 31°55'04.7"N, 109°07'40.4"W, Aug 2013, S. Heacox [2♀, UCRC: 00411593, 00411606]; Foothills and Portal Rd., 1443m, 31°54'03"N, 109°07'40"W, 27 Jul 2013, J. Herreid, *Chilopsis*, swp [1♀, UCRC: 00411563]; Foothills Rd., 1429m, 31°55'01"N, 109°07'38"W, 26 Jul 2013, J. Herreid, *Chilopsis*, swp [1♀,

UCRC: 00411569]; Foothills Rd., 1429m, 31°55'01"N, 109°07'38"W, 28 Jul 2013, J. Herreid, *Chilopsis*, swp [1♂, UCRC: 00411568]; Foothills Rd., 1429m, 31°55'01"N, 109°07'38"W, 7 Aug 2013, J. Herreid, *Chilopsis* (night), swp [1♀, UCRC: 00411567]; Foothills Rd., 1439m, 31°55'24"N, 109°07'49"W, 27 Jul 2013, J. Herreid, *Chilopsis*, swp [1♂, UCRC: 00411565]; Ghost Town Trail, 31°43'30"N, 109°48'41"W, 27 Aug 2013, J. Herreid, *Chilopsis*, swp [2♂ 2♀, UCRC: 00411559–62]; Portal area, 1454m, 31°54'00"N, 109°08'00"W, 6 Jun 1979, H.A. Hespenheide [1♀, UCRC: 00447161]; Portal Rd, 5.1 km SE Portal, 1354m, 31°53'51"N, 109°05'34"W, 15–16 Aug 2011, J. Heraty, *Chilopsis linearis*, swp [3♀, UCRC: 00292573–75]; Portal Rd. driveway, 1448m, 31°54'51"N, 109°07'59"W, 9 Aug 2013, S. Heacox [1♂ 3, UCRC: 00411590, 00411605, 00411608, 00436417]; Portal, 1454m, *31°54'49"N, 109°08'29"W*, 13 Aug 1974, H.M. Townes [1♀, AEIC: 00251346]; Portal, 1454m, *31°54'49"N, 109°08'29"W*, 29 Aug 1987, H.M. Townes [2♀, AEIC: 00251347, 00251349]; Portal, 1454m, *31°54'49"N, 109°08'29"W*, 7 Sep 1974, H.M. Townes [1♂, AEIC: 00251350]; Portal, 1454m, *31°54'49"N, 109°08'29"W*, H.M. Townes [1♀, AEIC: 00251348]; San Simon Road, 4 mi. NNW Portal, 1371m, 31°58'00"N, 109°09'00"W, 27 May 1995, H.A. Hespenheide, on foliage of *Chilopsis linearis* [7♀, UCRC: 00322689, 00322691, 00322693–94, 00322696, 00322699, 00322701]; Whitetail Canyon, 1448m, 32°00'13"N, 109°12'52"W, 25 Jul 2013, J. Herreid, *Chilopsis*, swp [1♂ 2♀, UCRC: 00411446–47, 00411449]; Whitetail Canyon, 1448m, 32°00'13"N, 109°12'52"W, 3 Aug 2013, Heacox S. [1♂ 2, UCRC: 00411591–92, 00411607]; Pima Co., Box Cyn. Coronado Nat. For., 31°47'52"N, 110°46'29"W, 13 Aug 2001, A. Owen, yellow pan trap [4♀, UCRC: 00091444–47];

Santa Clara Co., 4.5 mi. NE Patagonia Hwy 83, 1341m, *31°39'39"N, 110°41'21"W*, 9 Aug 1982 [2♂, CNC: 00321026–27]; Santa Cruz Co., Canelo, 1525m, *31°32'34"N, 110°30'52"W*, 10 Jul 1957, G.D. Butler [8♂ 4♀, UAIC: 00326477–79, 00326484, 00326486–88, 00326493, 00326495–96, 00326510, UCRC: 00322692]; Canelo, 1525m, *31°32'34"N, 110°30'52"W*, 14 Jul 1957, G.D. Butler [1♀, UAIC: 00326482]; Canelo, 1525m, *31°32'34"N, 110°30'52"W*, 18 May 1957, G.D. Butler [5♂ 2♀, UAIC: 00280013, 00326474, 00326483, 00326498–99, 00326503]; Canelo, 1525m, *31°32'34"N, 110°30'52"W*, 19 Jul 1958, M.S. Adachi [3♂ 3♀, UAIC: 00326491–92, 00326497, 00326502, 00326504, 00326507]; Canelo, 1525m, *31°32'34"N, 110°30'52"W*, 20 Jul 1958, M.S. Adachi [1♂, UAIC: 00326506]; Canelo, 1525m, *31°32'34"N, 110°30'52"W*, 21 Jun 1958, G.D. Butler [1♂ 4♀, UAIC: 00326475–76, 00326480–81, 00326509]; Canelo, 1525m, *31°32'34"N, 110°30'52"W*, 3 Aug 1956, G.D. Butler [1♂ 2♀, UAIC: 00326485, 00326489, 00326494]; Canelo, 1526m, *31°32'34"N, 110°30'52"W*, 10 Jul 1957, G.D. Butler [1♀, UCRC: 00320434]; Gardner Cny. 4.0 mi. N Sonoita, 4800m, *31°47'25"N, 110°35'22"W*, 10 Aug 1982, G. Gibson [10♂ 15♀, CNC: 00321025, 00321028–36, UCRC: 00320363–67, 00320369, 00320375–80, 00320383, 00320385, 00320400]; Harshaw, 4 mi. SE Patagonia, 1186m, *31°30'20"N, 110°48'26"W*, 5 Aug 1996, M. Gates, swp [1♀, UCRC: 00320382]; Harshaw Cr., ~4 mi SE Patagonia, 1296m, *31°31'23"N, 110°42'21"W*, 5 Aug 1996, M. Gates, swp [2♂, UCRC: 00408515–16]; Patagonia, 10 mi. S, 1195m, *31°25'34"N, 110°50'39"W*, 16 Jul 1950, F.G. Werner & G.D. Butler, *Chilopsis linearis* [2♀, UAIC: 00326472–73]; **California:** Riverside Co., Andreas Canyon nr Palm Springs, 183m, *33°55'43"N, 116°32'13"W*, 13 Oct 1983, N.J.

Smith [3♀, UCDC: 00280020, 00280023, 00280025]; Andreas Canyon, Palm Springs, 183m, *33°55'43"N, 116°32'13"W*, 25 Apr 1982, N.J. Smith [3♀, UCDC: 00280024, 00280026–27]; Chino Cyn., 526m, *33°50'41"N, 116°35'38"W,* 24 Apr 1978, J.B. Johnson, *Sarcostemma* [5♂, CNC: 00320672, UCRC: 00320453, WFBM: 00306537–39]; Deep Canyon, 242m, *33°38'57"N, 116°22'38"W*, 8 Oct 1977, N.J. Smith [1♂ 9♀, UCDC: 00280011–12, 00280014–19, 00280021–22]; Hwy 74 W of Palm Desert, 672m, 33°38'45"N, 116°24'29"W, 9 May 2007, J. Heraty, desert scrub, swp [1♂, UCRC: 00400701]; Whitewater Cyn, 573m, 33°57'51"N, 116°39'04"W, 13 Apr 2013, ENTM 109, *Chilopsis linearis*, swp [1♀, UCRC: 00352457]; Whitewater Cyn. Cmpgrd., 33°57'29"N, 116°38'49"W, 4 May 2014, A. Baker, swp desert willow [1♂, UCRC: 00437129]; Whitewater Cyn. Cmpgrd., 33°57'29"N, 116°38'49"W, 4 May 2014, A. Baker, swp desert willow, 9pm [1♀, UCRC: 00437128]; San Bernardino Co., Granite Cove, 1310m, 34°46'53"N, 115°39'13"W, 11 May 2013, J. Heraty, Mojave desert, swp [1♂ 1♀, UCRC: 00352463–64]; Granite Mountain, 1310m, 34°46'53"N, 115°39'13"W, 11 May 2013, J. Herreid, *Chilopsis* [1♂ 1♀, UCRC: 00411448, 00411450]; **New Mexico:** Dona Ana, Las Cruces, 1200m, *32°19'12"N, 106°45'49"W,* 2 Jun 1965, R.B. Bohart, Orchidaceous legume tree [2♀, UCDC: 00280007–08]; Hidalgo Co., 12 mi. W Animas, 1239m, *31°55'34"N, 109°00'24"W,* 6 Jul 1963, J.G. Rozen, D.K. Oliver, A.R. Moldenke, J.A. Woods [7♀, AMNH: 00237901–02, 00237904, FSCA: 00318604–05, UCDC: 00280006, UCRC: 00237903]; 14.9 km W Animas, 1326m, *31°56'13"N, 108°57'10"W*, 26–30 Jul 1982, G. Gibson [1♂, CNC: 00320663]; 9.3 mi W Animas, 1308m, 31°56'14"N, 108°56'45"W, 26–30 Jul 1982, G. Gibson [48♂ 112♀, CNC:

00320391, 00321016, 00321038–102, 00321105–06, 00321108, 00321110, 00321113–15, 00321117–18, 00321120–38, 00321140–41, UCRC: 00320388–90, 00320392–93, 00320395–99, 00320401–28, 00320430–32, 00320435, 00320437–39, 00320441–43, 00320445, 00320447–49, 00320451–52, 00321103–04, 00321109, 00321111–12, 00321116, UCRENT00001421–22]; Rodeo, 1255m, *31°50'39"N*, *109°01'40"W*, 18 Jun 1989, R.M. Bohart [2♂, UCDC: 00280010, UCLA: 00313804]; **Texas:** Brewster Co., Big Bend Nat'l Pk, Glenspring Pond (Glenn Springs) in 0.5 mi., 3000m, *29°12'60"N*, *103°15'59"W*, 9 Jul 1982, G. Gibson [1♂ 2♀, CNC: 00320660, 00320671, 00321139]; Big Bend Nat. Pk., 5.3 mi. W Panther Jct, 3900m, *29°12'60"N*, *103°15'59"W*, 29 Jun 1982, G. Gibson [1♂, UCRC: 00320440]; Big Bend Nat'l Pk 10.5 mi. NE Castalon, 3300m, *29°12'60"N*, *103°15'59"W*, 14 Jul 1982, G. Gibson [3♂ 3♀, CNC: 00320657, 00320662, 00320665, 00320669, 00321119, 00320429]; Big Bend Nat'l Pk 10.7 mi. W Panther Jct., 3650m, *30°01'20"N*, *103°46'29"W*, 28 Jun 1982, G. Gibson [5♂ 3♀, CNC: 00320658, 00320661, 00320666, 00320670, UCRC: 00320436, 00320444, 00320446, 00320450]; Glasscock Co., 9 mi. SE Stanton, 755m, *32°10'54"N*, *101°38'51"W*, 28 May 1973, Gaumer and Clark [1♀, TAMU: 00426704]. **Planidia Slides: USA: Arizona:** Cochise Co., nr Portal on San Simeon Rd, *31°56'16"N*, *109°08'09"W*, 2 Aug 2003, J. Heraty, *Chilopsis linearis* [5, UCRC: 00436228– 32].

2.4.4.6 *Orasema zahni* **sp. nov.**

(Figs 13, 14, 16, 35–37, 40, 61, 65, 66, 69)

Diagnosis. This species most closely resembles *O. simulatrix*, but can be recognized by the presence of a marginal wing fringe (Fig. 40). It is recognized from other species in the *simulatrix*-group by the following combination of characters: first funicular roughly equal to length of pedicel (Fig. 16); clypeus reticulate with straight lateral margin (Fig. 13); axillula reticulate (Fig. 36); acropleural sulcus not evenly reticulate (Fig. 35); distinct and crenulate frenal line (Fig. 36); acrosternite of female rounded in ventral view (Fig. 14).

Female. Length 2.6–3.2 mm. Body and coxae bluish green, dark green or black with metallic green and purple, gaster dark brown to black; pedicle and anellus yellowish brown; flagellum brown; mandibles yellow to light brown with dark outline; maxilla and labrum yellowish brown; femora slightly infuscate to dark brown basally; tibia and tarsi yellowish brown.

Head (Fig. 13), HDW:HDH 1.1–1.2. Face reticulate; lacks longitudinal groove; scrobal impression with similar sculpture to face. IOD:EYH 1.4–1.7. Malar space distinctly impressed between mouth and eye margin; GNL:EYH 0.7–0.8. Clypeus glabrate or weakly reticulate; epistomal sulcus strongly impressed; ventral margin of clypeus straight; supraclypeal area sculptured similarly to clypeus with weak striations, longer than broad and about equal length to clypeus.

Antenna with scape reaching 0.8X distance to median ocellus; anellus stout, close to twice as broad as long; FLG:HDH 0.7–0.8; F2L:F2W 1.0–1.3; F2L:F3L 1.2–1.4; following flagellomeres subequal in length, equal in width.

Mesosoma (Figs 35–37) with mid and lateral lobes reticulate with few fine rugose-areolate sections; axilla sculpture similar to the mesosoma, reticulate with some rugose-areolate; posterior margin of axilla abrupt, scutellar disc below dorsal margin of axilla (Fig. 35). Notauli moderately to deeply impressed and foveate. Scutellar disc reticulate with a rugose-areolate overlay and about 1.5X longer than broad, separated medially from TSA by a broadly impressed foveate channel (Fig. 36); frenal line a distinct crenulate groove, frenum with similar sculpture to scutellar disc; axillula with similar sculpture to scutellar disc, reticulate with a rugose-areolate overlay. Propodeal disc laterally reticulate-areolate, with rugose-areolate median carina (Fig. 37); callus rugulose to reticulate; metapleuron rugulose to reticulate. Upper mesepimeron reticulate. Lower mesepimeron rugose-areolate. Transepimeral sulcus weakly impressed. Femoral groove finely reticulate and broadly impressed; mesepisternum rugose. Prepectus reticulate or weakly rugulose. Hind coxa reticulate dorsally and smoother ventrally.

Forewing (Fig. 40), FWL:FWW 2.2–2.6; FWL:ML 2.1–2.4; costal cell with 5-10 setae, wing disc setose; marginal fringe present (Fig. 40); stigmal vein 2.0–2.5X as long as broad; postmarginal vein slightly longer than stigmal vein.

Metasoma with petiole 0.8–1.2X as long as hind coxa, 1.4–2.1X as long as broad and reticulate or weakly rugose; acrosternite semicircular in ventral view (Fig. 14).

Male. Length, 2.1–2.7 mm. Similar to female except for the following: femora sometimes infuscate but usually mostly all dark brown with metallic reflections basally; FLG:HDH 0.8–0.9; scape light to dark brown; F2L:F2W 0.6–0.8; metasoma with petiole 2.4–2.8X as long as hind coxa; petiole 5.1–7.9X as long as broad.

Oviposition Behavior and Immature Stages. *Orasema zahni* oviposits in straight lines on the ventral surface of leaves of *Prosopis glandulosa* and *Prosopis velutina* (Figs 65, 66). As many as six *O. zahni* oviposition punctures have been observed on a single leaf of *Prosopis*. The EFNs of *P. velutina* have a different location than *P. glandulosa* and are always found at the base of the pinnae and usually not at the base of the leaflets. Oviposition punctures seem to correlate with this difference in EFN location and on *P. velutina*, punctures are only found on the basal leaves close to where the EFNs are found.

Planidia of *O. zahni* are 0.18–0.21 mm in length and are identical to the *simulatrix*-group description. These planidia have been found within and near EFNs of *Prosopis* (Fig. 61). Their ant host is unknown.

Distribution. USA: Arizona, New Mexico, Texas (Fig. 69: black square). Collecting habitats are arid regions with *Prosopis* present. Localities are found in or near to the Sonoran and Chihuahuan deserts.

Etymology. Named after Levi Zahn.

Holotype: USA: Arizona: Cochise Co., Hwy 181, 1440m, 31°52'34"N, 109°31'33"W, 27 Jun 2014, J. Herreid, *Prosopis*, swp [1♀, UCRC: 00411581]. **Paratypes: USA:**

Arizona: Cochise Co., 1.0 mi. E Portal, 1432m, *31°54'49"N, 109°08'29"W*, 31 Jul 1982, G. Gibson [1♀, UCRC: 00320381]; Chiricahua Mtns, 2.4 mi. E Paradise, 1633m, *31°54'48"N, 109°14'24"W*, 14 Aug 1982, G. Gibson [3♂, CNC: 00320664, 00320667, 00320668]; Hwy 181, 1440m, 31°52'34"N, 109°31'33"W, 27 Jun 2014, J. Herreid, *Prosopis*, swp [1♂, UCRC: 00411574]; Paradise-Portal rd, 1608m, 31°55'56"N, 109°11'09"W, 26 Jun 2014, J. Herreid, *Prosopis*, swp [1♂, UCRC: 00411582]; Paradise-Portal rd, 1643m, 31°55'55"N, 109°11'17"W, 25 Jun 2014, K. Dominguez, *Prosopis*, swp [1♀, UCRC: 00411595]; Pima Co., Canoa, 943m, *31°47'19"N, 111°01'06"W*, 21 Jun 1960, G. Butler, alfalfa [1♀, UAIC: 00326512]; Continental, 869m, *31°51'03"N, 110°58'58"W*, 1 Jul 1960, G. Butler, suck/cotton [2♀, UAIC: 00326508, 00326520]; Sta Rita Destr. Site, 917m, *31°51'03"N, 110°58'58"W*, 12 Aug 1970 [1♀, UAIC: 00326500]; Sta Rita, Destr. Site, 917m, *31°51'03"N, 110°58'58"W*, 8 Jul 1970 [1♂, UAIC: 00326514]; Sta, Rita Destr. Site, 917m, *31°51'03"N, 110°58'58"W*, 12 Aug 1970 [3♀, UAIC: 00326518, 00326521, 00326523]; Sta. Rita Destr. Site, 917m, *31°51'03"N, 110°58'58"W*, 31 Jul 1970 [1♀, UAIC: 00326490]; Las Cienegas NCA, 1387m, 31°46'21"N, 110°37'55"W, 1 Jul 2014, J. Herreid, Mesquite tree, swp [1♀, UCRC: 00411578]; Las Cienegas NCA, 1387m, 31°46'21"N, 110°37'55"W, 2 Jul 2014, J. Herreid, Mesquite tree, swp [1♂, UCRC: 00411594]; Sahuarita, 825m, *31°57'26"n, 110°57'20"W*, 15 Jun 1957, G.T. Butler & F. Werner, swp, mesquite [1♀, UAIC: 00326516]; Santa Rita Rng. Res., 917m, *31°51'03"N, 110°58'58"W*, 23 May 1957, G. Butler, F. Werner, mesquite, swp [1♂, UAIC: 00326513]; Sycamore Canyon Rd., 31°23'22"N, 111°07'09"W, 29 Aug 2013, J. Herreid, mesquite, swp [1♂ 1♀, UCRC:

00411557–58]; Santa Cruz Co., Casa Blanca Canyon, 1447m, 31°38'57.4"N, 110°45'28.6"W, 14 Aug 2014, J. Heraty, mesquite, swp [1♂ 1♀, UCRC: 00412578, 00412580]; Harshaw Rd at 812, 1513m, 31°27'54"N, 110°43'10.6"W, 13 Aug 2014, J. Heraty, *Baccharis*, swp [1♀, UCRC: 00412579]; Nogales, 1170m, *31°20'25"N, 110°56'03"W*, 24 Aug 1939, R.H. Crandall [1♂ 1♀, UAIC: 00326505, 00326515]; Patagonia, 1237m, *31°32'22"N, 110°45'22"W,* 27 Jun 1961, P.H. Johnson[1♂, UAIC: 00326511]; Santa Rita Mtns., Josephine Cyn., 1650m, *31°49'33"N, 110°46'29"W*, 22 Jul 1990, R.K. Velten [1♂, UAIC: 00326522]; Tumacacori, 1000m, *31°34'07"N, 111°03'06"W*, 27 Aug 1975, C. Cinelly [1♀, UAIC: 00326519]; Yavapai Co., Skull Valley, 1300m, *34°30'19"N, 112°41'07"W*, 11 Aug 1967, D.A. Young [1♂, UCRC: 00322713]; Yuma Co., Colorado River at Parker, 126m, *34°09'00"N, 114°17'20"W*, C.A. Tosohi [1♀, UCRC: 00322718]; **New Mexico:** Lea Co., Site 14, 1189m, 32°22'08"N, 103°43'18"W, 14 Jun 1979, D.R. Delorme and H.L. Carrola, taken from *Prosopis glandulosa* Torr. [1♂, UCRC: 00320358]; Lincoln Co., 5 mi. N Angus Hwy 37, 2148m, *33°28'60"N, 105°43'27"W*, 8 Aug 1965, H.B. Leech [1♂, CASC: 00322704]; **Texas:** Culberson Co., McKittrick Canyon, 1584m, *31°58'45"N, 104°45'17"W,* 17 Aug 1961, F. & N. Gehlbach [1♀, UCRC: 00322719]. **Additional Material Examined: Planidia Slides: USA: Arizona:** Pima Co., Las Cienegas NCA, 1387m, 31°46'21"N, 110°37'55"W, 2 Jul 2014, J. Herreid, Mesquite tree, sweep [6, UCRC: 00447242–45, 00447318–19].

2.4.5 *Orasema wayqecha*-group

Diagnosis. Recognized from all other *Orasema* by the following combination of character states: postgena expanded and covering maxillary complex (Fig. 5); labrum with 7–10 segments (Fig. 6); face mostly smooth and shining with sparse setae, frons weakly reticulate or with weak vertical striae (Figs 47, 48); Forewing infuscate along impression of cubital vein distal to basal vein (Figs 49–52) and with or without dark brown spots, if present: one basal spot at base of marginal vein, one large apical spot distal to stigmal vein and trailing postmarginal vein (poststigmal spot), and a small third spot below the poststigmal spot spot and close to the posterior wing margin. Additional descriptive features include occiput strigate, with dorsal margin abrupt, slightly rounded and lacking full carina; eye bare and slightly protruding; face relatively flat; palpal formula 3-3 (Fig. 7); flagellum with 8 funiculars and 2 segmented clava; scape yellow; pedicel globose, broader than F2; clypeus glabrous, longer than broad, about 1.2X as long as clypeus; notali deeply impressed with many carina; mesepisternum ventral suface straight; posterior carina prominent; prepectus triangular in dorsal half, strongly narrowed ventrally; Forewings elongate and rounded with marginal wing fringe complete and easily visible; wing disc and costal cell completely and densely pilose with long postmarginal vein (Figs 52–55); stigmal vein 2.0–2.5X as long as broad, slightly angled distally; legs yellow; petiole cylindrical; acrosternite rounded in ventral view and shallowly crenulate, sometimes almost without sculpture.

Biology. The plant and ant host are known only for *O. wayqecha*. This species oviposits into two species of *Myrsine* (Primulaceae) on leaf surfaces with EFNs (Fig. 67). Planidia are often found near EFNs (Fig. 62). The planidia possess caudal cerci that are flexible and long, exceeding the apical 7 tergites in length. This species was found to parasitize *Pheidole* sp.. More detailed biology, host information and a description of the immatures for *O. wayqecha* will be described herein.

Distribution. Colombia, Peru (Fig. 71).

2.4.6 Species descriptions

2.4.6.1 *Orasema wayqecha* sp. nov.

(Figs 5–7 42–44, 46, 47, 49–50, 53, 55–59, 62, 67, 71)

Diagnosis. Differentiated from *O. quadrimaculata* by the following combination of characters: scutellar disk elongate, 1.5–2X longer than broad (Fig. 44); lack of male wing spots (Fig. 50); stigmal spot does not extend to the wing apex in females (Fig.49); vertical striae lateral to the eyes often strongly impressed (Fig. 47); labrum 7–8 digitate (Fig. 6); female femoral groove rugose-areolate (Fig. 43).

Female. Length, 3.2–3.7 mm. Head and mesosoma black, mesosoma with purplish reflections ventrally and bluish–green dorsally, coxae and petiole dark brown to black, apex of coxae yellowish brown; gaster dark brown to black, with faint bluish reflections; pedicel and anellus yellow.

Head (Fig. 47), HDW:HDH 1.2–1.3. Scrobal depression finely and irregularly sculptured medially, with two weak parallel channels and single fovea just above toruli; vertex almost completely smooth, ocellar triangle rugose; dorsal margin of occiput abrupt with single weak carina just behind lateral ocelli, occiput weakly strigate just below carina. IOD:EYH 1.7–1.8, GNL:EYH 0.9–1.0. Labrum with 8 digits.

Antenna with scape reaching to median ocellus; FLG:HDL 1.9–2.1; F2L:F2W 2.9–3.6, F2L:F3L 1.3–1.5; following flagellomeres equal in width and subequal in length.

Mesosoma (Figs 43, 44) with mid lobe coarse rugose-areolate, interstices sharp and broadly spaced, surface weakly verrucose; lateral lobe glabrate to transversely strigate, strongly swollen; axilla rugose-areolate, interstices narrow, posterior margin broadly rounded; scutellar disc sculptured as on mid lobe, areolate deeper posteriorly, closely spaced anteriorly, disc longer than broad (Fig. 44). Frenal area with similar sculpture to scutellar disc; axillula with similar sculpture to scutellar disc, obliquely carinate ventrally. Propodeal disc with median depression or carina lacking; callus fairly smooth and swollen with some setae; metepimeron mostly smooth. Lower mesepimeron weakly rugulose; transepimeral sulcus distinct; mesepisternum rugose-areolate. Prepectus posterior and dorsal margins swollen and weakly rugulose (Fig. 43). Proepisternum swollen, imbricate. Hind coxa weakly reticulate, with few transverse striae.

Forewing (Fig. 49) FWL:FWW 2.5–2.6; FWL:ML 3.1–4.1; postmarginal vein elongate, reaching 0.4 X distance to apex. Stigmal wing spot not extending to the apex of wing.

Metasoma with petiole 1.6–1.8X as long as hind coxa, 4.4–5.8X as long as broad and irregularly reticulate with weak longitudinal carinae basally. Hypopygium with single short hair on each side of midline apically. Ovipositor slightly curved cephalad; first valvula with subapical ridge, lateral line with 9 small narrowly spaced teeth; second valvula with 8–10 lateral teeth, broadly separated, weakly coalescing dorsally (Fig. 46).

Male. Length, 3.3–3.8 mm. Similar to female except for the following: wings spots absent but still infuscate along impression of cubital vein, distal to basal vein; labrum with 7–8 digits; scape reaching median ocellus; F1 broader than pedicel; prepectus weak reticulate; FLG:HDH 2.9–3.3; F2L:F2W 3.3–3.7; metasoma with petiole 1.9–2.7X as long as hind coxa, 6.9–9.1X as long as broad.

Oviposition Behavior and Immature Stages. *Orasema wayqecha* has been observed to oviposit near EFNs of two species of *Myrsine* (Primulaceae). On one species, as many as 80 eggs have been observed to be deposited in straight lines on the ventral surface of the leaves, on the other species of *Myrsine* over two hundred oviposition punctures have been recorded on a the ventral surface of a leaf. EFNs are on the dorsal plant surface at the base of the leaves, near the stems (Fig. 67). Planidia were observed congregating near the base of the leaves in close association to the EFNs (Fig. 62). *Orasema wayqecha* pupa and larvae (Figs 55–59) have been located in nests of *Pheidole* sp.. Nests of this ant were often located at the base of a *Myrsine* with oviposition punctures of *O. wayqecha*.

Planidium (Fig. 53): length 0.19–0.22 mm. Antenna, labial plates and tergopleural line are absent. Tergites I and II (TI, TII) separate. TI, TII, TIII with dorsal seta. TII, TVI with

very short lateral seta. TI, TIII, TV, TVII with ventral seta. TIX emarginate. Caudal pad present; caudal cerci present and long, about as long as apical 7–8 tergites. More developed first instars were found on ant larva (Figs 55, 56). Second Instar (Fig. 57): length 1.4 mm. Body white and smooth with no evident spiracles or mandibles. Prepupal stage (Fig. 58). Pupa (Fig. 59): length 4.1–4.4mm (n=2); recognized by: lateral swelling by mesothoracic spiracle; three pronounced tubercles over petiole; petiolar region relatively elongate and narrow; prominent transverse ridges on abdomen.

Distribution. Peru: Cuzco-Cosñipata Valley (Fig. 71: black circle). Specimens have been collected at elevations of 1700–2866 m and egg punctures have been observed up to 3400m in montane cloud forest.

Etymology. Named after the Wayqecha Biological Station where this species was first collected.

Holotype: Peru: Cuzco: Wayqecha Biological Station, Perdiz trail, 2866m, 13°10'38.1"S, 71°35'03.7"W, 28 Jul 2014, J. Heraty, cloud forest, swp [1♀, UCRC: 00412673]. **Paratypes: Peru: Cuzco:** Wayqecha Biological Station, Perdiz trail, 2866m, 13°10'38.1"S, 71°35'03.7"W, 28 Jul 2014, J. Heraty, cloudforest, swp [1♂ 2♀, UCRC: 00412571–73]; Santa Isabel, River Ceosnipata [Cosñipata], 660m, 13°00'00"S, 71°18'00"W, 9 Dec 1951, Woytkowski, rain forest [4♀, AEIC: 00415028–31]; Santa Isabel, Valle Cosñipata, 1600m, *13°00'00"S, 71°18'00"W,* Mar 1951, F. Woytkowski, forest [1♀, AEIC: 00415032]; Wayqecha, 2820m, 13°10'22"S, 71°35'30"W, 30 Nov 2011, J.M. Heraty, cloud forest, swp [1♂ 1♀, UCRC: 00352383–84]; Wayqecha, Oso

trail, 2600m, 13°10'12"S, 71°35'01"W, 3 Dec 2011, J.M. Heraty, montane forest, afternoon, swp [2♂ 1♀, UCRC: 00414009, 00414017–18]; Wayqecha, Oso trail, 2725m, 13°10'48"S, 71°34'55"W, 1 Dec 2011, J.M. Heraty, cloud forest, swp [3♂, UCRC: 00414014–16]; Wayqecha, Perdiz trail, 2865m, 13°10'38"S, 71°35'02"W, 2 Dec 2011, J.M. Heraty, cloud forest, afternoon, yellow pan trap [1♀, UCRC: 00414008]; Wayqecha, Perdiz trail, 2865m, 13°10'38"S, 71°35'02"W, 2 Dec 2011, J.M. Heraty, cloud forest, morning, yellow pan trap [3♂ 3♀, UCRC: 00333659, 00414003–05, 00414010–11]; Wayqecha, Shefflera trail, 2877m, 13°10'24"S, 71°35'23"W, 2 Dec 2011, J.M. Heraty, cloud forest, afternoon, yellow pan trap [1♂, UCRC: 00414019]; Wayqecha, Zorro trail, 2821m, 13°10'22"S, 71°35'32"W, 5 Dec 2011, J.M. Heraty, montane forest, swp [2♂ 2♀, UCRC: 00414006–07, 00414012–13]; Valle del Rio Cosñipata, Haciende Santa Isabel, 1700m, *13°00'00"S, 71°18'00"W*, 16 Jan 1952, F. Woytkowski [1♀, IMLA: 00313158]; Valle del Rio Cosñipata, Haciende Santa Isabel, 1700m, *13°00'00"S, 71°18'00"W*, 2 Jan 1952, F. Woytkowski [1♀, IMLA: 00274418]; Valle del Rio Cosñipata, Haciende Santa Isabel, 1700m, *13°00'00"S, 71°18'00"W*, 31 Dec 1951, F. Woytkowski [1♀, IMLA: 00313159]; Valle del Rio Cosñipata, Haciende Santa Isabel, 1700m, *13°00'00"S, 71°18'00"W*, 4 Jan 1952, F. Woytkowski [2♀, IMLA: 00313156–57]. **Other Material Examined: Planidia Slides: Peru: Cuzco Prov.:** Wayqecha, Perdiz trail, 2865m, 13°10'38"S, 71°35'02"W, 2 Dec 2011, J.M. Heraty, cloud forest [6, UCRC:00412500–05]; **Immature Stages:** Wayqecha Biological Station, 2866m, 13°10'38.1"S, 71°35'03.7"W, 26 Jul 2014, J. Heraty, J. Herreid & J. Mottern, in loose soil [5, UCRC:00447246–50].

2.4.6.2 *Orasema quadrimaculata* sp. nov.

(Figs 45, 48, 51, 52, 71)

Diagnosis. Differentiated from *O. wayqecha* by the following combination of characters: scutellar disk roughly as long as broad (Fig. 45); both males and females have wing spots; stigmal spot extends to wing apex (Figs 51, 52); face smooth with weak rugose sculpture lateral to the eye (Fig. 48); labrum 9–10 digitate; four maculate spots on forewing in males and females (Figs. 51, 52); female meseptisternum rugose-areolate with parallel carinae.

Female. Length, 4 mm (n=1). Head and body bluish green, mesosoma darker green dorsally with weak reddish reflections, forecoxa almost entirely yellowish brown, apex of mid and hind coxae yellowish brown; gaster dark brown to black, with purplish reflections; pedicel and anellus brown.

Head (Fig. 48), HDW:HDH 1.2 (n=1). Scrobal depression finely and irregularly sculptured medially, but smooth laterally; vertex smooth; dorsal occipital margin abrupt with weak carina just behind lateral ocelli, carina partially obscured by other fine carinae. IOD:EYH 1.9 (n=1). GNL:EYH 1.1(n=1). Labrum with 10 digits.

Antenna with scape reaching 0.8 X distance to median ocellus; FLG:HDL 2.4 (n=1); F2L:F2W 3.8 (n=1), F2L:F3L 1.7 (n=1); following flagellomeres equal in width and subequal in length.

Mesosoma (Fig. 45) with mid lobe coarse rugose-areolate, with weak verrucose surface sculpture; lateral lobe with similar sculpture, broadly rounded; axilla with similar sculpture to lateral lobe, posterior margin abrupt; scutellar disc coarse rugose-areolate, interstices broadly spaced, disc about equal length to width. Frenal area and axillula with similar sculpture to scutellar disc. Propodeal disc with weak median longitudinal carina; callus rugose-areolate, with patch of dense hairs; metepimeron rugose. Lower mesepimeron rugose; transepimeral sulcus weakly impressed; mesepisternum rugose-areolate, interstices closely spaced with parallel carinae. Prepectus reticulate, posterior and dorsal margins swollen and glabrate. Proepisternum swollen, smooth. Hind coxa weakly reticulate.

Forewing (Fig. 51) FWL:FWW 3.2 (n=1); FWL:ML 3.6 (n=1); postmarginal vein elongate, reaching 0.5–0.6 X distance to apex. Stigmal wing spot extends to apex of wing.

Metasoma with petiole 1.6X as long as hind coxa (n=1), 4.4X as long as broad (n=1), longitudinally ribbed, with weak cross carinae. Ovipositor hidden.

Male. Length, 3.6 mm (n=1). Similar to female except for the following: wings spots lighter in colour but basal spot more extensive and continuing along basal vein; labrum with 9 digits; scape reaching median ocellus; F1 broader than pedicel; prepectus weak reticulate; FLG: HDH 2.4 (n=1); F2L:F2W 3.6 (n=1); mesepisternum without parallel carinae; metasoma with petiole 2.3X as long as hind coxa (n=1), 8.7X as long as broad (n=1).

Oviposition Behavior and Immature Stages. Unknown.

Distribution. Colombia: Huila; Putumayo (Fig. 71: black triangle).

Etymology. Refers to four spots on forewing.

Holotype: Colombia: Huila: San Agustin, 1500m, *1°53'00"N, 76°15'58"W*, 8 Nov 1971, M. Cooper [♀, BMNH: 00309625]. **Paratype**: **Putumayo:** Cordillera Portachuelo, 2000mm, *1°07'00"N, 76°52'00"W*, 13 Jun 1974, M. Cooper, cloud forest [1♂, BMNH: 00239423].

2.5 Figures and Tables

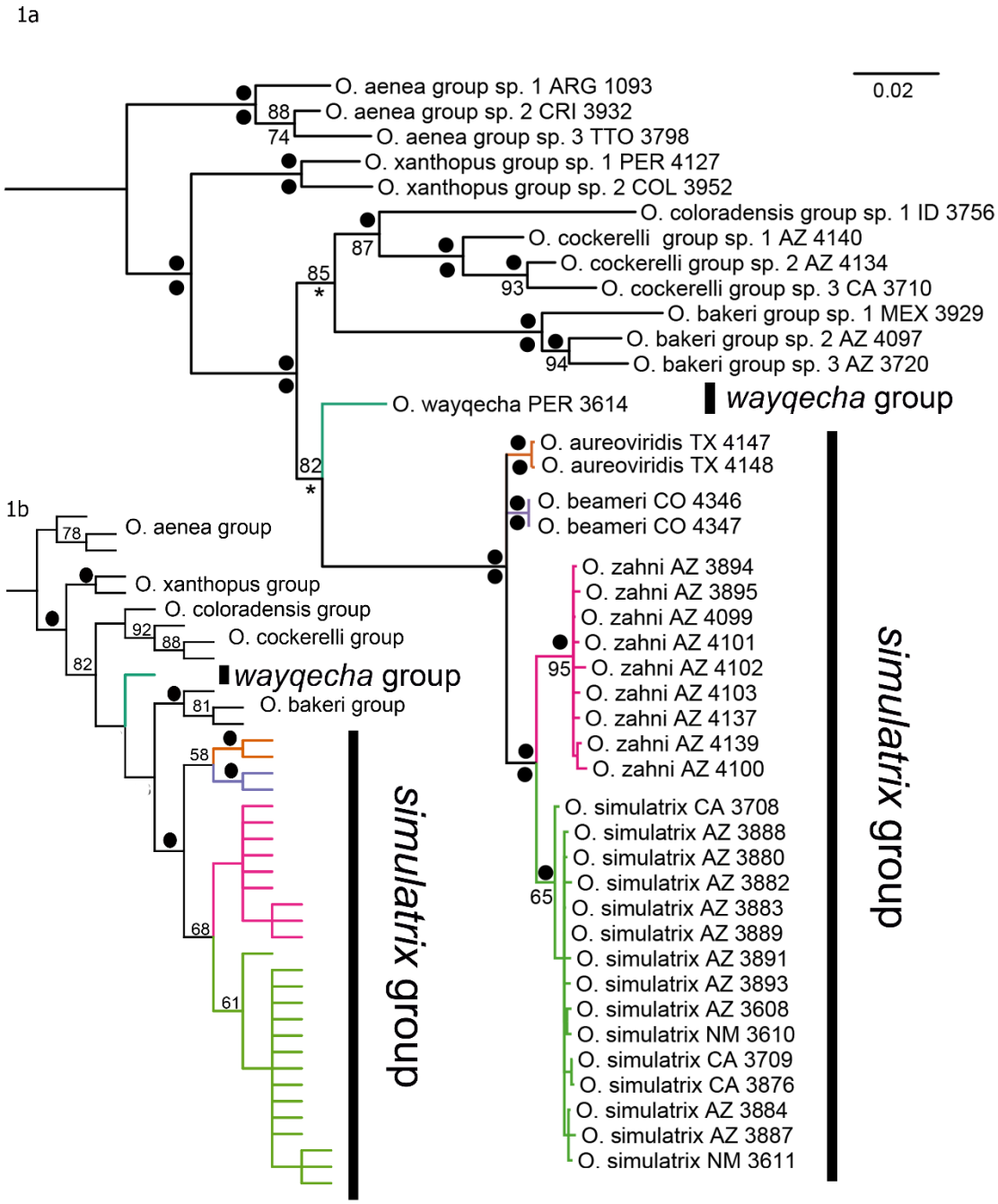

FIG. 1. (a) Maximum Likelihood and Bayesian phylogeny of *simulatrix*- and *wayqecha*-groups. (b) Parsimony strict consensus tree of *simulatrix*- and *wayqecha*-groups. 18S, 28S-D2, 28S-D3–5 and COI gene regions included in all analyses. Bayesian posterior probabilities >50 are placed above nodes of 1a, Maximum Likelihood bootstrap values >50 are shown below the nodes of 1a and, Parsimony bootstrap values >50 are placed above nodes of 1b. Values of 97 or greater are shown with a circle. Asterisk indicates the node was not recovered in Parsimony.

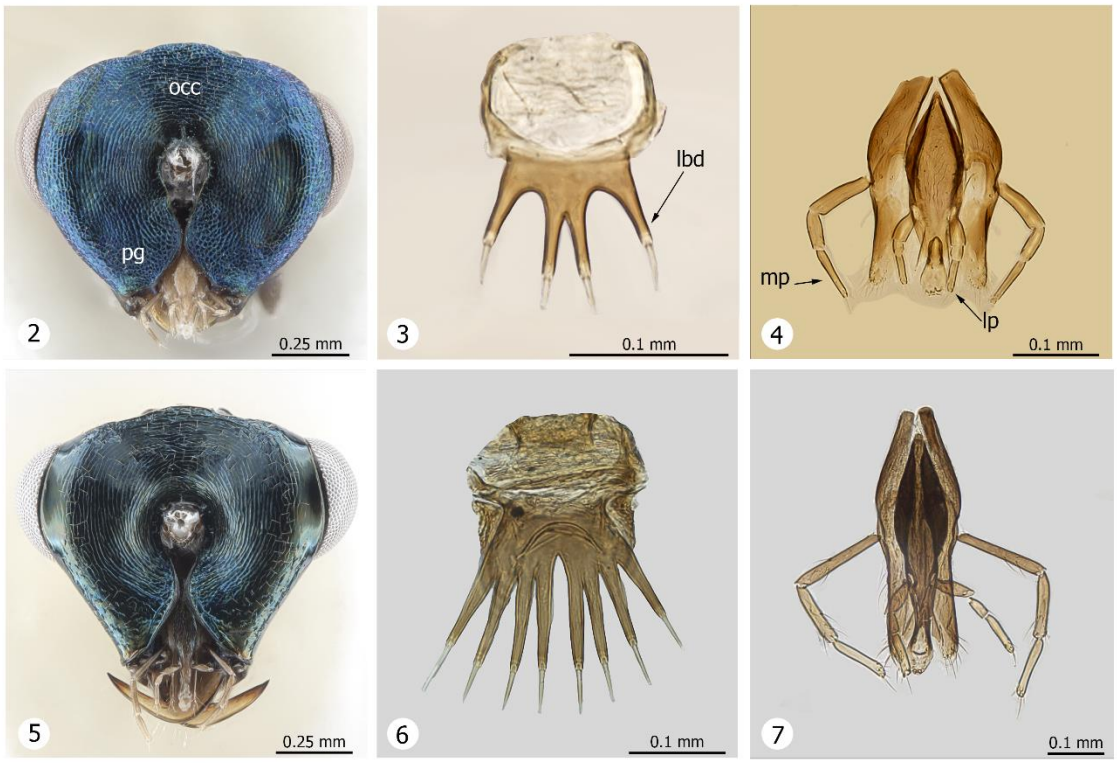

FIGS 2–7. 2–4 *Orasema simulatrix* (female): 2, head (posterior); 3, labrum (anterior); 4, maxillary complex (posterior). 5–7 *Orasema wayqecha* (female): 5, head (posterior); 6, labrum (anterior); 7, maxillary complex (posterior). Abbreviations: occ- occiput; pg- postgena; lbd- labral digit; mp- maxillary palp; lp- labial palp

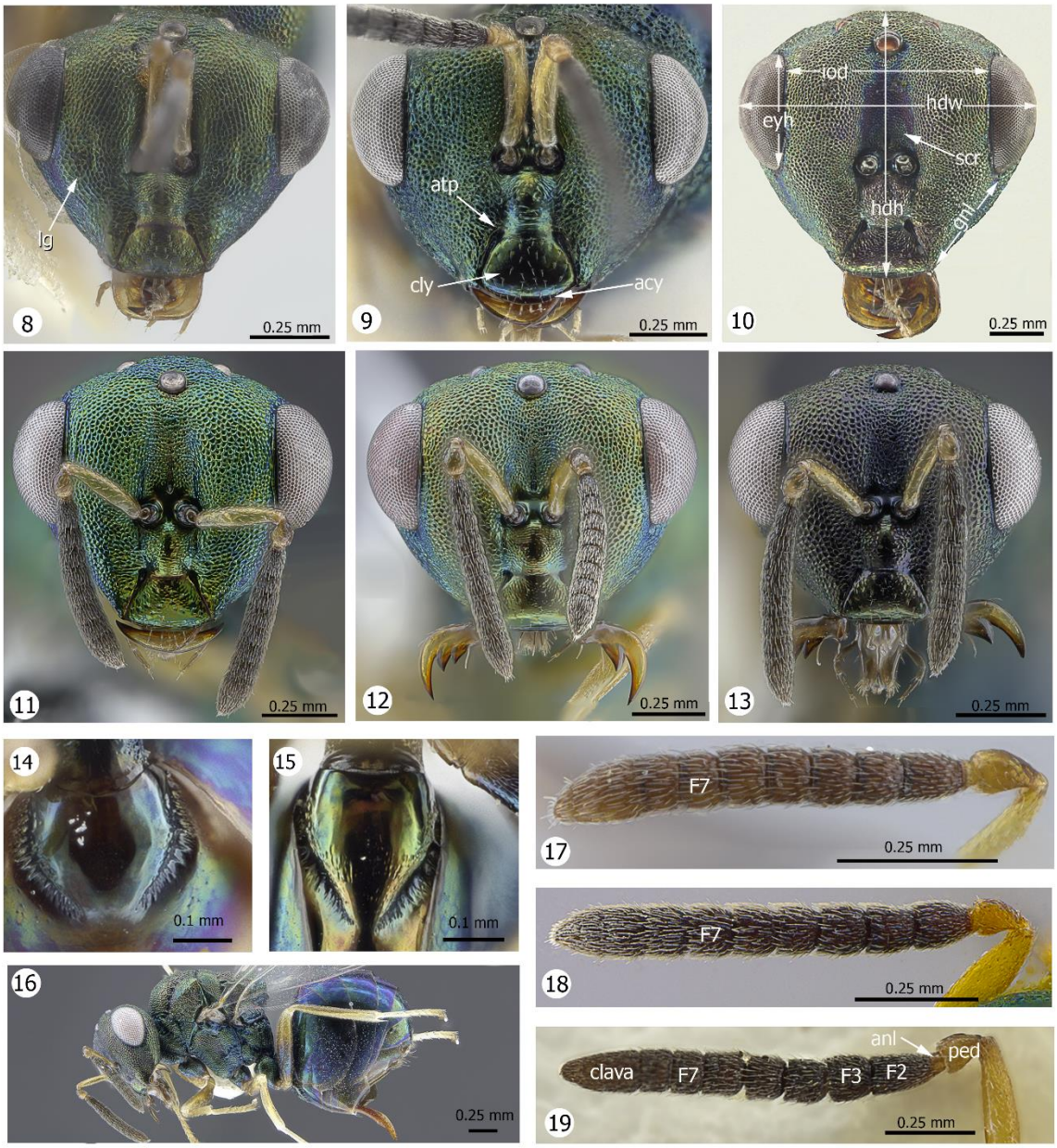

FIGS 8–19. 8, 15, 17 *Orasema beameri*: 8, head (anterior); 15, acrosternite; 17, antenna (lateral). 9, 18 *O. cancellata*: 9, head (anterior); 18, antenna (lateral). 10, 19 *O. difrancoae*: 10, head (anterior); 19, antenna (lateral). 11 *O. aureoviridis*: 11, head (anterior); 12 *O. simulatrix*: 12, head (anterior). 13, 14, 16 *O. zahni*: 13, head (anterior); 14, acrosternite; 16, habitus. Abbreviations: lg-longitudinal groove; atp- anterior tentatorial pit; cly- clypeus; acy- anteclypeus; eyh- eye height; iod- inner ocular distance; hdw- head width; hdh- head height; gnl- gena length; scr- scrobal depression; anl- annelus; ped- pedecile; F2- second flagellomere; F3- third flagellomere

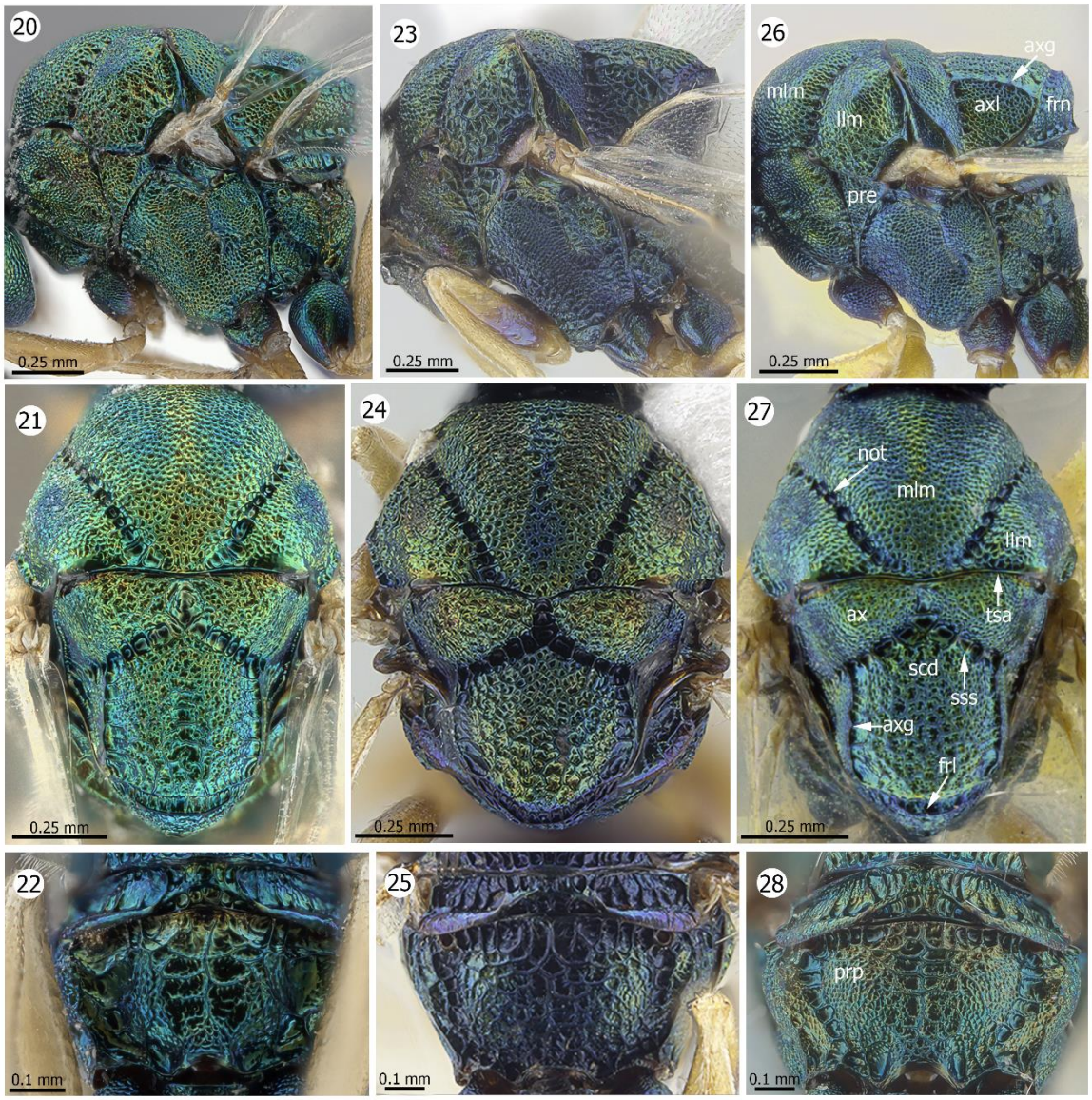

FIGS 20–28. 20–22 *Orasema aureoviridis*: 20, mesosoma (lateral); 21, mesosoma (dorsal); 22, propodeum. 23–25 *O. cancellata*: 23, mesosoma (lateral); 24, mesosoma (dorsal); 25, propodeum.26–28 *O. simulatrix*: 26, mesosoma (lateral); 27, mesosoma (dorsal); 28, propodeum. Abbreviations: pre- prepectus; axl- axillula; axg- axillular groove; frn- frenum; not- notaulus; mlm- midlobe of the mesoscutum; lml- lateral lobe of the mesoscutum; ax- axilla; tsap transscutellar articulation; scd- scutellar disc; sss- scutoscutellar sulcus ; prp- propodeum.

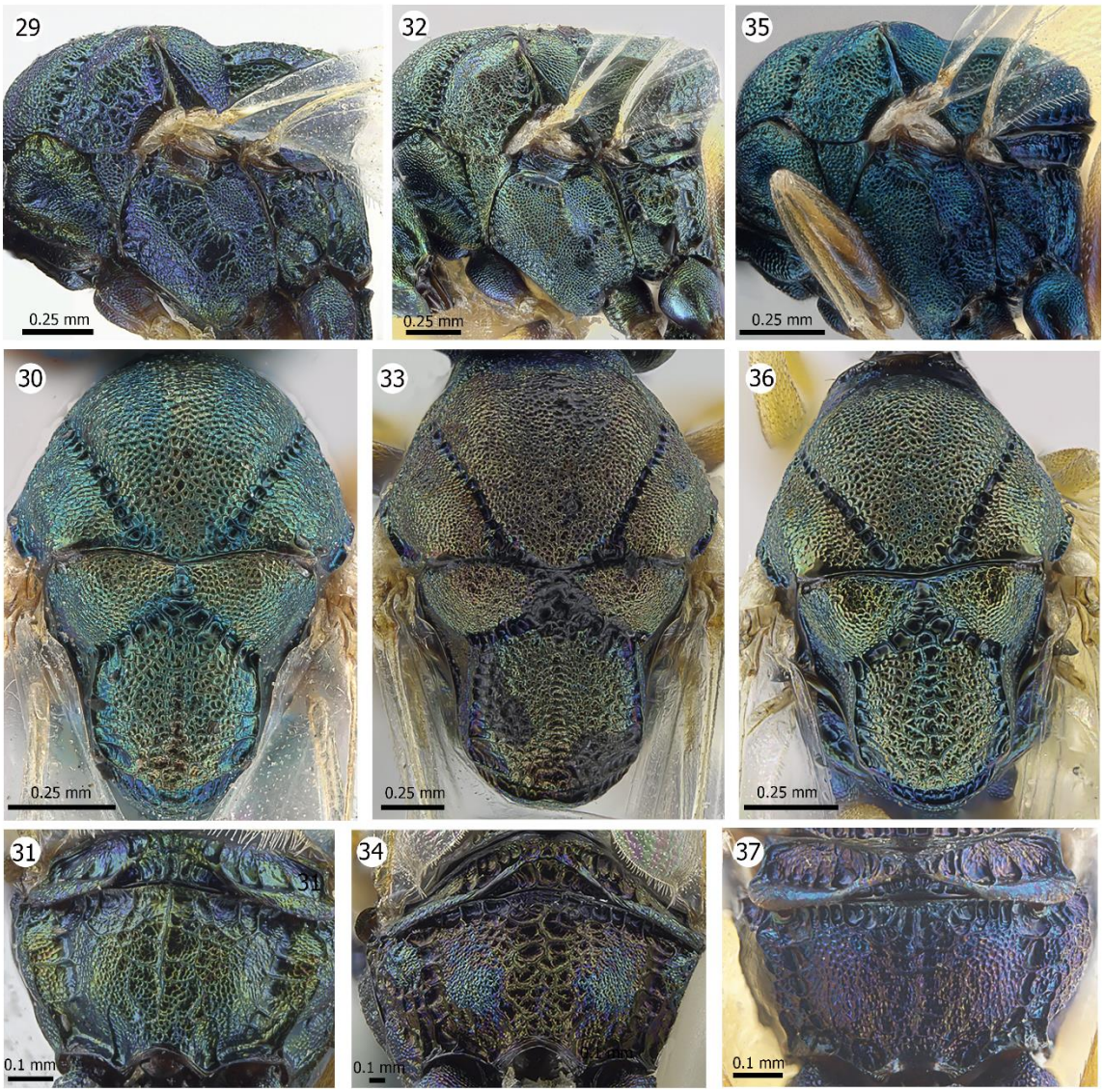

FIGS 29–37. 29–31 *Orasema beameri*: 29, mesosoma (lateral); 20, mesosoma (dorsal); 31, propodeum. 32–34 *O. difrancoae*: 32, mesosoma (lateral); 33, mesosoma (dorsal); 34, propodeum. 35–37 *O. zahni*: 35, mesosoma (lateral); 36, mesosoma (dorsal); 37, propodeum.

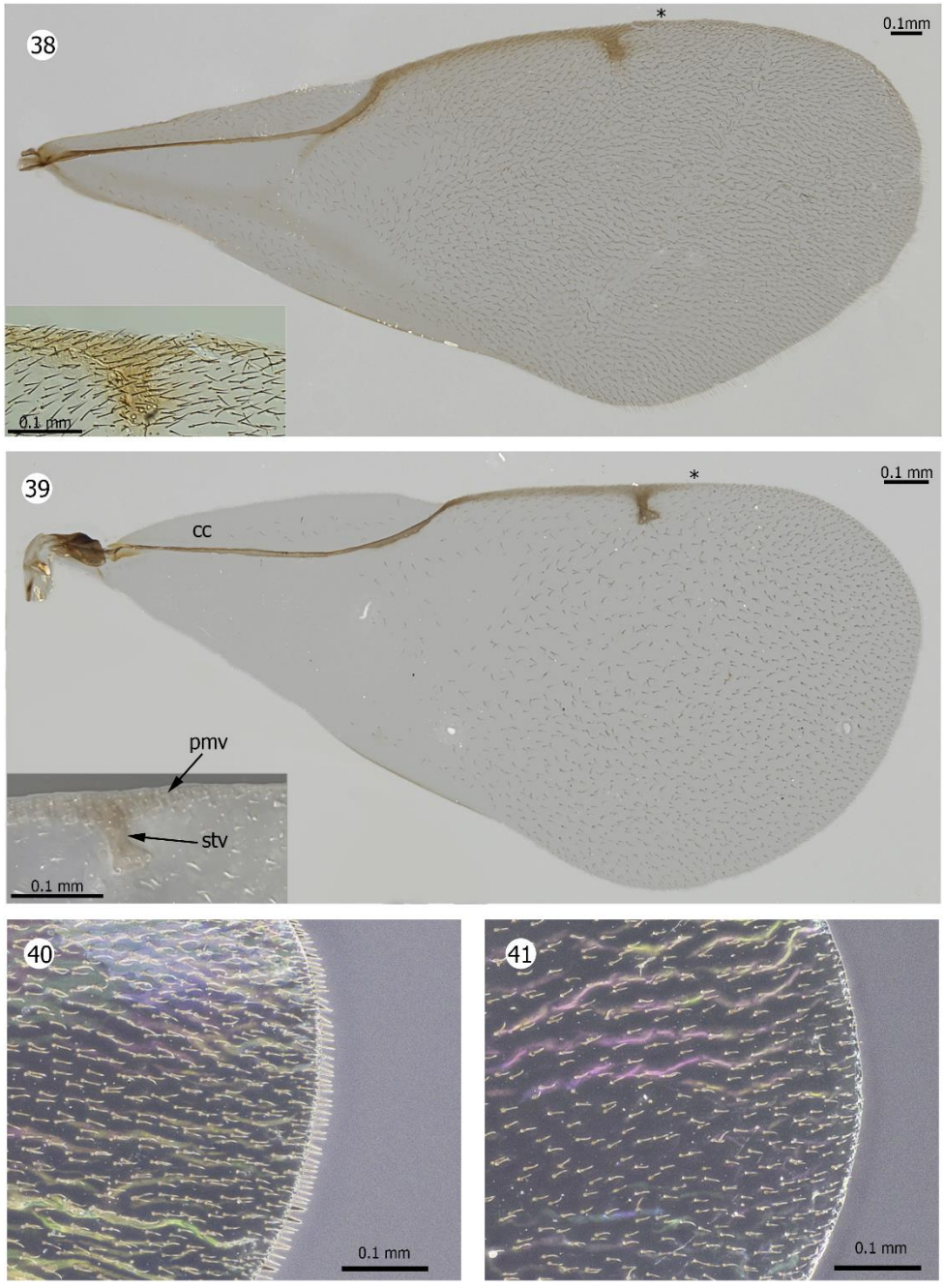

FIGS 38–41. Forewing: 38, 41 *Orasema simulatrix*: 41, marginal wing fringe (lateral). 39 *O. cancellata*. 40 *O. zahni*: 40, marginal wing fringe (lateral). Abbreviations: cc- costal cell; pmv- postmarginal vein; stv- stigma vein. Asterisks denote end of postmarginal vein.

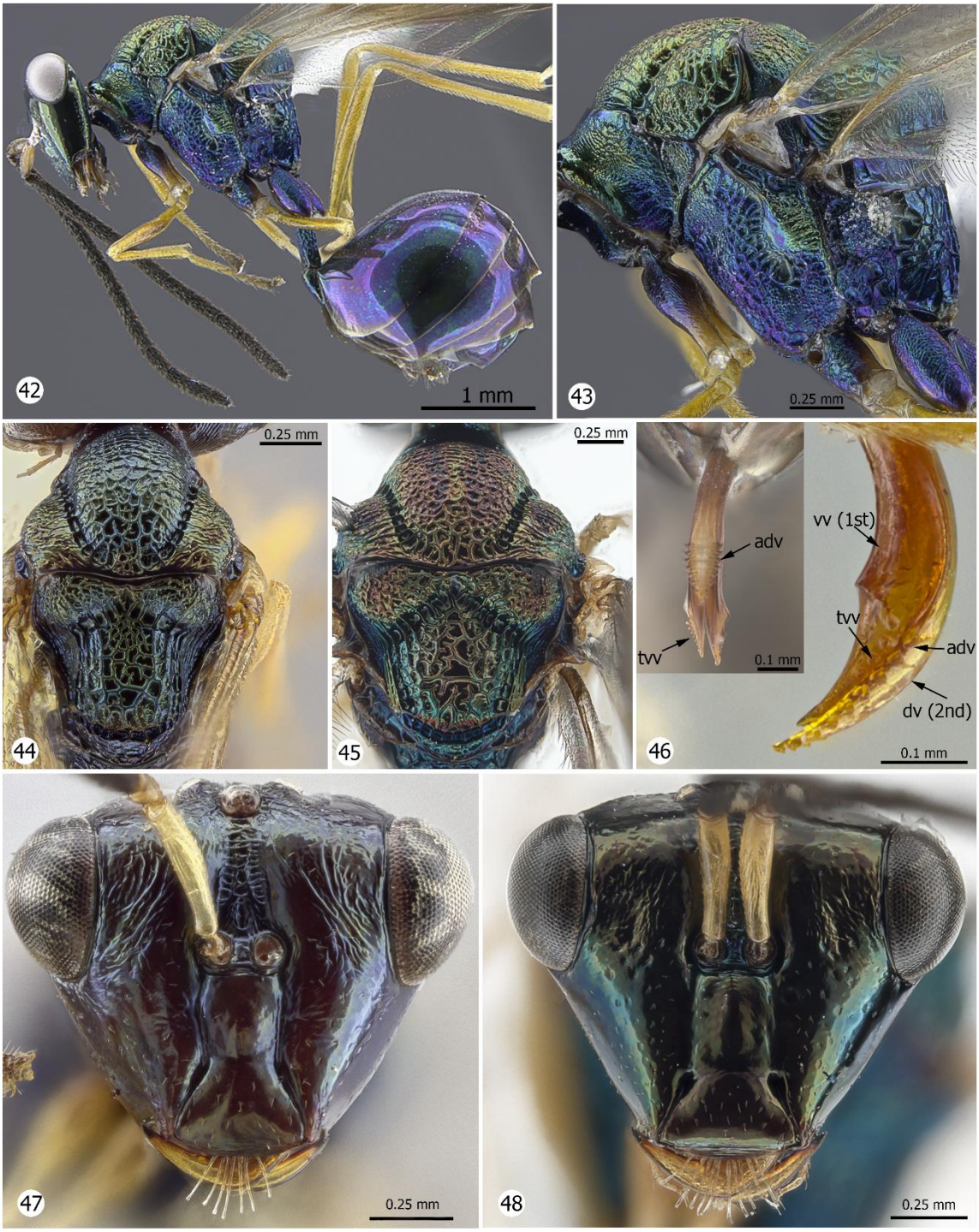

FIGS 42–48. 42–44, 46, 47, *Orasema wayqecha* (female): 42, habitus; 43, mesosoma (lateral); 44, mesosoma (dorsal); 46, ovipositor; 47, head (frontal). 45, 48, *O. quadrimaculata* (female): 45, mesosoma (dorsal); 58, head. Abbreviations: tvv- teeth of ventral valvula; adv- annuli of dorsal valvula; vv- ventral valvula; dv- dorsal valvula.

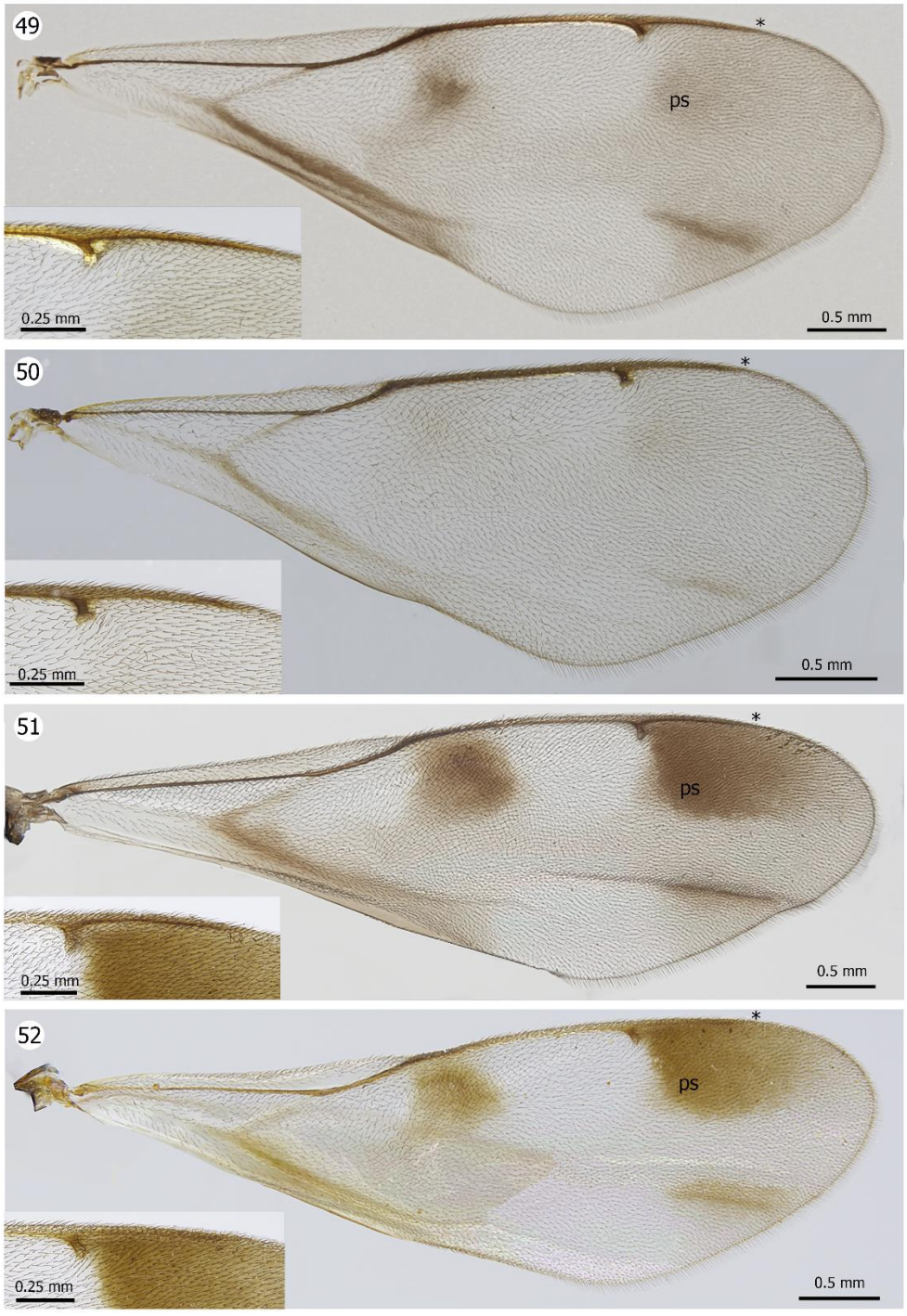

FIGS 49–52. Forewing: *Orasema wayqecha* (female): 49. *O. wayqecha* (male): 50. *O. quadrimaculata* (female): 51. *O. quadrimaculata* (male): 52. Asterisks denote end of postmarginal vein. Abbreviation: ps- poststigmal spot

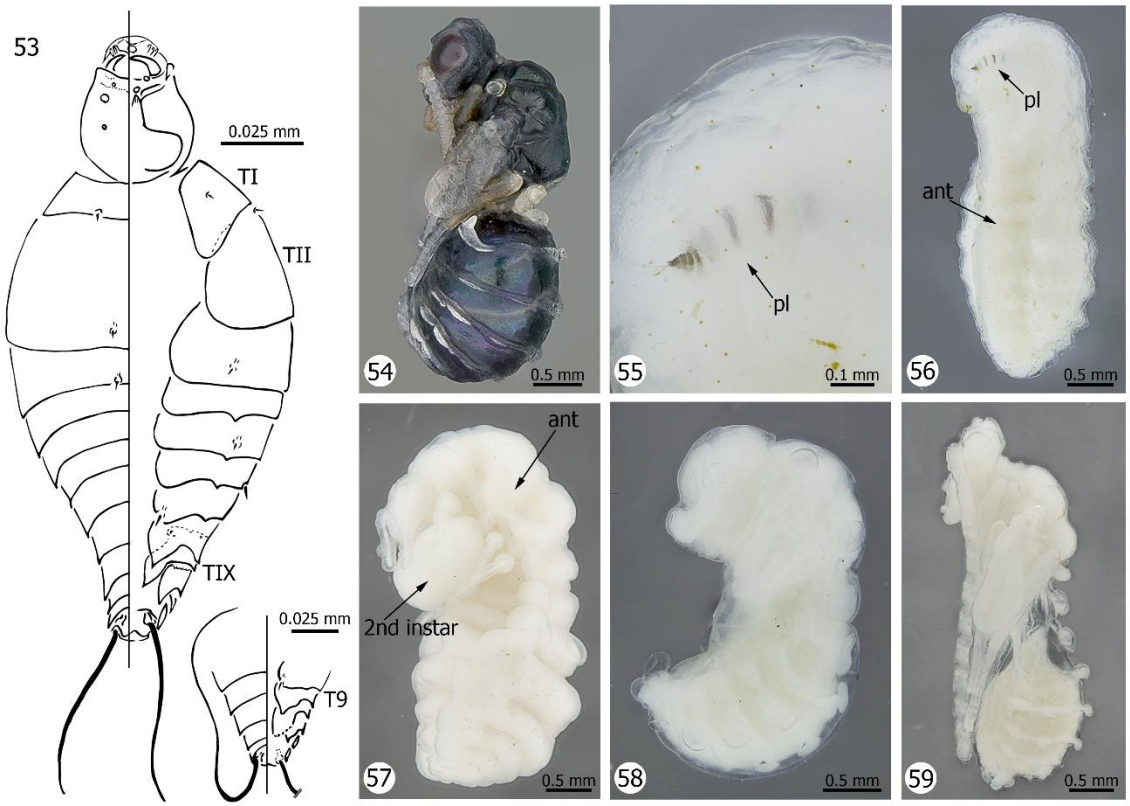

FIGS 53–59. 53 *Orasema simulatrix* planidia (full), *O. wayqecha* planidia (caudal end). 54, *O. simulatrix* mature pupa. 55–59 *O. wayqecha*: 55, 56, planidium embedded in *Pheidole* larvae; 57, 2nd instar larvae attached to immature *Pheidole*; 58, prepupae; 59, early pupae.

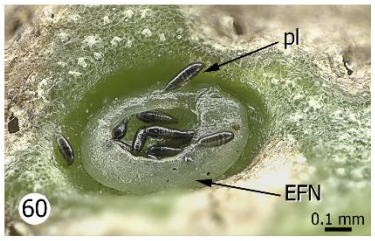
pl
EFN
60
0.1 mm

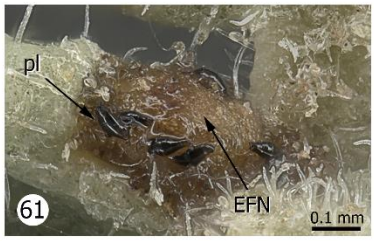
pl
EFN
61
0.1 mm

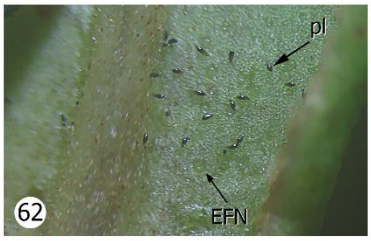
pl
EFN
62

63

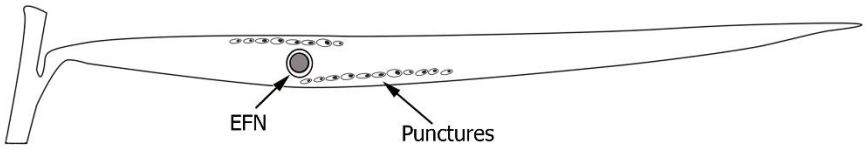
EFN
Punctures

64

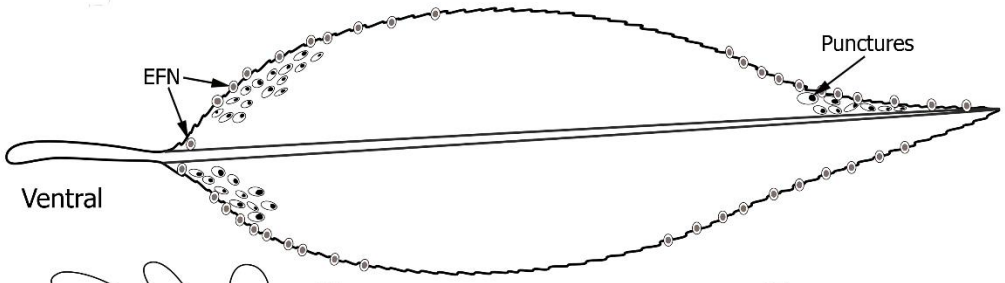
Punctures
EFN
Ventral

65

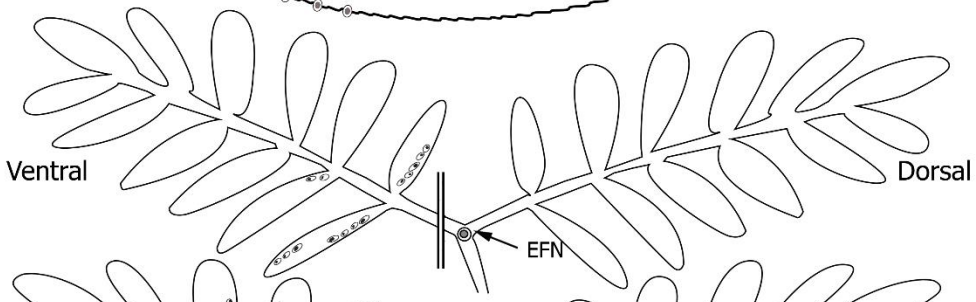
Ventral
Dorsal
EFN

66

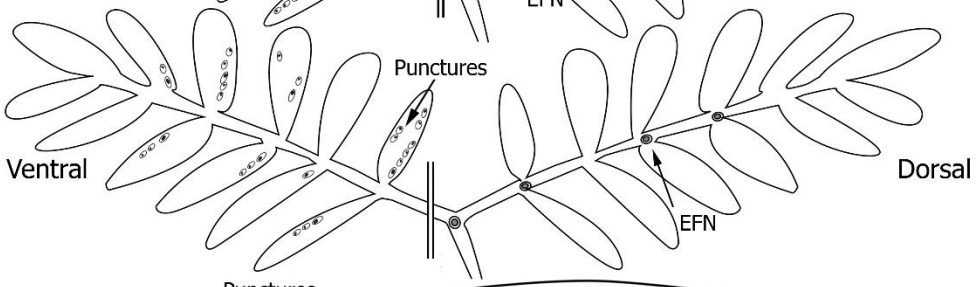
Punctures
Ventral
Dorsal
EFN

67

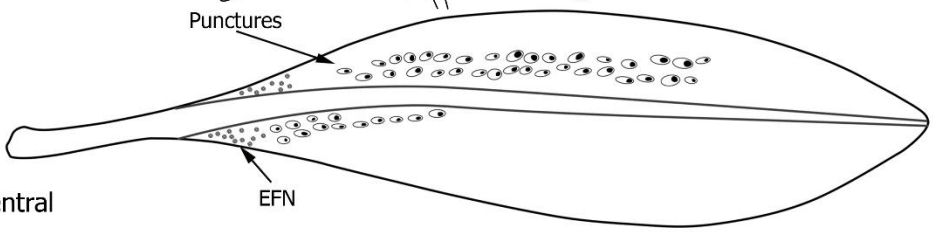
Punctures
EFN
Ventral

FIGS 60–67. 60, Planidia of *Orasema simulatrix* in *Chilopsis linearis* EFN; 61, *O. zahni* planidia in *Prosopis glandulosa* EFN; 62, *O. wayqecha* planidia near *Myrsine* EFNs; 63, *C. linearis* leaf with EFN and *O. simulatrix* oviposition punctures; 64, *Populus angustifolia* leaves with EFN and *O. beameri* oviposition punctures; 65, *P. velutina* leaves with EFN and *O. zahni* oviposition punctures; 66, *P. glandulosa* leaves with EFNs and *O. aureoviridis* or *O. zahni* oviposition punctures; 67, *Myrsine* leaf with EFNs and *O. wayqecha* oviposition punctures. Abbreviations: EFN- extrafloral nectary; pl- planidium

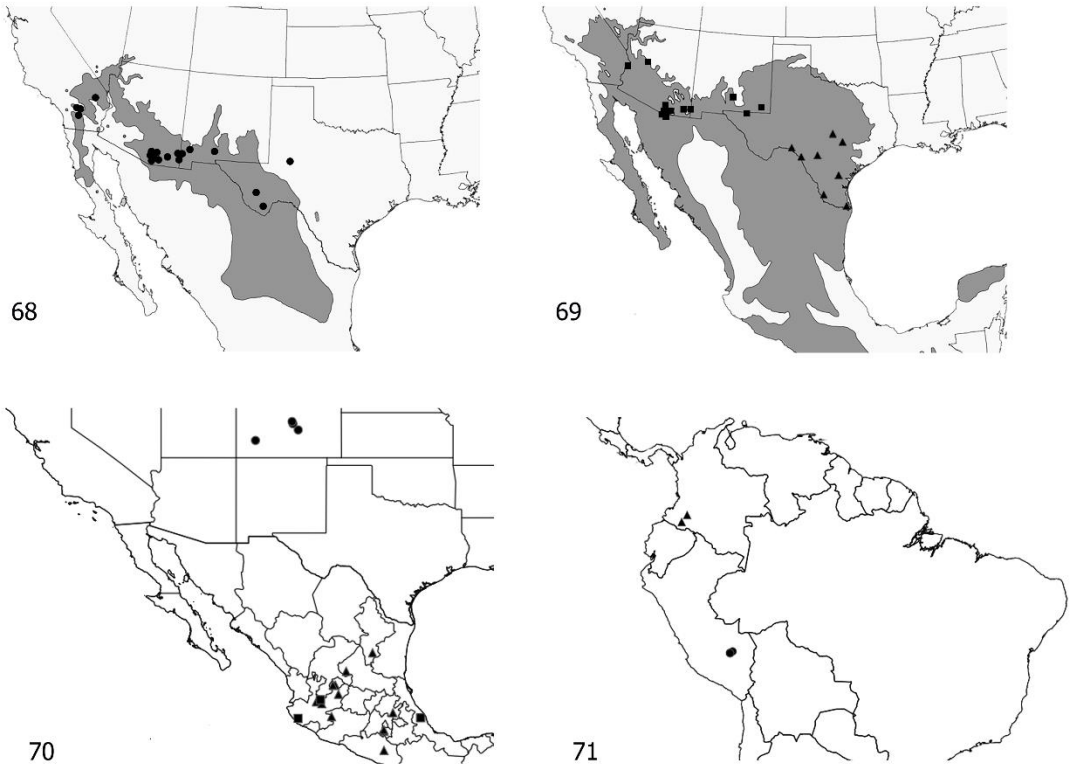

FIGS 68–71. Distribution maps: 68, *Orasema simulatrix* collecting localities (black circle) mapped onto *Chilopsis linearis* distribution; 69, *O. zahni* collecting localities (black square) and *O. aureoviridis* collecting localities (black triangle) mapped onto *Prosopis glandulosa* distribution; 70, *O. beameri* (black circle), *O. cancellata* (black square), *O. difrancoae* (black triangle) collecting localities; 71 *O. wayqecha* (black circle) and *O. quadrimaculata* (black triangle) collecting localities.

	species	UCRCENT ID	DNA ID	genes	18S	D2	D3-5	COI	COI
1	*aenea*-group sp. 1	447978	3710	5	KR632478	KR632409	KR632448	KR733129	KR733164
2	*aenea*-group sp. 2	412498	4134	4	KR632477	KR632408	KR632447	-	KR733163
3	*aenea*- group sp. 3	412116	3756	5	KR632472	KR632402	KR632441	KR733123	KR733158
4	*Orasema aureoviridis*	436489	3888	3	-	KR632390	KR632429	-	KR733146
5	*Orasema aureoviridis*	436488	3608	5	KR632479	KR632410	KR632449	KR733130	KR733165
6	*bakeri*-group sp. 1	412495	3880	4	-	KR632411	KR632450	KR733131	KR733166
7	*bakeri*-group sp. 2	411576	3882	3	-	KR632412	KR632451	-	KR733167
8	*bakeri*-group sp. 3	352479	3883	4	-	KR632413	KR632452	KR733132	KR733168
9	*Orasema beameri*	446406	3884	4	-	KR632414	KR632453	KR733133	KR733169
10	*Orasema beameri*	446407	3887	5	KR632480	KR632415	KR632454	KR733134	KR733170
11	*cockerelli*-group sp. 1	412581	3889	4	-	KR632416	KR632455	KR733135	KR733171
12	*cockerelli*-group sp. 2	352465	3891	4	-	KR632417	KR632456	KR733136	KR733172
13	*cockerelli*-group sp. 3	412575	3893	3	-	KR632418	KR632457	KR733137	-
14	*colradensis*-group sp. 1	352500	3708	5	KR632481	KR632419	KR632458	KR733138	KR733173
15	*Orasema simulatrix*	411564	3709	5	KR632482	KR632420	KR632459	KR733139	KR733174
16	*Orasema simulatrix*	352379	3876	4	-	KR632421	KR632460	KR733140	KR733175
17	*Orasema simulatrix*	411449	3610	5	KR632483	KR632422	KR632461	KR733141	KR733176
18	*Orasema simulatrix*	411446	3611	4	KR632484	KR632423	KR632462	-	KR733177
19	*Orasema simulatrix*	411569	3614	4	KR632486	KR632425	KR632464	-	KR733179
20	*Orasema simulatrix*	411568	4127	5	KR632487	KR632426	KR632465	KR733143	KR733180
21	*Orasema simulatrix*	411565	3952	4	KR632471	KR632401	KR632440	KR733122	KR733157
22	*Orasema simulatrix*	411563	3894	3	-	KR632391	KR632430	-	KR733147
23	*Orasema simulatrix*	411561	3895	4	-	KR632392	KR632431	KR733116	KR733148
24	*Orasema simulatrix*	411559	4099	4	-	KR632394	KR632433	KR733118	KR733150
25	*Orasema simulatrix*	352463	4101	3	-	KR632395	KR632434	-	KR733151
26	*Orasema simulatrix*	352464	4102	3	-	KR632396	KR632435	-	KR733152
27	*Orasema simulatrix*	411450	4103	3	-	KR632397	KR632436	-	KR733153
28	*Orasema simulatrix*	352381	4137	5	KR632469	KR632398	KR632437	KR733119	KR733154
29	*Orasema simulatrix*	352382	4139	4	-	KR632399	KR632438	KR733120	KR733155
30	*Orasema wayqecha*	352384	4100	4	-	KR632404	KR632443	KR733125	KR733160
31	*xanthopus*-group sp. 1	434572	3710	5	KR632478	KR632409	KR632448	KR733129	KR733164
32	*xanthopus*-group sp. 2	320847	4134	4	KR632477	KR632408	KR632447	-	KR733163
33	*Orasema zahni*	411558	3756	5	KR632472	KR632402	KR632441	KR733123	KR733158
34	*Orasema zahni*	411557	3888	3	-	KR632390	KR632429	-	KR733146
35	*Orasema zahni*	411594	3608	5	KR632479	KR632410	KR632449	KR733130	KR733165
36	*Orasema zahni*	411581	3880	4	-	KR632411	KR632450	KR733131	KR733166
37	*Orasema zahni*	411574	3882	3	-	KR632412	KR632451	-	KR733167
38	*Orasema zahni*	411582	3883	4	-	KR632413	KR632452	KR733132	KR733168
39	*Orasema zahni*	412578	3884	4	-	KR632414	KR632453	KR733133	KR733169
40	*Orasema zahni*	412580	3887	5	KR632480	KR632415	KR632454	KR733134	KR733170
41	*Orasema zahni*	411578	3889	4	-	KR632416	KR632455	KR733135	KR733171

Table 1: List of taxa used in the phylogenetic analyses, ID codes, and Genbank accession numbers.

gene	primer	sequence	references
18S 2			
	18S-441 F	5'-AAA TTA CCC CAC TCC CGG CA-3'	(Heraty et al., 2011)
	18S-1299 R	5'-TGG TGA GGT TCC CGT GTT-3'	(Heraty et al., 2011)
28S D2			
	D2 F	5'-CGG GTT GCT TGA GAG TGC AGC-3'	(Murray et al., 2013)
	D2Ra R	5'-CTC CTT GGT TCC GTG TTT C-3'	(Murray et al., 2013)
28S D3-5			
	D3F	5'-CCC GTC TTG AAA CAC GGA CC-3'	(Murray et al., 2013)
	D3Fa	5'-TTG AAA CAC GGA CCA AGG AG-3'	(Murray et al., 2013)
	D5Ra	5'-CGC CAG TTC TGC TTA CCA-3'	(Murray et al., 2013)
CoI			
	NJ F	5'-TAT ATT TTA ATY TWC CWG GAT TTG G-3'	(Murray et al., 2013)
	MD R	5'-ATT GCA AAT ACT GCA CCT AT-3'	(Dowton &Austin, 1997)
	LCO1490	5'-GGT CAA CAA ATC ATA AAG ATA TTG G-3'	(Folmer et al., 1994)
	HCO2198	5'-TAA ACT TCA GGG TGA CCA AAR AAT CA-3'	(Folmer et al. 1994)

Table 2. List of primers used for each gene region and their references.

3. Chapter 2

Into the nest: interactions of planidia (Eucharitidae: *Orasema*) and their ant host

3.1 Introduction

One of the most important behaviors in a parasitoid's lifecycle is locating its host. Among the majority of insect parasitoids, adult females are responsible not only for oviposition, but also for many behaviors associated with host finding and oviposition site selection (Vinson, 1976; Eggleton and Belshaw, 1992; Santos and Quicke, 2011). Both dipteran and coleopteran parasitoids commonly locate their host via the first instar larvae (Eggleton and Belshaw, 1992; Eggleton and Belshaw, 1993; Feener Jr and Brown, 1997). However, larval search and host location is not often found within Hymenoptera. Exceptions are members of the eucharitid-perilampid clade (Hymenoptera: Chalcidoidea). The first instar of these two families are characterized by being sclerotized, often highly mobile and responsible for locating their host (Heraty and Darling, 1984; Heraty et al., 2013; Heraty and Murray, 2013). Eggs are deposited into plant tissue away from the wasp's host and the first instars (planidia) emerges (Clausen, 1940a; Clausen, 1940b; Clausen, 1941; Heraty, 2000; Carey et al., 2012; Lachaud and Pérez-Lachaud, 2012). Both subfamilies of perilampids with known oviposition and planidial behaviors deposit eggs very close to the target host stage and plandia are directly responsible for host access (Darling and Miller, 1991; Darling and Roberts, 1999; Heraty and Murray, 2013). In all known eucharitids, eggs are deposited remotely from the host and planidia must use an ant forager as a carrier to gain access to the immature

ant host (Clausen, 1940b; Clausen, 1941; Clausen, 1976; Heraty, 2000; Heraty and Murray, 2013).

Within Eucharitidae, both adult females and planidia exhibit a variety of behaviors for achieving host access since eggs are deposited remotely. Known behaviors include adults ovipositing into or on specific plant structures, away from the host ant's nest. Eggs are placed into overwintering or expanding leaf or flower buds, randomly scattered onto leaves, inserted into leaf or fruit tissues, and in some peculiar cases placed onto seeds later dispersed by the wind (Parker and Thompson, 1925; Clausen, 1940b; Clausen, 1941; Heraty and Barber, 1990). Once emerged, the planidia, although mobile, cannot disperse to their host independently and require a "vector" to be transferred to the ant brood (Clausen, 1940b; Clausen, 1941; Clausen, 1976; Heraty and Murray, 2013). It has been proposed that planidia attach to a foraging adult ant or a food source of the host ant such as an immature thrips or auchenorrhynchous hemipteran (Parker, 1937; Ayre, 1962; Das, 1963; Johnson et al., 1986; Heraty and Barber, 1990; Heraty, 2000; Heraty, 2002). Another possibility is that planidia are picked directly up in the mouthparts of foraging adult ants through feeding on nectaries or fruit (Heraty and Barber, 1990).

A novel behavior facilitating host access was recently described for *Orasema simulatrix* Gahan (Hymenoptera: Eucharitidae). Females deposit eggs into incisions on leaf surfaces of *Chilopsis linearis* Cav. (Bignoniaceae), with eggs being placed in close proximity to extrafloral nectaries (EFNs) (Carey et al., 2012). Recently a species from Peru, *Orasema wayqecha*, was found to oviposit near EFNs of two species of *Myrsine*

(Myrsinaceae) (Herreid and Heraty, unpublished). EFNs are nectar secreting tissues that play no role in pollination and are usually found separate from the flower (Heil et al., 2000; Heil, 2011). EFNs are structurally diverse (Marazzi et al., 2013a). They can be found on a variety of plant structures including leaves, petioles, sepals and stipules, and their morphological expression ranges from a complex physical structure to undetectable, when nectar is absent, due to a lack of structure (Marazzi et al., 2013a; Marazzi et al., 2013b; Weber and Keeler, 2013). It has been shown that EFNs are actually somewhat common, but with a phylogenetically widespread distribution (Heil, 2011; Marazzi et al., 2013b). Weber and Keeler (2013) demonstrated that 21% of vascularized plant families possess some type of EFN. Their nectar is known to recruit ants and when given a choice, ants will preferentially forage on plants with EFNs (Heil et al., 2001; Heil et al., 2004). It is hypothesized that EFNs attract ants either to distract them from flowers so they will not impact pollination (Beattie et al., 1984; Wagner and Kay, 2002) or to provide indirect defense against herbivory (Heil and McKey, 2003). Either way this EFN-ant association has in some cases become obligate (Kost and Heil, 2005; González-Teuber and Heil, 2009). Emerging planidia can be found in an EFN more commonly than outside of an EFN, and they are rarely found distant from an EFN (Carey et al., 2012). It is hypothesized that planidia are picked up by their host ants while the ant is feeding at an EFN. The known ant host of *O. simulatrix*, *Pheidole desertorum* Wheeler, forages on *C. linearis* at night (Carey et al., 2012). Presumably, foraging *P. desertorum* are coming into contact with planidia. Although it has yet to be observed, it is likely that these ants are vectoring planidia to their brood. Something similar could potentially be happening with

O. wayqecha and its host, *Pheidole* sp., but as of yet *Pheidole* sp. has not been observed foraging on either species of *Myrsine*.

A narrowed petiole and the proventriculus both play a role in restricting adult ants to a liquid diet (Eisner and Wilson, 1952; Roche and Wheeler, 1991; Hunt, 1994; Cassill and Tschinkel, 1996). Even if large food particles could be transferred to the midgut, a lack of proteases makes digestion unlikely (Cassill et al., 2005; Dussutour and Simpson, 2009). Instead, they often forage on liquids such as EFN nectar, and then transfer solid food particles from their infrabuccal pocket, a filtering cavity within the mouthparts, to their larvae via trophallaxis (Eisner and Happ, 1962). Larval digestion of solids plays an important role in certain ant colonies, and within *Pheidole*, this trophallactic behavior has been observed (Abbott, 1978; Cassill et al., 2005; Dussutour and Simpson, 2009). Cassill et al. (2005) reported that the mature larvae (4^{th} instar) are responsible for solid food particle digestion with their regurgitate then fed to workers and other ant larvae. This behavior could potentially optimize the placement of *Orasema* planidia on to their host, because they initially parasitize mature larva (Heraty et al., 1993; Heraty, 1994b; Heraty, 2002).

Ayre (1962) originally examined planidial interactions with adult ants and reported that immature eucharitids can attach to any part of the worker ants but then migrate to the mouthparts, with the inference that planidia are orally transferred to ant larvae. Previous field observations have shown that eucharitid planidia from the genera *Gollumiella* and *Kapala* can be found within the infrabuccal pocket of their respective ant hosts,

Nylanderia and *Ectatomma* (Heraty, pers. comm). For these reasons, I hypothesize that *Orasema* planidia with EFN associations are transferred to the nest via the infrabuccal pocket of ant foragers. Planidia are possibly too small to be a direct target of the ant as prey. Likely they enter the infrabuccal pocket either while the host ant feeds from an EFN and accidentally collects the planidia into its mouthparts, or by attaching to the ant body when near an EFN, and then migrating or being groomed into the mouthparts. This latter transfer method was proposed by Ayre (1962).

Herein the relationship between adult ants and EFN associated planidia is examined using *O. simulatrix* and *O. wayqecha*. Several studies are undertaken to test if planidia are carried in the infrabuccal pocket. Results from these studies can elucidate the interactions between EFN associated planidia and their ant host vectors.

3.2 Materials and Methods

3.2.1 Foraging Ant Dissections: *Orasema simulatrix*

The purpose of this study was to determine if *Pheidole desertorum* and other ant species foraging on or near *Orasema* host plants carry planidia in their infrabuccal pocket.

Habitat

Foraging ants were collected from two main areas in the arid southwestern United States in Arizona and southern California. Collection areas for study were selected that had both the host plant and ant, *C. linearis* and *O. simulatrix*. Habitats tended to be desert with ephemeral watercourses, which is where *Chilopsis* usually grows (Petersen et al., 1982).

In southern California, ants were collected from Whitewater Canyon in Riverside County (33°57'51"N116°39'4"W) (Fig. 72). Ants from Arizona were collected along Foothills Road near Portal in Cochise County (31°55'5"N109°7'41"W) (Fig. 73).

Collection and Dissection Methods

The majority of ant collections took place at night since *Pheidole desertorum* is a species with nocturnal foragers (Chew, 1977; Carey et al., 2012). Collections in Arizona took place between July and September of 2013, 2014 and 2015, while collections in Whitewater Canyon, California happened only in 2014 of April and May. Eighteen total nights of collections were performed over these three years at various *Chilopsis* trees in Whitewater Canyon and along Foothills Road in Arizona (Table 3). Ant foragers were collected using a straight-tube aspirator and immediately placed in 95% EtOH for later identification and dissection. *Pheidole desertorum* along with other ants were collected directly from *Chilopsis* or from the ground near the host plant. Collections from the ground and plant were kept separate even if they came from the same site. Sweep netting and beating *C. linearis* over a canvas sheet was used for direct collection of ants from vegetation. Ground foraging ants were located passively or with baits then aspirated. Baits targeted myrmicine ants in general, but mostly *P. desertorum*, and were white 2x2 inch cards, placed on the ground, with a central placement of either peanut butter or crushed Keebler Sandies® (pecan cookies). Baits were generally placed before sunset or at night and checked periodically until ant activity was observed. After collection, ants were examined externally for planidia, and then heads were dissected to examine the

contents of the infrabuccal pocket. Dissections were performed with a fine forceps and an insect pin under magnification. No planidia were recovered from external examination, and planidia found in the infrabuccal pocket are recorded in Table 3. Some planidia were slide mounted and imaged with a Zeiss Axioskop 2 mounted with a 1.4 megapixel CCD camera (model LW1165C; Lumenera Corp., Ottawa, Ontario, Canada). Vouchers of a sampling of the ant genera were point mounted, labeled with a unique barcode, imaged and deposited in the UCR entomology museum. Specimen information and images were recorded in a FileMakerPro database.

3.2.2 Nest Ant Dissections: *Orasema simulatrix* & *O. wayqecha*

This study was undertaken to determine if *Pheidole* workers collected directly from their nest harbor planidia in their infrabuccal pocket.

Habitat

Ant nest excavations took place in two locations. *Pheidole desertorum*, the host ant of *O. simulatrix*, were collected near Portal, AZ in Cochise County along Foothills Road (31°55'01"N109°07'41"W) (Figs 73 & 75). This location, arid flatland, was dominated by desert scrub vegetation including *Chilopsis linearis, Larrea tridentata* Coville (Zygophyllaceae), *Acacia constricta* Benth. (Fabaceae) and *Prosopis* sp. (Fabaceae) and various desert grasses (Carey et al., 2012). An unidentified species of *Pheidole* that is host to a new species of *Orasema, O. wayqecha,* was collected at the Wayqecha Biological Station located in the Andes of southeastern Peru (13°10'38"S71°35'04"W)

(Figs 74 & 76). This location can be categorized as high elevation montane cloud forests. *Orasema* activity was found as high as 3400 m in this area.

Collection and Dissection Methods

Four individual nests of *Pheidole* were excavated from sites in Arizona and Peru. Excavated ant nests used in this study had either evidence of *Orasema* parasitism or were near to a parasitized nest. Parasitism of a nest was determined both by presence of immature stages of *Orasema* on ant larva or pupa, *Orasema* pupae or the ant prepupal remains, which have a characteristic morphology (Wheeler, 1907; Heraty et al., 1993). Nests were excavated or discovered under rocks, and adult and immature ants aspirated into fluon-lined plastic containers, where they could be examined for parasitism, sorted and preserved in 95% EtOH. Mature ants from excavated nests were identified, examined externally for planidia, and then dissected. Dissections followed the same protocol as the foraging ant dissections. Vouchers from each nest excavated were point mounted, given a unique barcode, and information was deposited in a FileMakerPro database. Information about the four excavated nests and the ants dissected is recorded in Table 4.

3.2.3. Planidia Ant Interactions: *Orasema simulatrix*

This experiment was to determine if *O. simulatrix* planidia are transferred to the infrabuccal pocket of ***P. desertorum*** when they are placed on the ant's legs and body.

Habitat

Four separate sites in Whitewater Canyon, California, were used for collecting of worker ants and planidia. The canyon is a unique mix of riparian and California desert habitat (Fig. 72). The study sites were adjacent to Whitewater Canyon Road and *Chilopsis linearis* was present.

Study Sites

Planidia used in this experiment were collected from trees at three sites (**S1**: 33°57'31.36"N116°38'51.45"W; **S2**: 33°57'36.19"N116°38'56.53"W (Fig. 77); **S3**: 33°57'49.56"N116°39'3.52"W). To obtain ants that were not associated with *Orasema* I collected *P. desertorum* adults from a fourth site (**S4**: 33°58'56.2"N116°39'11.23"W) that lacked any noticeable *Orasema* activity as assessed by sweeping vegetation and examining the leaves for oviposition scars.

Collecting Methods

Shoots of *C. linearis* with oviposition punctures were cut from trees at sites 1-3 and placed in sealed, 1 gallon plastic ziploc® bags to preserve moisture. Leaves were examined for live planidia with a Zeiss Stemi SV 6 microscope. Planidia were manipulated with a minutien pin mounted on a 1/16" wooden dowel and placed together near a wet EFN until they could be used.

Pheidole desertorum was collected from a single nest at site 4. The nest was located by baiting worker ants using a white 2x2 inch card with crushed Keebler Sandies®

(pecan cookies) mixed with Shannon Luminous powder, which fluoresces under black light so that ants may be tracked. Baits were placed about an hour before sunset and checked periodically after dark for *P. desertorum* activity. Workers at baits were followed back to the nest using a black light. Workers collected at baits were not used in the planidia trials, but instead I used ants aspirated from the ground near their nest entrance. Ants were placed in plastic fluon-lined containers that were at least 6" x 3". Workers were fed a 50% sucrose solution using a vial and cotton stopper until they were used in the experiment.

Experimental Design

Single *P. desertorum* were placed into a plastic 3.5 inch diameter Falcon® disposable petri dish with lid. The petri dish was then placed in a refrigerator or in a container with ice to cool the ant until it was slowed or inactive. The ant was then held by the leg with a curved medium tipped forceps under a microscope and a variable number of active planidia then placed on the legs and body of the ant with a minutien pin mounted on a 1/16” wooden dowel. Each ant with planidia was kept for approximately 24 hours. All ants were dead after 24 hours, possibly due to stress and starvation. Running the experiment until the ants died allowed the adult ants as much time as possible to transfer planidia to their mouthparts. Ant bodies were examined for planidia and the contents of their infrabuccal pockets examined in 95% EtOH with a fine forceps and an insect pin. The petri dish was also examined for planidia but not all planidia placed on the ant could be accounted for. This is possibly due to their small size or they escaped from the dish.

The number of planidia initially placed on the ant and remaining on the body and in the infrabuccal cavity are recorded for each ant (Table 5). A sampling of planidia that remained on the ant was imaged (Figs 78–81) using a Leica Imaging System with a Z16 APOA microscope and are deposited in a FileMakerPro database.

3.3 Results

3.3.1. Foraging Ant Dissections: *Orasema simulatrix*

A total of 1122 foraging ants from twelve different ant genera were collected in Arizona and dissected. No planidia were found in the infrabuccal pocket of ants belonging to the genera *Dorymyrmex* (Dolichoderinae) (109), *Forelius* (Dolichoderinae) (21), *Paratrechina* (Formicinae) (18), *Crematogaster* (Myrmicinae) (8), *Solenopsis* (Myrmicinae) (6), *Myrmica* (Myrmicinae) (3) and *Tetramorium* (Myrmicinae) (3). These accounted for 168 of the total ant dissections. A total of 801 *Pheidole desertorum* (Myrmicinae) were collected either directly from *Chilopsis* (52) or off the ground near *Chilopsis* (749). When dissected, planidia were not found even though *P. desertorum* made up most of the ants collected. However, planidia were recovered in the mouthparts of two genera of Formicine ants, *Camponotus* (2) and *Formica* (1). In one of the species, *Camponotus ocreatus* (Emery), planidia were recovered from the infrabuccal pocket in almost 40% of individuals dissected. Eighteen individuals from *Camponotus ocreatus* were dissected and seven were found to have between 1 and 18 planidia in their mouth parts ($\bar{x}$=4.9, SD=6). Eighty-seven *Camponotus* sp. foragers were collected and five had a single planidium in their infrabuccal pocket. Two of the 48 dissected *Formica* had one

planidium in their mouthparts. The number of individuals dissected from each genus and proportion of specimens with planidia is outlined in Table 3.

3.3.2 Nest Ant Dissections: *Orasema simulatrix* & *O. wayqecha*

Four *Pheidole* nests were excavated: two *Pheidole desertorum* nests from southwestern Arizona and two *Pheidole* sp. nests from southeastern Peru. One nest from each area had direct evidence of *Orasema* parasitism while the others were in close proximity to parasitized nests or plants with active planidia. A total of 426 *P. desertorum*, the host of *O. simulatrix*, were dissected from the two nests in Arizona, and 225 *Pheidole* sp., the host of *O. wayqecha*, were dissected from two nests in Peru, but none had planidia in their mouthparts (Table 4).

3.3.3 Planidia Ant Interactions: *Orasema simulatrix*

Of 80 planidia placed on 32 live *P. desertorum*, 12.5% remained on the ants. Ten planidia were found on seven of the 32 ant specimens: eight planidia externally on ant bodies (Figs 80 & 81) and two planidia in the infrabuccal pockets (Figs 78 & 79). A single ant had planidia in both the mouthparts and on the body, while five of the seven ants had planidia solely on the body, and the remaining ant had a single planidium in the infrabuccal pocket. The number of planidia placed on each individual *P. desertorum* and the number recovered are outlined in Table 5.

3.4 Discussion

Pheidole are known to be host for both *O. simulatrix* and *O. wayqecha.* If their EFN associated planidia are being transferred to their immature host by oral transfer from the workers, one would expect to find *Pheidole,* in *Orasema* infested areas, to have planidia in their infrabuccal pocket. This was not the case. No field-collected *Pheidole* carried planidia in their mouthparts. However the planidia-ant interaction experiments demonstrated that *Pheidole* are capable of transferring planidia that were placed externally on the body into the infrabuccal pocket. Other ant genera such as *Camponotus* and *Formica* collected from planidia infested *Chilopsis* were found to carry planidia in their infrabuccal pockets, even though there has been no evidence of parasitism of either host by this species. *Camponotus* and *Formica* are both members of the formicine subfamily, but *Orasema* are assumed to almost exclusively parasitize species of Myrmicinae (Heraty et al., 1993; Heraty, 1994a; Heraty, 1994b). Johnson et al. (1986) did collect adult *O. coloradensis* from nests of *F. subnitens* (Creighton) with emergence traps placed over them and during nest excavations but this record could be potentially misleading. *Formica* brood was never found to be parasitized by *O. coloradensis* and it is possible that *Formica* was a mistaken association or was living in cleptobiosis with the actual ant host (Wheeler, 1907; Heraty, 1994a). This was something previously seen by Wheeler (1907) with *F. ciliate* and *S. molesta* (Say), another proposed host of *O. coloradensis*. Finding *O. simulatrix* planidia in the mouthparts of *Camponotus* and *Formica* is potentially due to the fact that they are primarily nectivorous ants that likely

frequent EFNs which increases their chances of picking up planidia (Cosens and Toussaint, 1986; Medan and Josens, 2005; Falibene et al., 2009).

The lack of planidia in the mouthparts of *Pheidole* potentially means either more *Pheidole* may need to be sampled to discover planidia in their mouthparts or there is a different means of transfer not yet discovered. Planidia are potentially being transferred via the *Pheidole* infrabuccal pocket but the occurrence of them in forager's mouthparts is so rare that more ants would need to be collected and dissected in order to confirm this mechanism of transfer. If true, rareness of planidia could be due to a few compounding factors. It is possible that planidia are so efficient at transferring from forager mouthparts to the brood that at any given time only ants that have been recently foraging on *Orasema* host plants harbor planidia. Also, *Pheidole* may only forage on nectaries only at certain times making the discovery of planidia in the mouthparts unlikely if sampling is not carried out at the correct time of day or year. It may mean that planidia are not being transferred via their ant host's infrabuccal pocket and there is a different means of host access. These EFN associated *Orasema* are potentially transferred to their immature host when ants with planidia filled mouthparts like *Camponotus* and *Formica* are carried into the nest as prey items.

These studies have helped formulate this new hypothesis even though questions still remain as to how EFN-associated planidia make their way to the ant host. Planidia were only discovered in the mouthparts of non-host ants, *Camponotus* and *Formica*. Recent nest excavations at the Arizona site found dead *Camponotus ocreatus* inside a colony of

P. desertorum (Dominguez & Heacox, pers. comm.). *Pheidole* are known predators of small invertebrates including ants (Feener, 2000; Wilson, 2005). It is possible *P. desertorum* foraging on *Chilopsis* are in search of other ants. If this is the case, a new hypothesis may be that planidia are using non-host ants as an intermediate host, similar to other *Orasema* that potentially use immature thrips or auchenorrynchous hemipterans as intermediate hosts which are taken to the brood as prey items (Clausen, 1940b; Das, 1963; Johnson et al., 1986; Heraty, 2000). *Orasema* planidia could possibly be playing a part in the death of their intermediate ant host. It was recently proposed that eucharitid planidia from the genus *Chalcura* Kirby (Eucharitinae) attach to ants and cause their death (Schwitzke et al., 2015). Ants were found to die within an hour of having planidia placed on their body. Perhaps *Pheidole* are scavenging ants that planidia have killed. This new hypothesis should be considered and tested.

Future studies examining how planidia are transferred in EFN associated *Orasema* should continue to look at *Pheidole* mouthpart dissections but with more focused collections. Appendices 5.1–5.3 outline modified protocols that could help further improve these studies. Some modifications include increasing the number of *Pheidole* nests excavated and the number of individuals collected. Also, the planidia-ant protocols should be optimized to increase ant survival. These changes could raise the chances of capturing individuals with planidia in the infrabuccal pocket and bring us closer to understanding how EFNs facilitate host access for certain *Orasema*.

3.5 Figures and Tables

FIGS 72–74. 72, Whitewater Canyon, Riverside County, California; 73, Foothills Road, Cochise County, Arizona; 77, Wayqecha Biological Station, Cuzco, Peru .

FIGS 75–77. 75, nest 2 location along Foothills Road, Cochise County, Arizona; 73, *Myrsine* at the Wayqecha Biological Station, Cuzco, Peru; 77, site 2 at Whitewater Canyon, Riverside County, California.

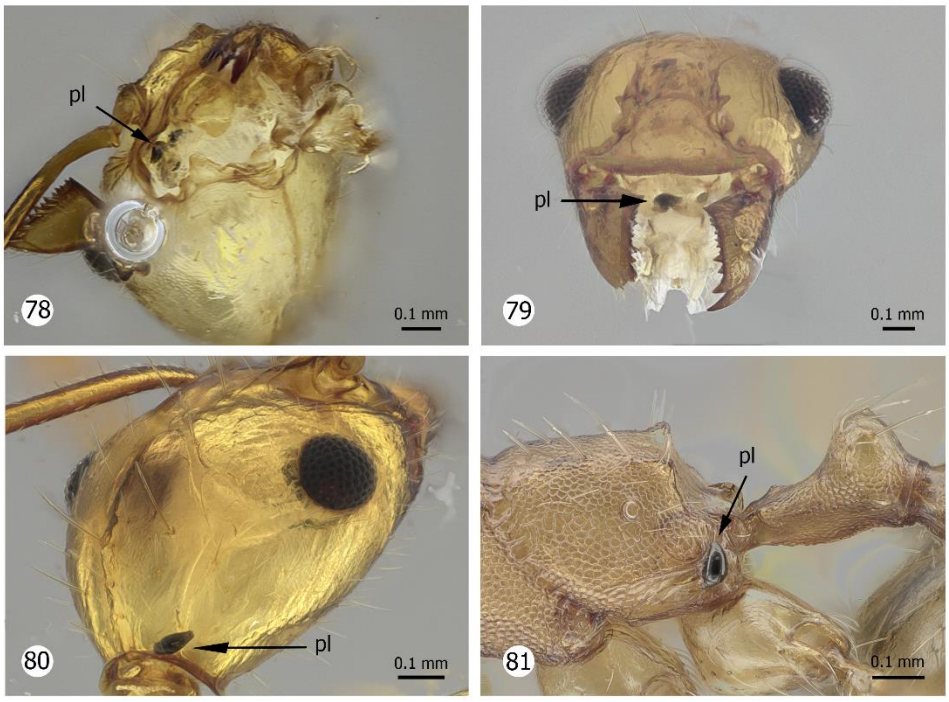

FIGS 78–81. Plandia-ant trials: 78 & 79, planidium in the infrabuccal pocket of *Pheidole desertorum*; 80, planidium attached to the exterior head of *P. desertorum*; 81, planidium attached to the mesosoma of *P. desertorum*.

Ant Species	**Individuals from tree**	**Individuals from ground**	**Individuals with planidia**	**No. of planidia in buccal cavity**
Pheidole desertorum	52	749	0	-
Camponotus ocreatus	13*	5*	7	1-18
Camponotus sp.	87*	0	5	1
Formica sp.	47*	1	2	1
Dorymyrmex sp.	109	0	0	-
Forelius sp.	14	7	0	-
Paratrechina sp.	18	0	0	-
Crematogaster sp.	8	0	0	-
Solenopsis sp.	0	6	0	-
Myrmica sp.	3	0	0	-
Tetramorium sp.	0	3	0	-

Table 3**.** Summary of ant species and genera collected from *Chilopsis* and from the ground around *Chilopsis* and the number of ants harboring planidia in their mouthparts for the foraging ant dissections.

Nest	Species	No. Dissected (No. with pl)	Date
1	*Pheidole desertorum*	98 (0)	14 Sept. 2012
2*	*Pheidole desertorum*	328 (0)	13 Sept. 2012
3*	*Pheidole* sp.	70 (0)	26 July 2014
4	*Pheidole* sp.	155 (0)	28 July 2014

Table 4. Number of individuals dissected from four different ant nests. Nests with asterisks had evidence of *Orasema* parasitism. Other nests were in the vicinity of parasitized nests or infested host plants.

No. planidia placed on ant	No. trials	Mean No. planidia remaining on body (n=total trials)	Mean No. planidia in mouthparts (n=total trials)	No. negative trials
1	6	-	-	6
2	8	1 (n=1)	-	7
3	14	1.3 (n=3)	1 (n=2)	10
4	4	2 (n=1)	-	3

Table 5. Results from the planidia-ant interaction experiments. Number of trials with 1–4 planidia placed on a worker ant is shown. Mean number of planidia that remained on the body and were found in the mouthparts are reported. Calculated means exclude the negative runs. Number of trials with no planidia remaining on the ant (negative trial) are outlined.

4. Conclusions

At present, relatively little is known about EFN associated eucharitids. Until recently the only published eucharitid EFN associations were from *O. simulatrix* (Carey et al., 2012). With the inclusion of recent publications and observations, nectary associations are expanded to include two genera from the subfamily Eucharitinae, *Kapala* Cameron and *Chalcura* Kirby. Field observations have shown eucharitid planidia from the genera *Kapala* can be found perched near floral nectaries of *Hamelia patens* (Rubiaceae) that their ant host, *Ectatomma* Smith (Formicidae), frequents (Heraty, pers. comm). Recently there has been evidence of another genus of eucharitid possessing an EFN association. A species of *Chalcura* was discovered to oviposit into stipules of *Leea manillensis* (Leeaceae) (Schwitzke et al., 2015). EFNs are located in close proximity to the oviposition sites and planidia would emerge and concentrate around them. My research both expands the number of species described with EFN associations, the *wayqecha*- and *simulatrix*-groups, and examined how these EFN associated groups are transported into the ant nest.

The *simulatrix*- and *wayqecha*-groups are revised using an integrative taxonomic approach that includes a molecular phylogeny, morphological descriptions, distribution data and a synopsis of oviposition behaviors. These two species groups are supported as a clade by phylogenetic analyses, morphology and shared behaviors. The Bayesian analysis from Chapter 1 (Fig. 1a) and analyses with a larger taxon set (Mottern et al. unpublished) support a monopyletic *simulatrix*- and *wayqecha*-group. Both groups possess a unique morphology as adults, convergent postgenae (Figs 2, 5), and planidia, elongate cerci and

an emarginated tergite IX (Fig. 59). Also their habit of ovipositing near EFNs (Figs 63-65) is both novel within *Orasema* and something they have in common. In the future increased sampling efforts could help include, *O. cancellata*, *O. difrancoae*, and *O. quadrimaculata* in both the phylogenetic analyses and behavior descriptions. Having this data would help elucidate relationships within and between the two species groups. It would also determine if an EFN association is found across all of both the *simulatrix*- and *wayqecha*-groups.

Orasema simulatrix and *O. wayqecha*, species that are revised in Chapter 1, are used to examine the hypothesis that EFN associated *Orasema* are transferred to the nest via the infrabuccal pocket of their host ant. Mouthpart dissections of both foraging and nest ants did not uncover planidia in the infrabuccal pocket of *Pheidole*, but instead in the mouthparts of *Camponotus* and *Formica*. Meanwhile the ant-planidia trials determined that it is possible for *Pheidole* to transfer planidia to the infrabuccal pocket if they are attached to the exterior of the ant's body. The implication of these findings are that the original hypothesis is correct but more *Pheidole* need to be collected and dissected to confirm it or that the hypothesis is incorrect and there is an alternate means for planidia to access the ant brood. The results from these three studies in tandem with the recent observation of dead *Camponotus ocreatus* within the nest of *Pheidole* has allowed for the synthesis of a novel hypothesis that EFN associated planidia are transferred to their immature host when dead ants with planidia in their mouthparts are carried into the nest as prey items and fed to the immature host ant. Research carried out in the future should

examine both hypotheses and continue to look for other possible mechanisms of host access all EFN associated eucharitids.

The revisionary work, phylogenetic analyses and behavior trials helped to elucidate EFN-eucharitid relationships. The use of EFNs in three different eucharitid genera indicates this behavioral character is potentially widespread across the family or even within *Orasema*. Expanding this type of work to include more groups from Eucharitidae will improve our understanding of these tritrophic relationships that include a parasitoid, ant host and plant host. It would also help elucidate the evolution of EFN associations within *Orasema* and across Eucharitidae as a whole and examine if an EFN association is correlated with adult and larval morphology such as an expanded postgenae and elongate cerci.

Species with a possible nectary association include members of the *simulatrix*- and *wayqecha*-groups whose biology is still unknown and the numerous species across Eucharitidae whose biology is either unknown or not well characterized. Future research should further examine species that oviposit into EFN bearing plants and species with morphology that potentially correlates with an EFN relationship. An undescribed species from the *coloradensis*-group was recently found to have a convergent postgenae but its biology is unknown. Including novel EFN associations in this research will lead to a better understanding of this complex and fascinating system.

5. Appendix

Improving Ant-Planidia Studies

This appendix was designed to highlight some of the pitfalls faced while trying to determine the host-larval parasitoid interactions both in the field and in the laboratory. Some of the problems of design were based on some potentially flawed ideas of how interactions were taking place that have evolved over the course of our studies. In particular, whether an intermediate ant host from a different genus (*Camponotus* or *Formica*) is being used to vector the *Orasema* parasitoid to their correct brood host. These notes may provide benefit to future studies of the group.

5.1 Foraging Ant Dissections: *Orasema simulatrix*

Improving foraging ant collections and dissections would make this study more informative and help better answer how planidia are traveling from their host plant, *Chilopsis linearis*, to the brood of their ant host, *Pheidole desertorum*. This study addressed the hypothesis that planidia are being transferred to *P. desertorum* brood by traveling in the infrabuccal pocket of *P. desertorum* workers. The objective was to determine if *P. desertorum* and other ant species foraging on or near *Chilopsis* carry planidia in their infrabuccal pocket under natural conditions. In the current study, *P. desertorum* and other ants were collected by either sweeping or beating the tree, or by aspirating ants from the ground near *Chilopsis.* In future studies, optimal collection methods should be determined and used to increase the number of foraging ants, specifically *P. desertorum*, collected. A minimum or threshold number of ants to be

collected for each collecting event needs to be determined. Finally, this study is based on the idea that planidia would be coming in contact with foraging ants when they are near EFNs of *Chilopsis.* Future studies should examine which ant species are actually foraging on or near the EFN of *Chilopsis*.

Two different methods were implemented for collecting foraging ants on *Chilopsis*. Trees were either swept with a net or beat with a canvas sheet placed below. Additional methods such as screen-sweep techniques and fogging desert willow could be employed in future collections of tree foraging ants. Screen-sweeping is similar to standard sweeping, but uses a specialized net with a screen attached (Noyes, 1982) this would filter out large plant debris then all contents of the net could be emptied into alcohol and later examined for ants. This method could be used to sample trees multiple times per night over a period of days, similar to beating or sweeping *Chilopsis*. Insecticide fogging the *Orasema* host plant would be a technique that could only sample a tree at one point in time (residue would prevent or alter insect activity over at least a 24 hour period). Fogging would involve using a canned pyrethroid insecticide to kill insects over an entire tree and the placing traps around the tree to collect falling insects into alcohol (Noyes, 1989). Preliminary studies should compare these four collection methods. The technique that yields the highest number of *P. desertorum* and other ants collected should then be implemented for this experiment.

Pheidole desertorum were the only ants collected off of the ground near *Chilopsis*. Ground foragers were located passively or by baiting with Keebler® Pecan Sandies®

(pecan cookies) or peanut butter placed centrally on 2x2 white paper cards. Future studies should determine which bait results in more *P. desertorum* collected and should be used for all study baits. With this information, a novel type of baiting could also take place. Baits could be placed on the branches of *Chilopsis*, to determine what ants are foraging on *Chilopsis*. Also, future studies could implement visual observations of EFNs to discover if *P. desertorum* are actually consuming nectar. If they are found to not feed at the EFNs this could indicate that planidia are being transferred to *P. desertorum* brood via some mechanism other than traveling in the infrabuccal pocket of *P. desertorum* workers.

5.2 Nest Ant Dissections: *Orasema simulatrix* & *O. wayqecha*

The objective of this study was to determine if planidia are found in the infrabuccal pocket of *Pheidole* workers collected from parasitized nests. The hypothesis is that if planidia are transferred to the ant brood via oral regurgitation from forager ant some *Pheidole* may harbor them in their mouthparts at any given time. The most important aspect of future nest ant dissection studies is to increase the number of *Pheidole* nests excavated and the number of workers collected during the excavations. An increased number of nests and ant specimens for dissection elevates the chance of uncovering planidia if indeed they are being transferred in the mouthparts of worker *Pheidole*.

5.3 Planidia Ant Interactions: *Orasema simulatrix*

If EFN-associated planidia are transferred to their host in the mouthparts of their foraging host ant, then there are multiple ways the immature wasp might enter the infrabuccal

pocket. While the host ant is feeding from an EFN it could accidentally collect the planidia into its mouthparts, or the planidia may phoretically attach to the ant body when it is near an EFN, and then migrate or being moved into the mouth parts during ant grooming. The planidia-ant interaction experiment addressed the latter means of transfer and examined if planidia of *Orasema simulatrix* are able to be transferred to the infrabuccal pocket of *Pheidole desertorum* if placed on the exterior of the ant.

The majority of the alterations for future experiments would deal with the unaccounted planidia and the death of the ants in the trial. Not all of the planidia could be accounted for, which was likely due to an arena that was too large so all of the planidia could not be visually located, or planidia were escaping because the trials were not run in a sealed container. A modified arena design could improve this study. It was recently proposed that the planidia from a eucharitid in the genus *Chalcura* Kirby (Eucharitinae) attach to ants and cause their death (Schwitzke et al., 2015). Ants were found to die within an hour of having planidia placed on their body. Although ant death was not observed to be this rapid in our planidia-ant trials they were all deceased within 24 hours. In future studies, the optimization of ant survival, ending the trials before ants are deceased, and including a control group (unparasitized) would help address why ant death is happening.

A sealed trial arena container should be used so planidia off of the ant are easier to find and they cannot escape. The current trial used plastic 3.5 inch diameter Falcon® disposable petri dishes with lid, which are not sealed and large with the potential of larval

escape. This was associated with the difference in numbers of recovered planidia. In future studies, smaller sealed containers such as gel capsules or small snap-lid petri dish containers could be used. One issue that might arise with sealed containers is maintaining arena humidity, which could be dealt with by placing a wetted cotton string in the arena, using a wetted dental cement base, or by placing the arena over a saturated salt solution (Winston and Bates, 1960). Since *P. desertorum* are nocturnal foragers (Carey et al., 2012), a red film could be placed over the arena to simulate darkness and create a less artificial environment. Modifications to the arena that decrease time to individual ant mortality are essential.

The planidia-ant trials could also be improved with the following alterations: optimize ant's survival before and during the trials, modify the trials timing protocols (both starting point and end point), and include control trials of *P. desertorum* that have not been exposed to planidia. Importantly, the number of trials needs to account for the different age class of the ants that are being collected, as the date of eclosion remains unknown. Similar trials should be conducted on other ant genera/species to determine their vectoring capacity for *Orasema* planidia.

In the current study, all trial ants died within a 24 hour period. Preliminary testing of different ant treatment variables before and during the trials could help maximize ant survival before and during the trials. It should be determined if a 24 hour acclimation period increases ant survival or if trials with recently collected ants yields the same results. It also needs to be resolved whether ants should be fed or watered before the

trials. Ants could be fed a sucrose-water solution or only water before and during the trials. Preliminary tests should determine if there will be a rise in ant survivorship if 75% humidity is maintained for the ants. Lastly, methods to anesthetize the ant before a trial should be tested. A Carbon Dioxide Anesthetizer could be a method that results in less mortality than cooling. Once optimal conditions are determined, they should be standardized and consistently used in all trials.

Optimizing conditions will allow the survival time of an ant in a trial setting to be determined. With this knowledge the trials should be set to end before the *P. desertorum* are deceased and the ant's condition (*e.g.* active, inactive, dead) should be monitored and recorded at various intervals. At the trial's conclusion live ants should be killed and then examined for planidia. The final alteration to the planidia-ant trials would be to add a control group that have not had any previous exposure to planidia as based on the sampling area. This will control for 1) any effect that planidia may be having on the ants survival, and 2) as a measure that the trial ants showed no previous exposure to planida. The purpose of these trials are to 1) observe the number of planidia remaining on the ant, transferred to the infrabuccal pocket, or leaving the ant, 2) observe the potential impact of the planidia on ant mortality, and 3) observe whether there is a differential mortality caused by the planidia to different ant species genera being used as vectors.

6. References

Abbott, A. 1978. Nutrient dynamics of ants. In: Brian, M. V. (Ed.) Production Ecology of Ants and Termites. Cambridge University Press, London, pp. 233-244.

Ayre, G. 1962. *Pseudometagea schwarzii* (Ashm.) (Eucharitidae: Hymenoptera), a parasite of *Lasius neoniger* Emery (Formicidae: Hymenoptera). Canadian Journal of Zoology 40, 157-164.

Beattie, A. J., Turnbull, C., Knox, R. B., Williams, E. 1984. Ant inhibition of pollen function: a possible reason why ant pollination is rare. American Journal of Botany, 421-426.

Bentley, B. L. 1976. Plants bearing extrafloral nectaries and the associated ant community: interhabitat differences in the reduction of herbivore damage. Ecology 57, 815-820.

Burks, R. A., Mottern, J., Heraty, J. M. 2015. Revision of the *Orasema festiva* species group (Hymenoptera: Chalcidoidea: Eucharitidae). Zootaxa 3972, 521-534.

Cameron, P. 1884. Hymenoptera (Families Tenthredinidae-Chrysididae). Taylor and Francis, London.

Carey, B., Visscher, K., Heraty, J. 2012. Nectary use for gaining access to an ant host by the parasitoid *Orasema simulatrix* (Hymenoptera, Eucharitidae). Journal of Hymenoptera Research 27, 47-65.

Cassill, D. L., Butler, J., Vinson, S. B., Wheeler, D. E. 2005. Cooperation during prey digestion between workers and larvae in the ant, *Pheidole spadonia*. Insectes Sociaux 52, 339-343.

Cassill, D. L., Tschinkel, W. R. 1996. A duration constant for worker-to-larva trophallaxis in fire ants. Insectes Sociaux 43, 149-166.

Chew, R. M. 1977. Some ecological characteristics of the ants of a desert-shrub community in southeastern Arizona. American Midland Naturalist 98, 33-49.

Clausen, C. 1976. Phoresy among entomophagous insects. Annual Review of Entomology 21, 343-368.

Clausen, C. P. 1940a. The immature stages of the Eucharidae. Proceedings of the Entomological Society of Washington 42, 161-170.

Clausen, C. P. 1940b. The oviposition habits of the Eucharidae (Hymenoptera). Journal of the Washington Academy of Sciences 30, 504-516.

Clausen, C. P. 1941. The habits of the Eucharidae. Psyche 48, 57-69.

Cosens, D., Toussaint, N. 1986. The dynamic nature of the activities of the wood ant *Formica aquilonia* foraging to static food resources within a laboratory habitat. Physiological Entomology 11, 383-395.

Dallwitz, M., Paine, T., Zurcher, E. 1999. User's Guide to the DELTA Editor. URL: http://delta-intkey.com/www/overview.htm.

Dallwitz, M. J. 1980. A general system for coding taxonomic descriptions. Taxon, 41-46.

Dallwitz, M. J., Paine, T. A., Zurcher, E. J. 1993. Delta user's guide: a general system for processing taxonomic descriptions. Division of Entomology.

Darling, D. C., Miller, T. D. 1991. Life history and larval morphology of *Chrysolampus* (Hymenoptera: Chalcidoidea: Chrysolampinae) in western North America. Canadian Journal of Zoology 69, 2168-2177.

Darling, D. C., Roberts, H. 1999. Life history and larval morphology of *Monacon* (Hymenoptera: Perilampidae), parasitoids of ambrosia beetles (Coleoptera: Platypodidae). Canadian Journal of Zoology 77, 1768-1782.

Das, G. M. 1963. Preliminary studies on the biology of *Orasema assectator* Kerrich (Hym., Eucharitidae), parasitic on *Pheidole* and causing damage to leaves of tea in Assam. Bulletin of Entomological Research 54, 373-378.

Dayrat, B. 2005. Towards integrative taxonomy. Biological Journal of the Linnean Society 85, 407-415.

Dowton, M., Austin, A. D. 1997. Evidence for AT-transversion bias in wasp (Hymenoptera: Symphyta) mitochondrial genes and its implications for the origin of parasitism. Journal of Molecular Evolution 44, 398-405.

Dussutour, A., Simpson, S. J. 2009. Communal nutrition in ants. Current Biology 19, 740-744.

Díaz-Castelazo, C., Sánchez-Galván, I. R., Guimarães, P. R., Raimundo, R. L. G., Rico-Gray, V. 2013. Long-term temporal variation in the organization of an ant–plant network. Annals of Botany 111, 1285-1293.

Eggleton, P., Belshaw, R. 1992. Insect parasitoids: An evolutionary overview. Philosophical Transactions: Biological Sciences 337, 1-20.

Eggleton, P., Belshaw, R. 1993. Comparisons of dipteran, hymenopteran and coleopteran parasitoids: provisional phylogenetic explanations. Biological Journal of the Linnean Society 48, 213-226.

Eisner, T., Happ, G. M. 1962. The infrabuccal pocket of a formicine ant: a social filtration device. Psyche 69, 107-116.

Eisner, T., Wilson, E. O. 1952. The morphology of the proventriculus of a formicine ant. Psyche 59, 47-60.

Falibene, A., de Figueiredo Gontijo, A., Josens, R. 2009. Sucking pump activity in feeding behaviour regulation in carpenter ants. Journal of insect Physiology 55, 518-524.

Feener, J. D. H. 2000. Is the assembly of ant communities mediated by parasitoids? Oikos 90, 79-88.

Feener Jr, D. H., Brown, B. V. 1997. Diptera as parasitoids. Annual Review of Entomology 42, 73-97.

Folmer, O., Black, M., Hoeh, W., Vrijenhoek, R. 1994. DNA primers for amplification of mitochondrial cytochrome c oxidase subunit I from diverse metazoan invertebrates. Molecular Marine Biology and Biotechnology 3, 294-299.

Goloboff, P. A., Farris, J. S., Nixon, K. C. 2008. TNT, a free program for phylogenetic analysis. Cladistics 24, 774-786.

González-Teuber, M., Heil, M. 2009. Nectar chemistry is tailored for both attraction of mutualists and protection from exploiters. Plant Signaling & Behavior 4, 809-813.

Grissell, E. E. 1999. Hymenopteran diversity: some alien notions. American Entomologist 45, 235-244.

Gross, P. 1993. Insect behavioral and morphological defenses against parasitoids. Annual Review of Entomology 38, 251-273.

Heil, M. 2008. Indirect defence via tritrophic interactions. New Phytologist 178, 41-61.

Heil, M. 2011. Nectar: generation, regulation and ecological functions. Trends in Plant Science 16, 191-200.

Heil, M., Fiala, B., Baumann, B., Linsenmair, K. 2000. Temporal, spatial and biotic variations in extrafloral nectar secretion by *Macaranga tanarius*. Functional Ecology 14, 749-757.

Heil, M., Hilpert, A., Krüger, R., Linsenmair, K. E. 2004. Competition among visitors to extrafloral nectaries as a source of ecological costs of an indirect defence. Journal of Tropical Ecology 20, 201-208.

Heil, M., Koch, T., Hilpert, A., Fiala, B., Boland, W., Linsenmair, K. E. 2001. Extrafloral nectar production of the ant-associated plant, *Macaranga tanarius*, is an induced, indirect, defensive response elicited by jasmonic acid. Proceedings of the National Academy of Sciences of the United States of America 98, 1083-1088.

Heil, M., McKey, D. 2003. Protective ant-plant interactions as model systems in ecological and evolutionary research. Annual Review of Ecology, Evolution, and Systematics 34, 425-453.

Heil, M., Rattke, J., Boland, W. 2005. Postsecretory hydrolysis of nectar sucrose and specialization in ant/plant mutualism. Science 308, 560-563.

Heraty, J., Ronquist, F., Carpenter, J. M., Hawks, D., Schulmeister, S., Dowling, A. P., Murray, D., Munro, J., Wheeler, W. C., Schiff, N. 2011. Evolution of the hymenopteran megaradiation. Molecular Phylogenetics and Evolution 60, 73-88.

Heraty, J. M. 1985. A revision of the nearctic Eucharitinae (Hymenoptera: Chalcidoidea: Eucharitidae). Proceedings of the Entomological Society of Ontario 116, 61-103.

Heraty, J. M. 1994a. Biology and importance of two eucharitid parasites of *Wasmannia* and *Solenopsis*. In: Williams, D. (Ed.) Exotic ants: biology, impact and control of introduced species. Westview Press, Boulder, CO, pp. 104-120.

Heraty, J. M. 1994b. Classification and evolution of the Oraseminae in the old world, including revisions of two closely related genera of Eucharitinae (Hymenoptera: Eucharitidae). 157, 1-174.

Heraty, J. M. 2000. Phylogenetic relationships of Oraseminae (Hymenoptera: Eucharitidae). Annals of the Entomological Society of America 93, 374-390.

Heraty, J. M. 2002. A revision of the genera of Eucharitidae (Hymenoptera: Chalcidoidea) of the world. American Entomological Institute 68, 1-367.

Heraty, J. M. 2014. Catalog of World Eucharitidae, 2014. University of California, Riverside.

Heraty, J. M., Barber, K. N. 1990. Biology of *Obeza floridana* (Ashmead) and *Pseudochalcura gibbosa* (Provancher) (Hymenoptera: Eucharitidae). Proceedings of the Entomological Society of Washington 92, 248-258.

Heraty, J. M., Burks, R. A., Cruaud, A., Gibson, G. A. P., Liljeblad, J., Munro, J., Rasplus, J.-Y., Delvare, G., Janšta, P., Gumovsky, A., Huber, J., Woolley, J. B., Krogmann, L., Heydon, S., Polaszek, A., Schmidt, S., Darling, D. C., Gates, M. W., Mottern, J., Murray, E., Dal Molin, A., Triapitsyn, S., Baur, H., Pinto, J. D.,

van Noort, S., George, J., Yoder, M. 2013. A phylogenetic analysis of the megadiverse Chalcidoidea (Hymenoptera). Cladistics 29, 466-542.

Heraty, J. M., Darling, D. C. 1984. Comparative morphology of the planidial larvae of Eucharitidae and Perilampidae (Hymenoptera: Chalcidoidea). Systematic Entomology 9, 309-328.

Heraty, J. M., Murray, E. 2013. The life history of *Pseudometagea schwarzii*, with a discussion of the evolution of endoparasitism and koinobiosis in Eucharitidae and Perilampidae (Chalcidoidea). Journal of Hymenoptera Research 35, 1-15.

Heraty, J. M., Wojcik, D. P., Jouvenaz, D. P. 1993. Species of *Orasema* parasitic on the *Solenopsis saevissima*-complex in South America (Hymenoptera: Eucharitidae, Formicidae). Journal of Hymenoptera Research 2, 169-182.

Howard, R. W., Pérez-Lachaud, G., Lachaud, J. P. 2001. Cuticular hydrocarbons of *Kapala sulcifacies* (Hymenoptera: Eucharitidae) and its host, the ponerine ant *Ectatomma ruidum* (Hymenoptera: Formicidae). Annals of the Entomological Society of America 94, 707-716.

Huelsenbeck, J. P., Larget, B., Alfaro, M. E. 2004. Bayesian phylogenetic model selection using reversible jump Markov chain Monte Carlo. Molecular Biology and Evolution 21, 1123-1133.

Hunt, J. 1994. Nourishment and social evolution in wasps sensu lato. In: Hunt, J. H., Nalepa, C. A. (Eds.), Nourishment and evolution in insect societies. Westview Press, Inc., pp. 211-244.

Hölldobler, B., Wilson, E. O. 1990. The ants. Harvard University Press.

Johnson, J. B., Miller, T. D., Heraty, J. M., Merickel, F. W. 1986. Observations on the biology of two species of *Orasema* (Hymenoptera: Eucharitidae). Proceedings of the Entomological Society of Washington 88, 542-549.

Katoh, K., Standley, D. M. 2013. MAFFT multiple sequence alignment software version 7: improvements in performance and usability. Molecular biology and evolution 30, 772-780.

Koptur, S., Palacios-Rios, M., Díaz-Castelazo, C., Mackay, W. P., Rico-Gray, V. 2013. Nectar secretion on fern fronds associated with lower levels of herbivore damage: field experiments with a widespread epiphyte of Mexican cloud forest remnants. Annals of Botany 111, 1277-1283.

Kost, C., Heil, M. 2005. Increased availability of extrafloral nectar reduces herbivory in Lima bean plants (*Phaseolus lunatus*, Fabaceae). Basic and Applied Ecology 6, 237-248.

Lachaud, J.-P., Lenoir, A., Hughes, D. P. 2012. Ants and their parasites. Psyche 2012, 5.

Lachaud, J.-P., Pérez-Lachaud, G. 2012. Diversity of species and behavior of hymenopteran parasitoids of ants: a review. Psyche 2012, 1-24.

Little, E. L., Jr. 1976. Atlas of United States trees, minor western hardwoods. U.S. Department of Agriculture Miscellaneous Publication.

Madison, W., Madison, D. 2011. Mesquite: a modular system for evolutionary analysis. Version 2.75. htttp://mesquiteproject. org.

Marazzi, B., Bronstein, J. L., Koptur, S. 2013a. The diversity, ecology and evolution of extrafloral nectaries: current perspectives and future challenges. Annals of Botany 111, 1243-1250.

Marazzi, B., Conti, E., Sanderson, M. J., McMahon, M. M., Bronstein, J. L. 2013b. Diversity and evolution of a trait mediating ant–plant interactions: insights from extrafloral nectaries in *Senna* (Leguminosae). Annals of Botany 111, 1263-1275.

Medan, V., Josens, R. B. 2005. Nectar foraging behaviour is affected by ant body size in *Camponotus mus*. Journal of Insect Physiology 51, 853-860.

Miller, M., Pfeiffer, W., Schwartz, T. 2010. Creating the CIPRES science gateway for inference of large phylogenetic trees. Proceedings of the gateway computing environments workshop (GCE), New Orleans, Louisiana, United States of America.

Mottern, J. L., Heraty, J. M. 2014. Revision of the *Cales noacki* species complex (Hymenoptera, Chalcidoidea, Aphelinidae). Systematic Entomology 39, 354-379.

Murray, E. A. 2014. Systematics and evolution of eucharitidae (Hymenoptera: Chalcidoidea), with a focus on the new world *Kapala*. University of California, Riverside.

Murray, E. A., Carmichael, A. E., Heraty, J. M. 2013. Ancient host shifts followed by host conservatism in a group of ant parasitoids. Proceedings of the Royal Society B: Biological Sciences 280 20130495.

Noyes, J. S. 1982. Collecting and preserving chalcid wasps (Hymenoptera: Chalcidoidea). Journal of Natural History 16, 315-334.

Noyes, J. S. 1989. A study of five methods of sampling Hymenoptera (Insecta) in a tropical rainforest, with special reference to the Parasitica. Journal of Natural History 23, 285-298.

Padial, J. M., Miralles, A., De la Riva, I., Vences, M. 2010. Review: The integrative future of taxonomy. Frontiers in Zoology 7, 1-14.

Parker, H., Thompson, W. 1925. Notes on the larvae of the Chalcidoidea. Annals of the Entomological Society of America 18, 384-398.

Parker, H. L. 1937. The oviposition habits of *Stilbula cynipiformis* Rossi (Hymenoptera, Eucharitidae). Proceedings of the Entomological Society of Washington 39, 1-3.

Petersen, C., Brown, J., Kodric-Brown, A. 1982. An experimental study of floral display and fruit set in *Chilopsis linearis* (Bignoniaceae). Oecologia 55, 7-11.

Rambaut, A. 2012. FigTree v1. 4. Molecular evolution, phylogenetics and epidemiology. Edinburgh, UK: University of Edinburgh, Institute of Evolutionary Biology.

Rambaut, A., Suchard, M., Xie, D., Drummond, A. 2014. Tracer v1. 6. Computer program and documentation distributed by the author, website http://beast.bio.ed.ac.uk/Tracer [accessed 27 July 2014].

Roche, R., Wheeler, D. 1991. Proventriculus morphology of the turtle ant, *Zacryptocercus rowheri*. J. Electron Microscopy Technique 18, 329.

Ronquist, F., Teslenko, M., van der Mark, P., Ayres, D. L., Darling, A., Höhna, S., Larget, B., Liu, L., Suchard, M. A., Huelsenbeck, J. P. 2012. MrBayes 3.2: efficient Bayesian phylogenetic inference and model choice across a large model space. Systematic Biology 61, 539-542.

Santos, A., Quicke, D. L. 2011. Large-scale diversity patterns of parasitoid insects. Entomological Science 14, 371-382.

Schlick-Steiner, B. C., Steiner, F. M., Seifert, B., Stauffer, C., Christian, E., Crozier, R. H. 2010. Integrative taxonomy: a multisource approach to exploring biodiversity. Annual Review of Entomology 55, 421-438.

Schmid-Hempel, P. 1998. Parasites in social insects. Princeton University Press.

Schwitzke, C., Fiala, B., Linsenmair, K. E., Curio, E. 2015. Eucharitid ant-parasitoid affects facultative ant-plant *Leea manillensis*: top-down effects through three trophic levels. Arthropod-Plant Interactions 9, 497-505.

Sharkey, M. J. 2007. Phylogeny and classification of Hymenoptera. Zootaxa 1668, 521-548.

Stamatakis, A. 2014. RAxML version 8: a tool for phylogenetic analysis and post-analysis of large phylogenies. Bioinformatics 30, 1312-1313.

Stamatakis, A., Hoover, P., Rougemont, J. 2008. A rapid bootstrap algorithm for the RAxML web servers. Systematic biology 57, 758-771.

Stephenson, A. G. 1982. The Role of the Extrafloral Nectaries of *Catalpa speciosa* in Limiting Herbivory and Increasing Fruit Production. Ecology 63, 663-669.

Trelease, W. 1881. The foliar nectar glands of *Populus*. Botanical Gazette, 284-290.

Vaidya, G., Lohman, D. J., Meier, R. 2011. SequenceMatrix: concatenation software for the fast assembly of multi-gene datasets with character set and codon information. Cladistics 27, 171-180.

Vander Meer, R. K., Jouvenaz, D. P., Wojcik, D. P. 1989. Chemical mimicry in a parasitoid (Hymenoptera: Eucharitidae) of fire ants (Hymenoptera: Formicidae). J Chem Ecol 15, 2247-2261.

Varone, L., Briano, J. 2009. Bionomics of *Orasema simplex* (Hymenoptera: Eucharitidae), a parasitoid of *Solenopsis* fire ants (Hymenoptera: Formicidae) in Argentina. Biological Control 48, 204-209.

Vinson, S. B. 1976. Host selection by insect parasitoids. Annual Review of Entomology 21, 109-133.

Wagner, D., Kay, A. 2002. Do extrafloral nectaries distract ants from visiting flowers? An experimental test of an overlooked hypothesis. Evolutionary Ecology Research 4, 293-305.

Walsh, P. S., Metzger, D. A., Higuchi, R. 1991. Chelex 100 as a medium for simple extraction of DNA for PCR-based typing from forensic material. Biotechniques 10, 506-513.

Weber, M. G., Keeler, K. H. 2013. The phylogenetic distribution of extrafloral nectaries in plants. Annals of Botany 111, 1251-1261.

Wheeler, W. M. 1907. The polymorphism of ants. Annals of the Entomological Society of America 1, 39-69.

Wilson, E. 2005. Oribatid mite predation by small ants of the genus P*heidole*. Insectes Sociaux 52, 263-265.

Winston, P. W., Bates, D. H. 1960. Saturated solutions for the control of humidity in biological research. Ecology 41, 232-237.

Yoder, M. J., Miko, I., Seltmann, K. C., Bertone, M. A., Deans, A. R. 2010. A gross anatomy ontology for Hymenoptera. PloS one 5, e15991.